

## Simulation of the Behavior of Supported Metal Catalysts in Real Reaction Atmospheres by Means of Model Catalysts

SUNG H. LEE AND E. RUCKENSTEIN

*Department of Chemical Engineering, State University of New York, Buffalo, New York 14260*

Received January 10, 1987; revised April 13, 1987

Model catalysts formed of small crystallites of Ni, Co, or Fe supported on thin, electron transparent films of nonporous alumina were heated in chemical atmospheres having compositions in the range encountered in the steam-reforming reaction. Electron microscopy and electron diffraction were used to investigate the physical and chemical changes that occurred. For a better understanding of the phenomena involved, the effect of the mixture is compared to the effects caused by the individual components and by their combinations. It is shown that, depending upon the nature of the catalyst as well as upon the composition of the mixture, sintering or/and coking can occur much more rapidly in mixtures than in single-component atmospheres. This suggests that a cooperative action of the reaction components is the cause of the early deactivation of the steam-reforming catalysts. Various phenomena such as carbon deposition (as films or patches on the surface of the catalyst and on the substrate or as filaments), deformation of the crystallites, severe sintering, and permanent loss of metal to the gas stream were observed. Explanations are provided for the behavior of the Ni/Al<sub>2</sub>O<sub>3</sub>, Co/Al<sub>2</sub>O<sub>3</sub>, and Fe/Al<sub>2</sub>O<sub>3</sub> catalysts, in various atmospheres, by considering the competition between carbon deposition and its gasification, as well as the strength of the interactions between crystallites and substrate. Two kinds of filaments were observed: carbonaceous filaments and metal oxide filaments which probably contain some carbon. A thermodynamic condition for the formation of filamentous carbon is suggested. If the sum of the interfacial free energies between carbon and crystallite, and carbon and substrate is smaller than that between crystallite and substrate, then carbon could penetrate between crystallites and substrate and filaments would be generated. Indeed, carbonaceous filaments were identified only when the catalyst particles were present as metals. In such cases, the interfacial free energy between the metal crystallite and alumina is much greater than that between the oxidized metal and alumina and the above thermodynamic condition is more likely to be satisfied. Permanent loss of active metal to the gas stream occurred, either because of the disintegration of the crystallites caused by carbon precipitation inside the particles, and/or possibly because of the formation of volatile carbonyls. © 1987 Academic Press, Inc.

### INTRODUCTION

The loss of activity and/or selectivity of industrial catalysts in the course of reaction can be attributed to a wide variety of causes, which may be grouped into sintering, coking, poisoning, and phase transformation. However, in real situations these processes coexist and influence each other, and the deactivation of the catalyst is a result of their cooperative action. Therefore, an investigation of deactivation by the cooperative action of various processes should be undertaken; this is the scope of the present paper.

A meaningful case for such studies is the steam-reforming reaction, in which steam reacts with natural gas, primarily methane, to form H<sub>2</sub>, CO, CO<sub>2</sub>. While supported nickel is employed as the commercial catalyst (1), cobalt and iron can also be used, though they are less active. The high temperature (about 700-1000°C) and the presence of steam, methane, and hydrogen set severe conditions on the catalyst. As is well known, when these compounds are alone, the heating in hydrogen stimulates sintering, the heating in methane causes coking, while the heating in the presence of steam

results in a phase transformation of alumina (2) as well as in the formation of a solid solution between the oxidized metal and support (3). However, when the above gases are together these processes influence one another. For instance, when carbon deposition constitutes the dominant process, steam and hydrogen are expected to have an influence on carbon formation, on the morphologies of carbon deposits, and on the rate of carbon growth. Indeed, carbon deposits and/or coke precursors, which are formed by the dissociation of CO or decomposition of hydrocarbons, are removed as CH<sub>4</sub> or CO by the reaction with H<sub>2</sub> or H<sub>2</sub>O (4-6). The presence of sufficient amounts of H<sub>2</sub> or H<sub>2</sub>O minimizes the formation of condensed hydrocarbons and amorphous carbon or graphite (7). Therefore, coking under such conditions differs from that in pure methane or carbon monoxide. On the other hand, carbon formation may enhance or deter sintering. Indeed, sintering is stimulated by carbon gasification, since the resulting gases enhance the mobility of the crystallites on the substrate; in contrast the deposition of carbon around the particles impedes their migration.

In the very extensive literature dealing with deactivation in the steam-reforming reaction, the investigators have studied only the individual processes leading to deactivation of the catalysts, such as coking, sintering, or poisoning. Coking has received the greatest attention and the results have been summarized in numerous reviews (5-10). Only a few investigators have, however, studied carbon formation in real reaction systems. Rostrup-Nielsen (5) reported that, during steam reforming of naphtha, the coking rate on the nickel surface at temperatures near 500°C depends on the steam-to-carbon ratio and other factors. No coking was observed to occur on the cobalt/alumina catalyst, which has a poor activity for the reaction, though in atmospheres without steam, coke was generated (from methane, carbon monoxide, or ole-

fins) on cobalt as on nickel. The deactivation of nickel supported on alumina was explained as a result of the blockage of the pore mouth by the coke deposited mainly close to the external surface. This blockage impedes the adsorption of steam on the crystallites and therefore steam can no longer depress carbon formation. In contrast, the poor activity of cobalt for steam reforming was explained by the blockage of the pore mouth by the metal oxide which rapidly forms in steam, rather than by the blockage by carbon. Jackson *et al.* (11) reported different deactivation mechanisms for Ni catalysts in a real reaction atmosphere and in one without steam. He noted that the filamentous carbon, which is generated on the catalysts when the hydrocarbon is alone, is no longer present to any appreciable extent under real conditions.

Sintering is also considered to be an important cause for catalyst deactivation in the steam reforming reaction (12, 13). Williams *et al.* (14) suggested that the principal cause of sintering in steam reforming is the thermal instability of the alumina support, namely the transformation, due to the presence of steam, of the  $\gamma$ -alumina to the alpha phase, which triggers the sintering of the metal particles. These investigators observed a very sharp early decrease in the surface areas of both nickel and alumina with time in the presence of steam and hydrogen. As pointed out by Satterfield (12), the crystallite size is increased to about 1  $\mu$ m, as soon as the catalyst is brought in contact with the steam-reforming mixture.

The formation of an inactive phase in the metal crystallites is also a problem of concern. Borowiecki *et al.* (15) suggested that the surface reaction as well as the deposition of carbon promote the formation of an inactive "oxidized" metal form at the boundary between metal and support.

The poisoning by the additional constituents of the hydrocarbon feed stock also contributes to the loss of catalyst activity

(16). However, this problem is beyond the scope of the present paper.

There is a lack of comparative studies regarding the cooperative deactivation (due to sintering, coking, and phase transformation) of various catalysts in atmospheres similar to those encountered in steam-reforming reactions. In the present investigation, model catalysts of Ni/Al<sub>2</sub>O<sub>3</sub>, Co/Al<sub>2</sub>O<sub>3</sub>, and Fe/Al<sub>2</sub>O<sub>3</sub> were heated in various chemical atmospheres, such as methane, carbon monoxide, steam plus methane, steam plus methane and hydrogen, and steam plus methane, hydrogen, and carbon monoxide. The composition of these mixtures simulates either the inlet or the outlet composition of the industrial primary reformer furnace. The effect of steam was already reported (17). The object of the present investigation is to examine the cooperative deactivation in simulated reaction atmospheres, and to identify the dominant event or events in various atmospheres and for various metals as well as the interrelationship between them.

## EXPERIMENTAL

### *a. Preparation of the Specimen*

Thin, electron transparent alumina films, about 30 nm thick, were prepared by anodization of high-purity aluminum foils (99.999% Alfa Products) and the dissolution of the remaining aluminum in mercury chloride solutions (18). The thin alumina films were then deposited on gold microscope grids and heated at 800°C for 40 h. Nickel (99%, Alfa Products), cobalt (99.8%, Alfa Products), and iron (99.998% Alfa Products) were then vacuum deposited on the alumina substrate to a thickness of 1.5 nm. The specimens were heated in flowing ultrahigh-purity H<sub>2</sub> (99.999% pure, but containing traces of O<sub>2</sub> (less than 1 ppm) and H<sub>2</sub>O (less than 3 ppm); Linde Division, Union Carbide Co.) at 500°C for at least 5 h and then at 700°C for at least 5 additional hours in order to change the metal films to well-defined crystallites. In

addition, the as-supplied hydrogen was further purified to eliminate the traces of O<sub>2</sub> and water by passing it through a Deoxo unit (Engelhard Industries) and then through a molecular sieve bed immersed in liquid nitrogen. This further-purified H<sub>2</sub> was always employed when heating in H<sub>2</sub> alone. In all the other cases, the as-supplied hydrogen was employed.

### *b. Heat Treatment*

The heating of the above specimen was carried out at 1 atm and 700°C in a quartz tube located in a furnace. After the specimen was introduced in the tube, ultrahigh-purity helium (99.999% pure, Linde Division, Union Carbide Co.) was allowed to flow through the tube during the period in which the temperature was raised to 700°C. Helium was then replaced by the desired feed stream, such as methane (ultrahigh-purity, 99.97%, <10 ppm O<sub>2</sub> and <6 ppm moisture; Linde Division, Union Carbide Co.), carbon monoxide (ultrahigh-purity, 99.8%; Matheson Gas Products), and three sets of gas mixtures containing at least two components among hydrogen, steam, methane, carbon monoxide, and helium. The compositions of the gas mixtures are listed in Table 1. The amounts of the individual components in the gas mixtures were adjusted with individual flow meters and the total flow rate without steam was maintained at about 200 ml/min. Steam was introduced into the gas mixtures by means of a water saturator maintained at a temperature at which the water vapor pressure can provide the desired concentration of steam

TABLE 1  
A List of the Composition of Gas Mixtures

Gas mixture	Volume (%)				
	CH <sub>4</sub>	Steam	H <sub>2</sub>	CO	He
Mixture 1	50	50	0	0	0
Mixture 2	5	43	40	0	12
Mixture 3	5	43	40	12	0

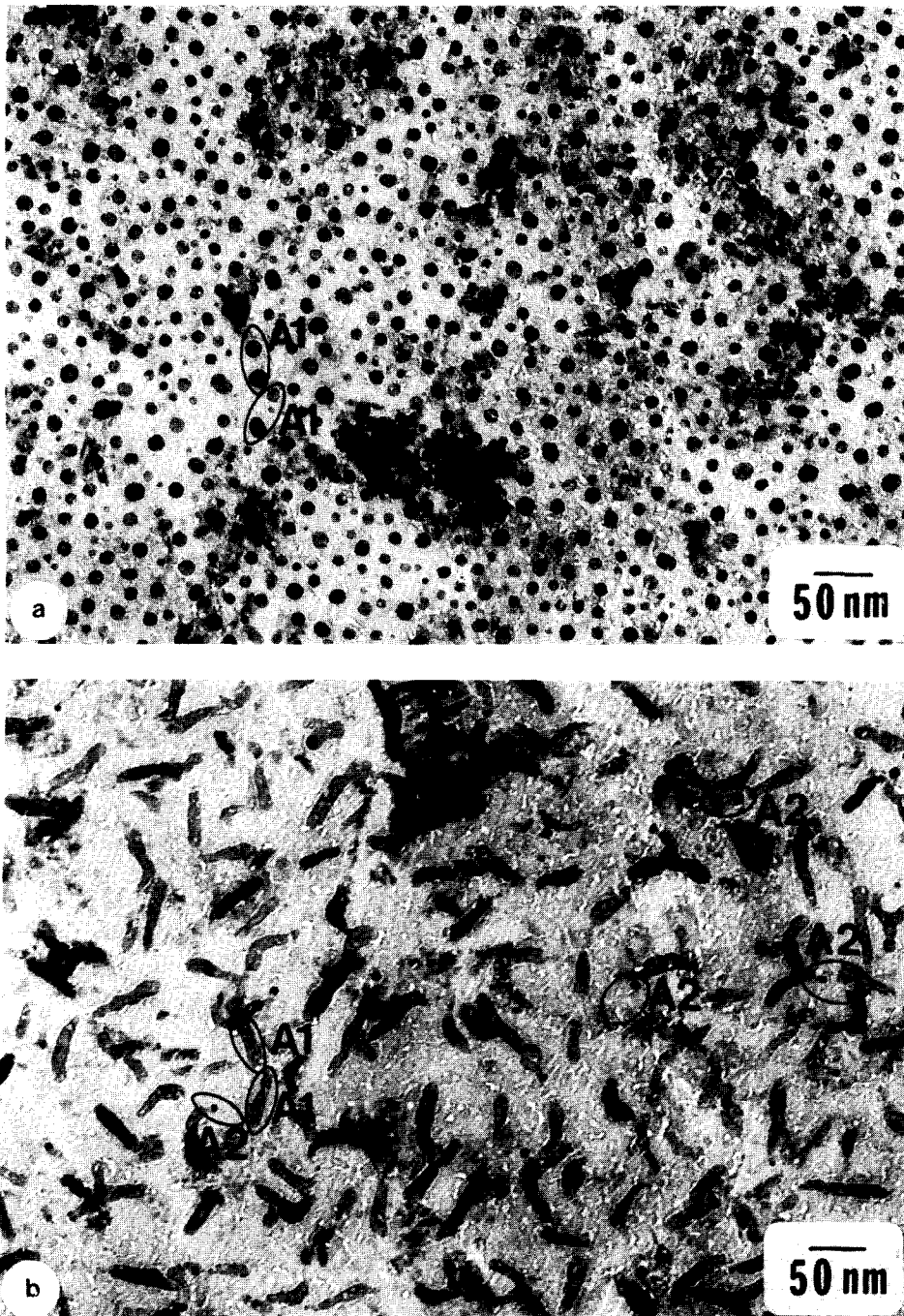


FIG. 1. Sequence of changes on heating a Ni/Al<sub>2</sub>O<sub>3</sub> specimen in methane at 700°C after pretreatment in hydrogen. When the heating in a given atmosphere has taken place in several steps, the total time is indicated at each step. (a) 10 h (5 h at 500°C and 5 h at 700°C) H<sub>2</sub>; (b) 1.5 h CH<sub>4</sub>; (c) 3 h CH<sub>4</sub> (the specimen was heated for 1.5 more hours in CH<sub>4</sub> after the heat treatment (c)); (d) 2 h O<sub>2</sub>; (e) 3 h H<sub>2</sub>; (f) 1.5 h CH<sub>4</sub>.

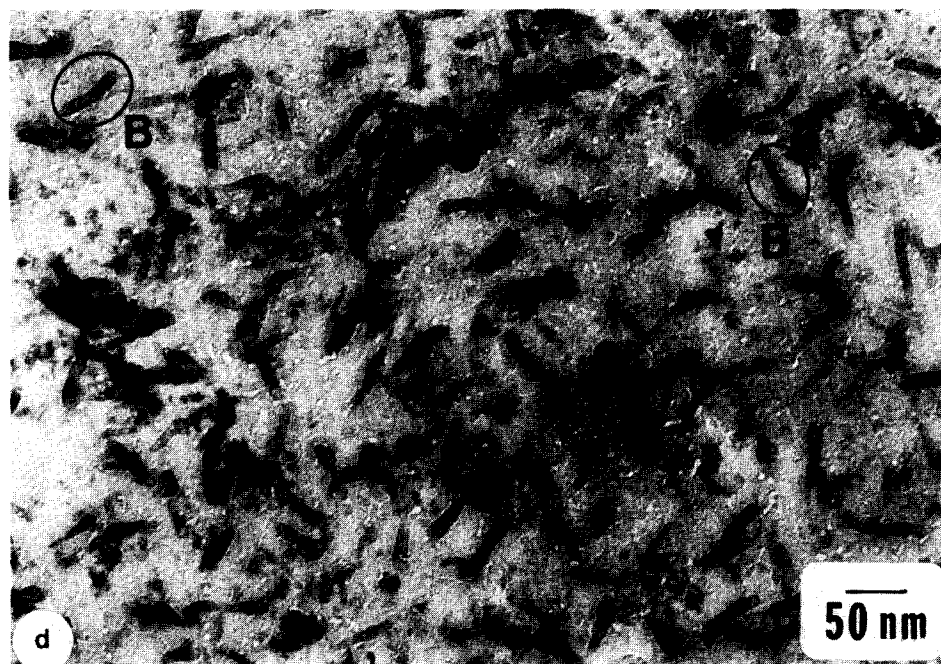
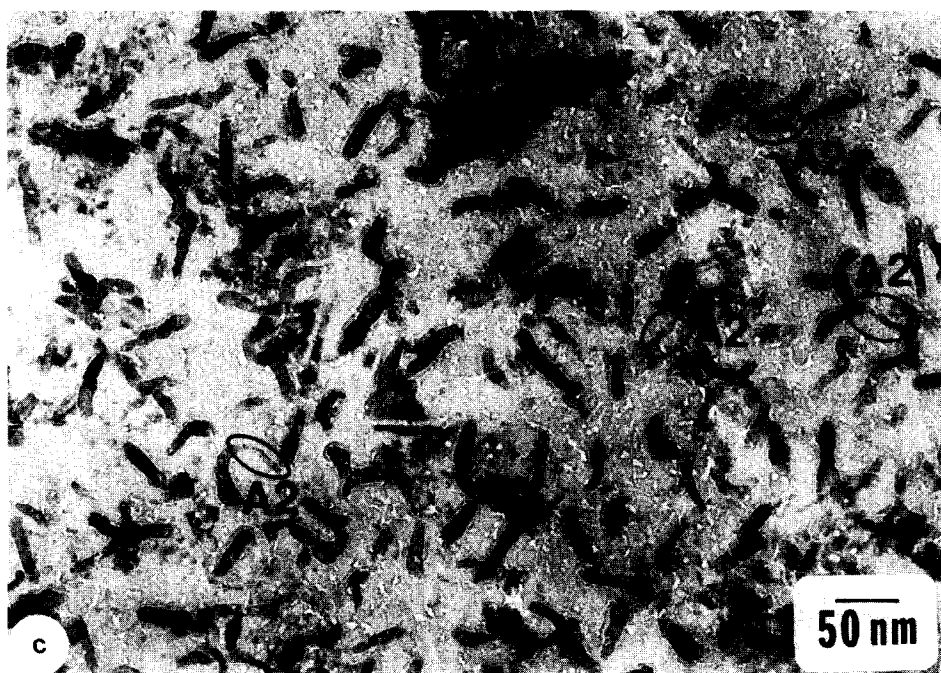


FIG. 1—Continued.

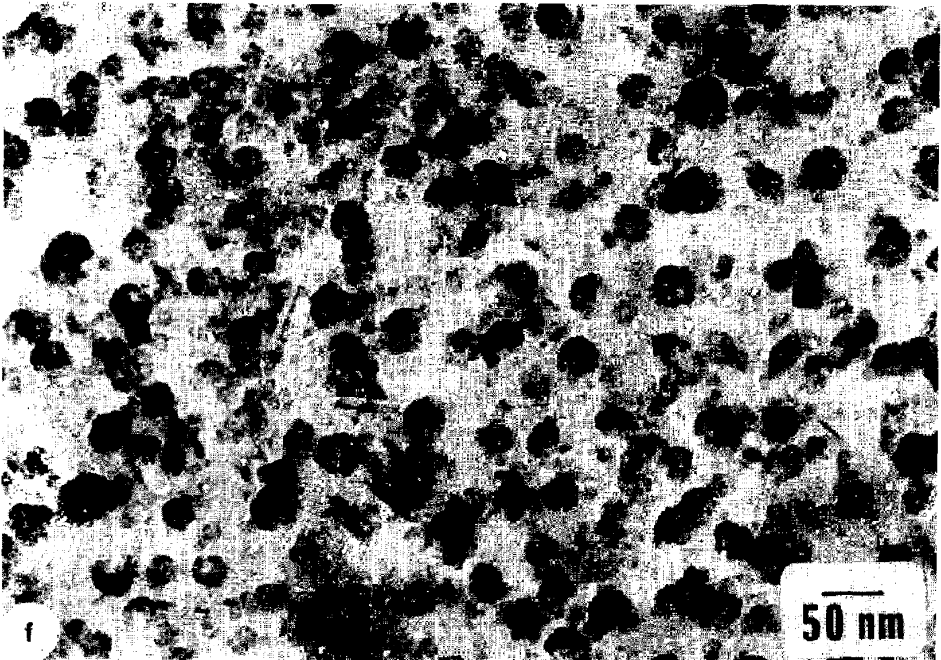
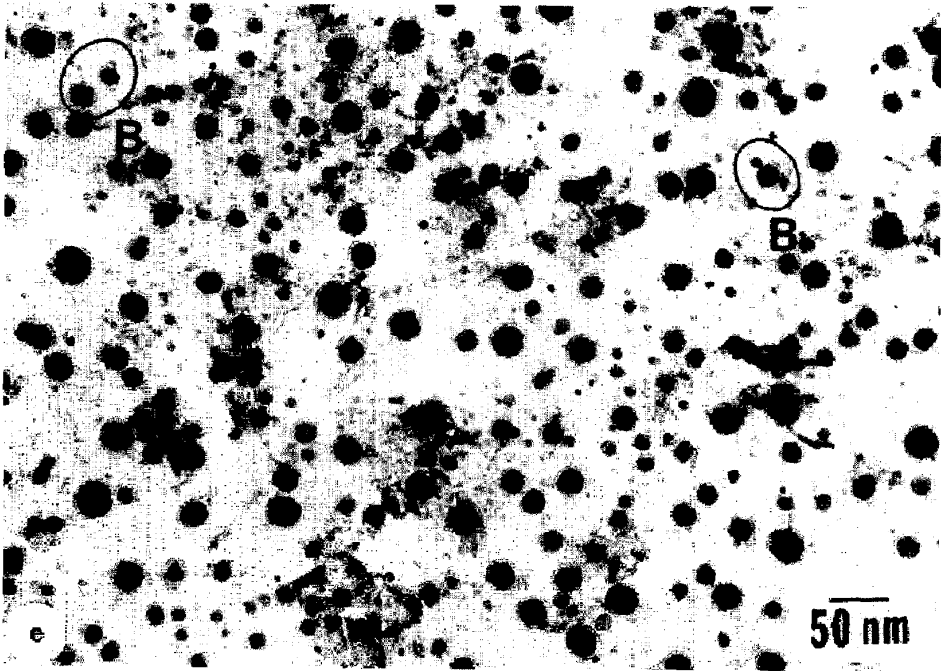


FIG. 1—Continued.

in the gas mixture. Before being taken out for observation, the samples were cooled down slowly to room temperature, in a helium atmosphere. The observations have been made in the same region of the sample after each heat treatment, by means of a JEOL 100U TEM.

## RESULTS

### 1. HEATING IN METHANE

#### A. $Ni/Al_2O_3$

*a. Heating in  $CH_4$  after pretreatment in  $H_2$ .* On heating in hydrogen for 10 h (5 h at 500°C and subsequently 5 h at 700°C), globular particles were formed (Fig. 1a). The electron diffraction pattern indicated the presence of Ni. Subsequently, the specimen was heated in  $CH_4$ . During heating in  $CH_4$  for 1.5 h, filamentous (elongated) structures replaced the globular particles (Fig. 1b). Following elongation, most of the particles coalesced with their neighbors (A1 in Fig. 1b). At the tip of some filaments, dark particles were detected (A2 in Fig. 1b). On further heating for 1.5 additional hours, these darker particles moved over the substrate and decreased in size or disappeared, generating filaments along their trajectories (A2 in Fig. 1c). It is likely that the lost material from the particles was left behind in the filaments. After particles were heated for a total of 4.5 h, no significant change was observed. The electron diffraction patterns indicated the presence of NiO, probably because of the presence of moisture and oxygen in methane. Hence the major component of the filament was, most probably, NiO. It is, however, likely that carbon deposition and its penetration into the particles is in some way responsible for the filamentous structure. In some of the specimens, the particles extended, maintaining however the globular shape, and no filament formation was observed during heating in  $CH_4$ . In such cases, it is not clear whether carbon was deposited around the particles, because of the difficulty in discerning carbon deposition from extension

of the particle. The specimen of Fig. 1c was subsequently heated in oxygen for 2 h. The filaments which contained mostly NiO remained almost unaffected (Fig. 1d), with only marginal loss of material, probably due to carbon gasification. There was no change in the diffraction pattern. The specimen was subsequently heated in  $H_2$  for 3 h (Fig. 1e). During this heat treatment, the filaments transformed to globular shapes, as a result of contraction. In some regions (B in Figs. 1d and 1e), two or more particles were formed from a filament. The diffraction pattern indicated that NiO was reduced to Ni. The specimen was again heated in  $CH_4$ . After heating for 1.5 h, the particles extended and split into several interconnected subunits (Fig. 1f). Some small particles disappeared, most probably because of spreading out as thin undetectable films. One may note that most of the extended particles have a small darker particle supported on a very extended patch. On further heating in  $CH_4$ , for up to 15.5 h, the particles extended a little further and the darker remnant particles decreased in size or disappeared. However, filaments were not generated, indicating that the already coked specimens do not act in the same way as the fresh specimens do. However, on another sample, whose micrographs are not included in this paper, filaments which contained mostly NiO were generated in  $CH_4$  even after heating the coked specimen in  $O_2$  and subsequently in  $H_2$ , but to a much smaller extent than the first time.

It is inevitable to expose the specimen to air during repeated heating and subsequent observation by TEM. In order to check whether the exposure to air affects the morphology of the particles, a sample was continuously heated in  $CH_4$  for 5 h at 700°C. The result is shown in Fig. 2 and is quite similar to that obtained by heating a specimen in several steps for almost the same total heating time (Fig. 1c). These results point out that the repeated exposure to air does not affect in an important way the morphology of the particles.

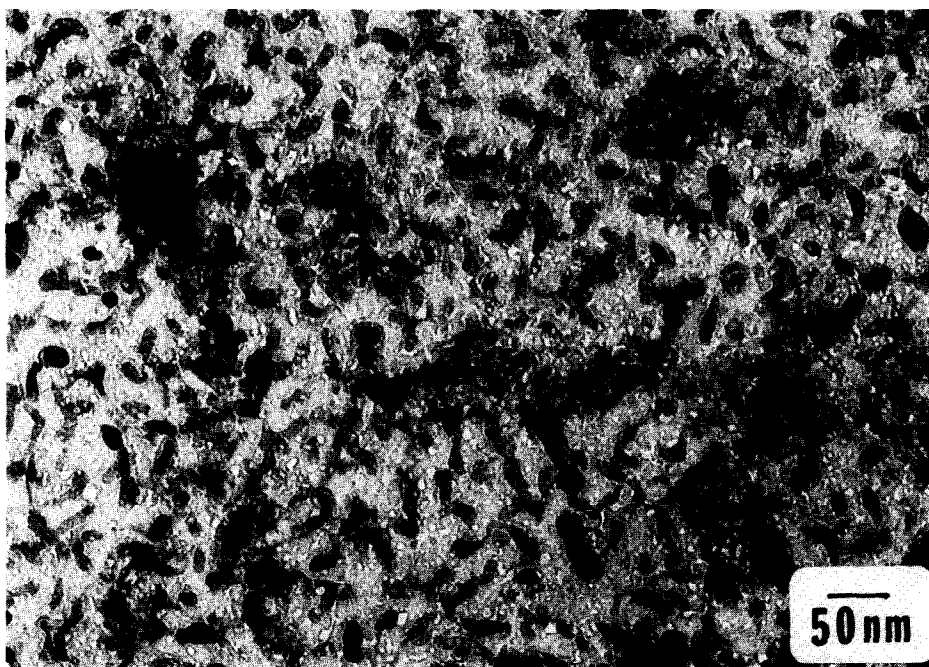


FIG. 2. Ni/Al<sub>2</sub>O<sub>3</sub> specimen after heating in CH<sub>4</sub> for 5 h continuously at 700°C following heating in H<sub>2</sub> for 10 h (5 h at 500°C and 5 h at 700°C).

*b. Heating in CH<sub>4</sub> after pretreatment in steam.* Since particles were not generated on heating in steam at 700°C for up to 15 h, the specimen was first heated in H<sub>2</sub> for 10 h (5 h at 500°C and 5 h at 700°C) and subsequently in steam also at 700°C. Figure 3a shows the result of heating in steam for 5 h. Compared to the pretreatment in H<sub>2</sub> (Fig. 1a), the particles appear to be thinner. On heating the specimen of Fig. 3a in CH<sub>4</sub> for 4 h, dark patches, most likely carbon deposits, but no filaments appeared (C in Fig. 3b).

#### B. Co/Al<sub>2</sub>O<sub>3</sub>

After heating in H<sub>2</sub> for 10 h the particles acquired globular shapes (Fig. 4a). Electron diffraction indicated the presence of  $\alpha$ -Co. However, some rings of Co<sub>2</sub>O<sub>3</sub> and Co<sub>3</sub>O<sub>4</sub> were also identified. On further heating in CH<sub>4</sub> for 30 min, most of the large particles increased in size (D in Fig. 4b), either

because of their extension, or, most likely, because of carbon deposition around and on the extended particles. In some regions (E in Fig. 4b), some neighboring particles coalesced. In region F, two neighboring particles deformed and became interconnected, possibly by carbonaceous films. After heating for up to 15 h, in several steps, some of the particles extended marginally and some became so thin that one could see the structure of the substrate beneath them (Fig. 4c). Some particles decreased in size, probably because of the spreading out from them of thin films undetectable by electron microscopy. On subsequent heating in H<sub>2</sub> for 2 h at 700°C (Fig. 4d), numerous new small particles appeared in regions where no particles were observed before, indicating that indeed during heating in CH<sub>4</sub> some particles and part of other particles spread out over the substrate as undetectable films. These undetectable films ruptured during heating in H<sub>2</sub>



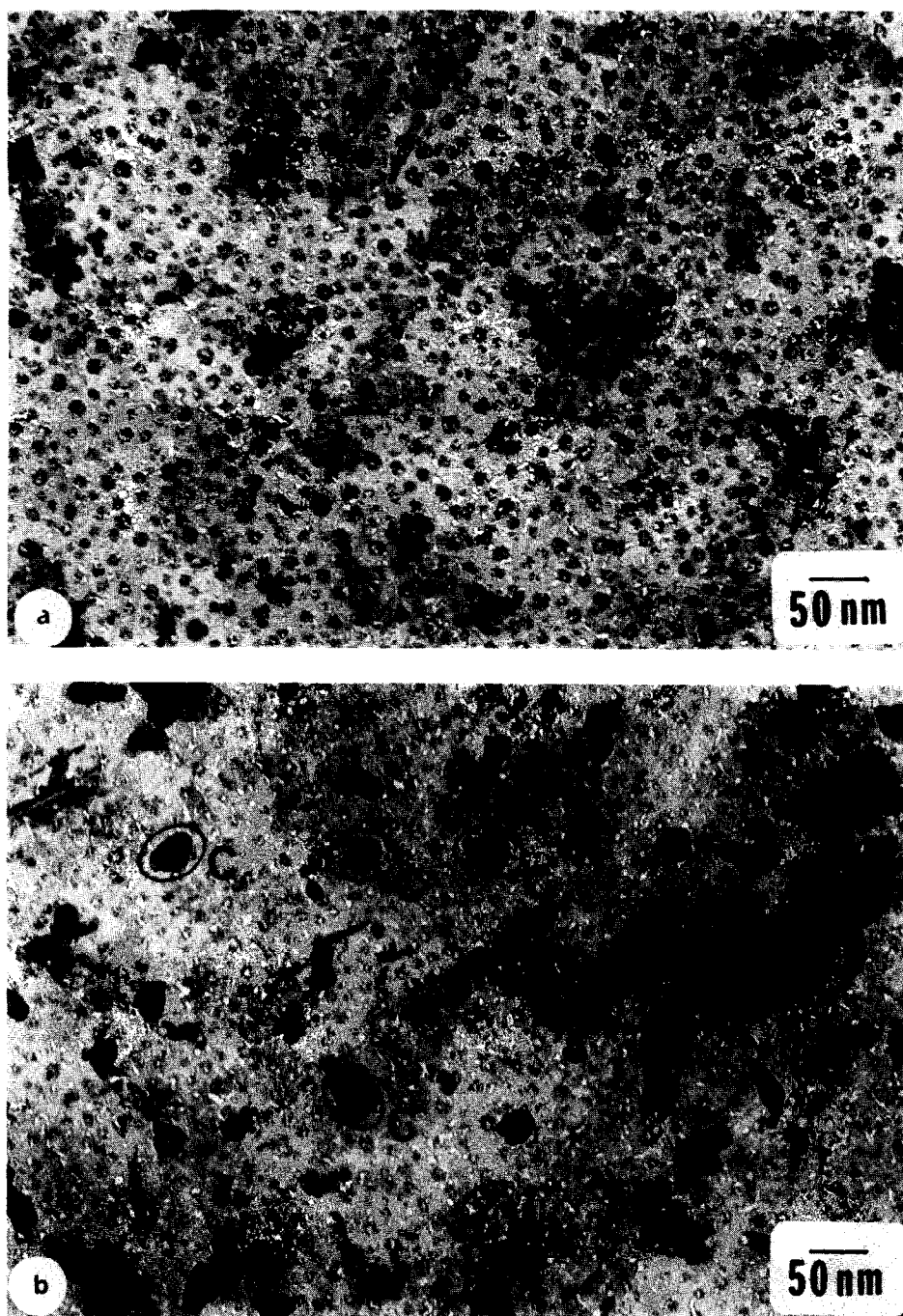


FIG. 3. Sequence of changes on heating a Ni/Al<sub>2</sub>O<sub>3</sub> specimen in methane at 700°C after pretreatment in steam. (a) 10 h (5 h at 500°C and 5 h at 700°C) in H<sub>2</sub> and subsequently 5 h in steam at 700°C; (b) 4 h CH<sub>4</sub>.

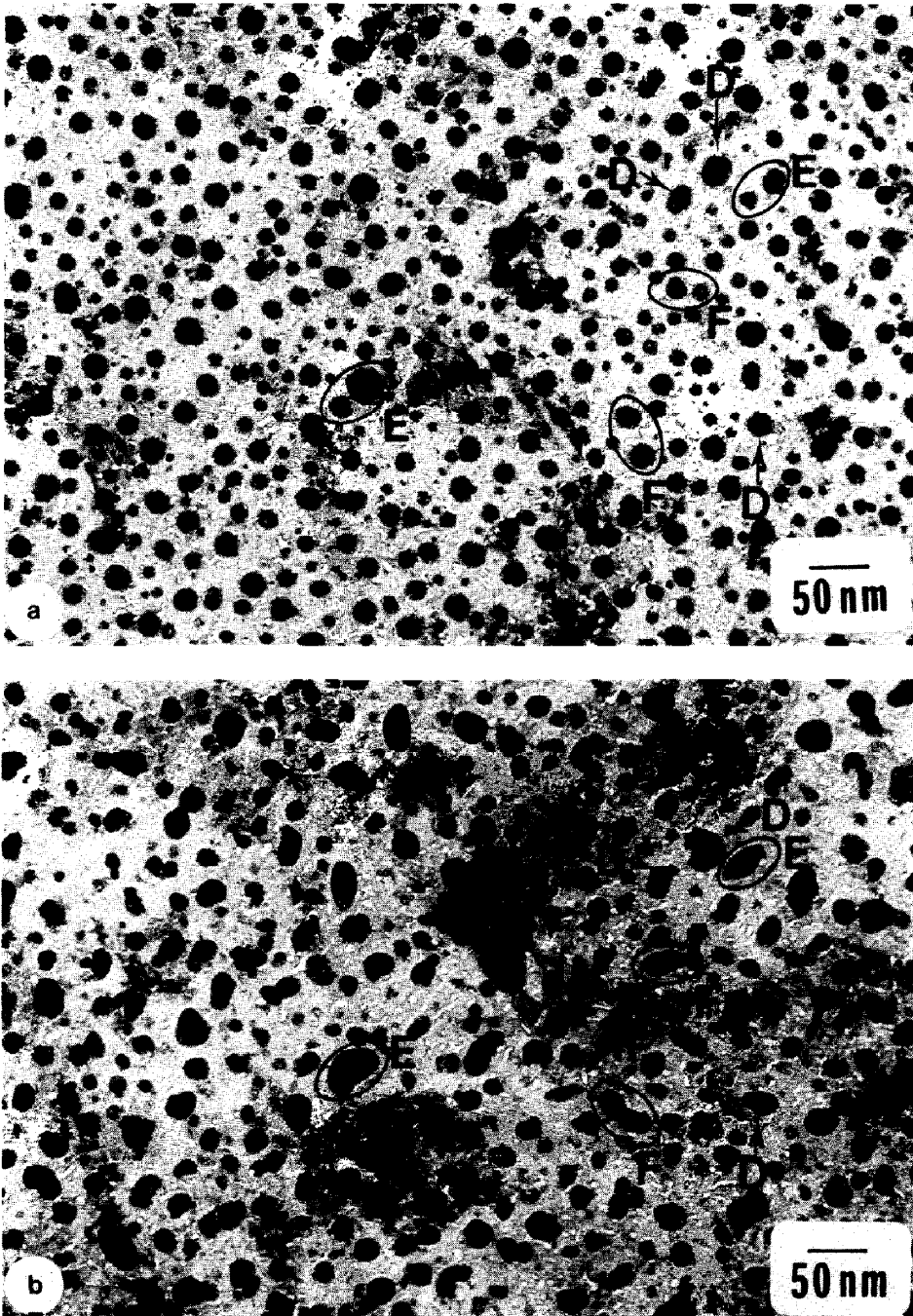


FIG. 4. Sequence of changes on heating a Co/Al<sub>2</sub>O<sub>3</sub> specimen in methane at 700°C. (a) 10 h (5 h at 500°C and 5 h at 700°C) H<sub>2</sub>; (b) 0.5 h CH<sub>4</sub>; (c) 15 h CH<sub>4</sub>; (d) 2 h H<sub>2</sub>.

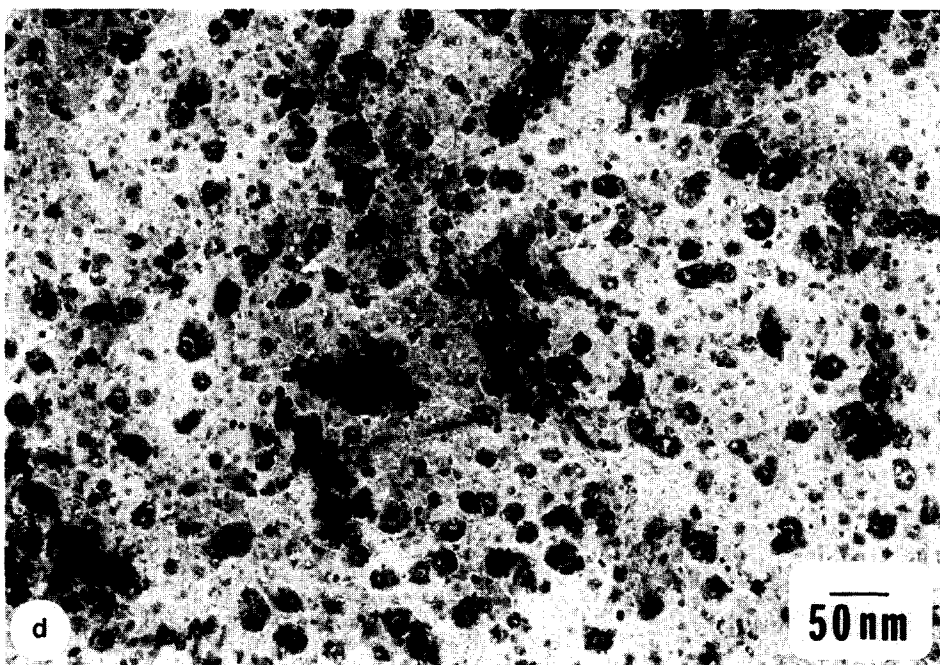
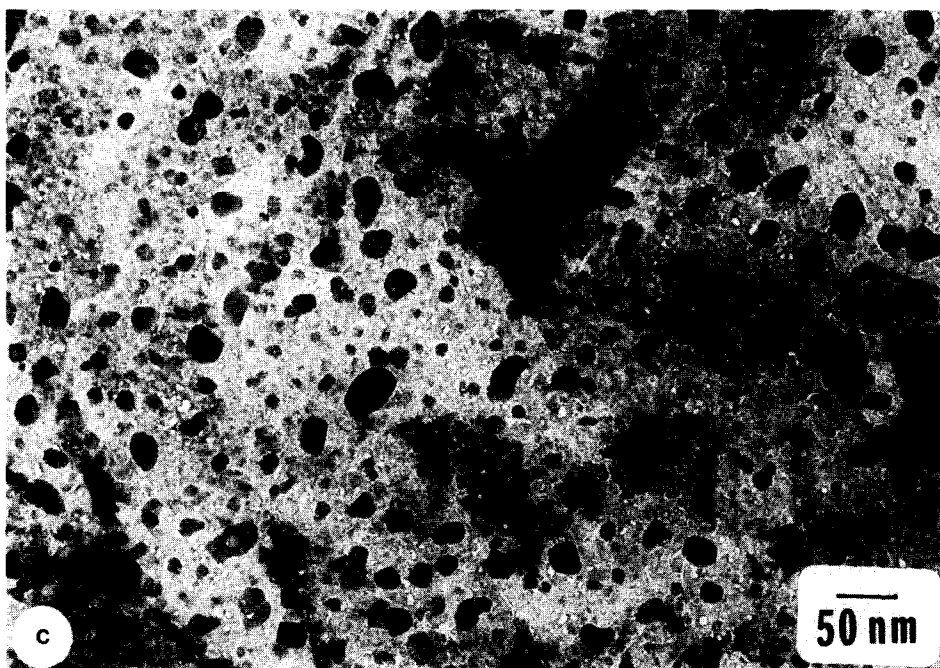


FIG. 4—Continued.

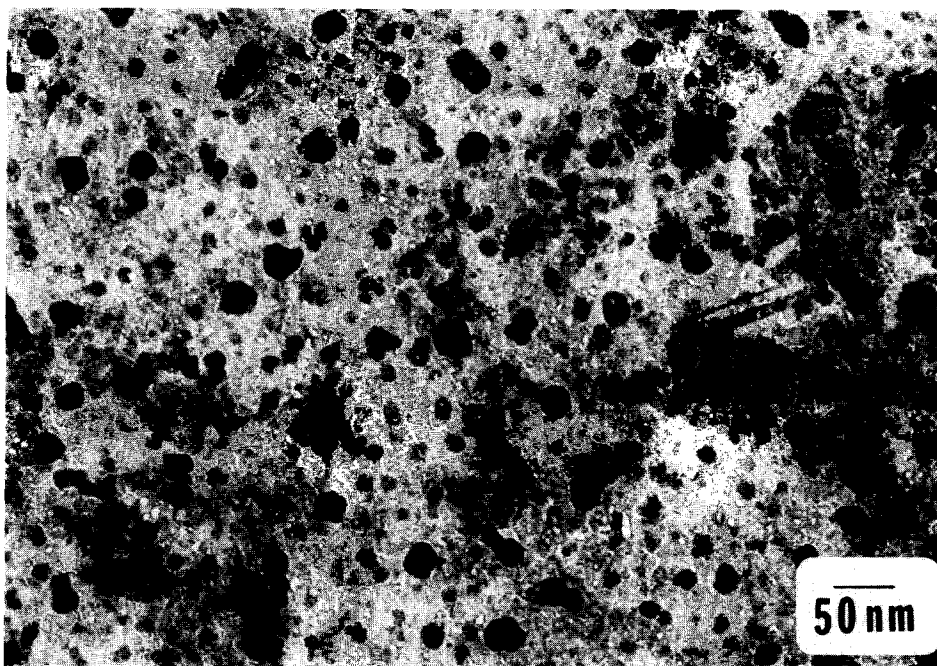


FIG. 5. Co/Al<sub>2</sub>O<sub>3</sub> specimen after heating in CH<sub>4</sub> for 15 h continuously at 700°C following heating in H<sub>2</sub> for 10 h (5 h at 500°C and 5 h at 700°C).

and contracted to form small particles as suggested and explained in Ref. (19). A specimen which was heated continuously in CH<sub>4</sub> for 15 h (Fig. 5) provided results similar to those observed on heating in several steps for the same length of time (Fig. 4c).

### C. Fe/Al<sub>2</sub>O<sub>3</sub>

Figures 6a–6e show the micrographs of a specimen which had a 7.5-Å-thick initial loading. The initial particles were generated on heating in H<sub>2</sub> for 5 h at 500°C and an additional 5 h at 700°C (Fig. 6a).  $\alpha$ -Fe and  $\gamma$ -Fe<sub>2</sub>O<sub>3</sub> (or Fe<sub>3</sub>O<sub>4</sub>) were identified in the electron diffraction pattern. (Since  $\gamma$ -Fe<sub>2</sub>O<sub>3</sub> and Fe<sub>3</sub>O<sub>4</sub> have the same lattice constant, one cannot differentiate between them in the electron diffraction pattern.) Upon heating in CH<sub>4</sub> for 20 min, some particles extended (Fig. 6b), and other particles disappeared, leaving sometimes small remnant particles, most likely as a result of their

spreading out as thin films undetectable by electron microscopy. After a total of 2 h of heating in CH<sub>4</sub>, most of the particles increased in size (Fig. 6c). They continued to grow, acquiring more elongated or disordered shapes, on additional heating in several steps, for up to 15 h (Fig. 6d). The growth of the particles was, most likely, a result of carbon deposition around and on the particles. The specimen was subsequently heated in H<sub>2</sub>. After 1 h of heating in H<sub>2</sub> (Fig. 6e), most of the particles decreased in size, probably because of the gasification of carbon. Figures 7a–7c provide information about a 15-Å loading specimen on heating in CH<sub>4</sub>. Its behavior was quite similar to that of the 7.5-Å loading. Figure 7a shows the initial particles which were formed after heating in H<sub>2</sub> for 5 h at 500°C and 5 additional hours at 700°C.  $\alpha$ -Fe and  $\gamma$ -Fe<sub>2</sub>O<sub>3</sub> (or Fe<sub>3</sub>O<sub>4</sub>) were detected in the electron diffraction pattern. Upon heating in CH<sub>4</sub> for 1.5 h, large patches of irregular

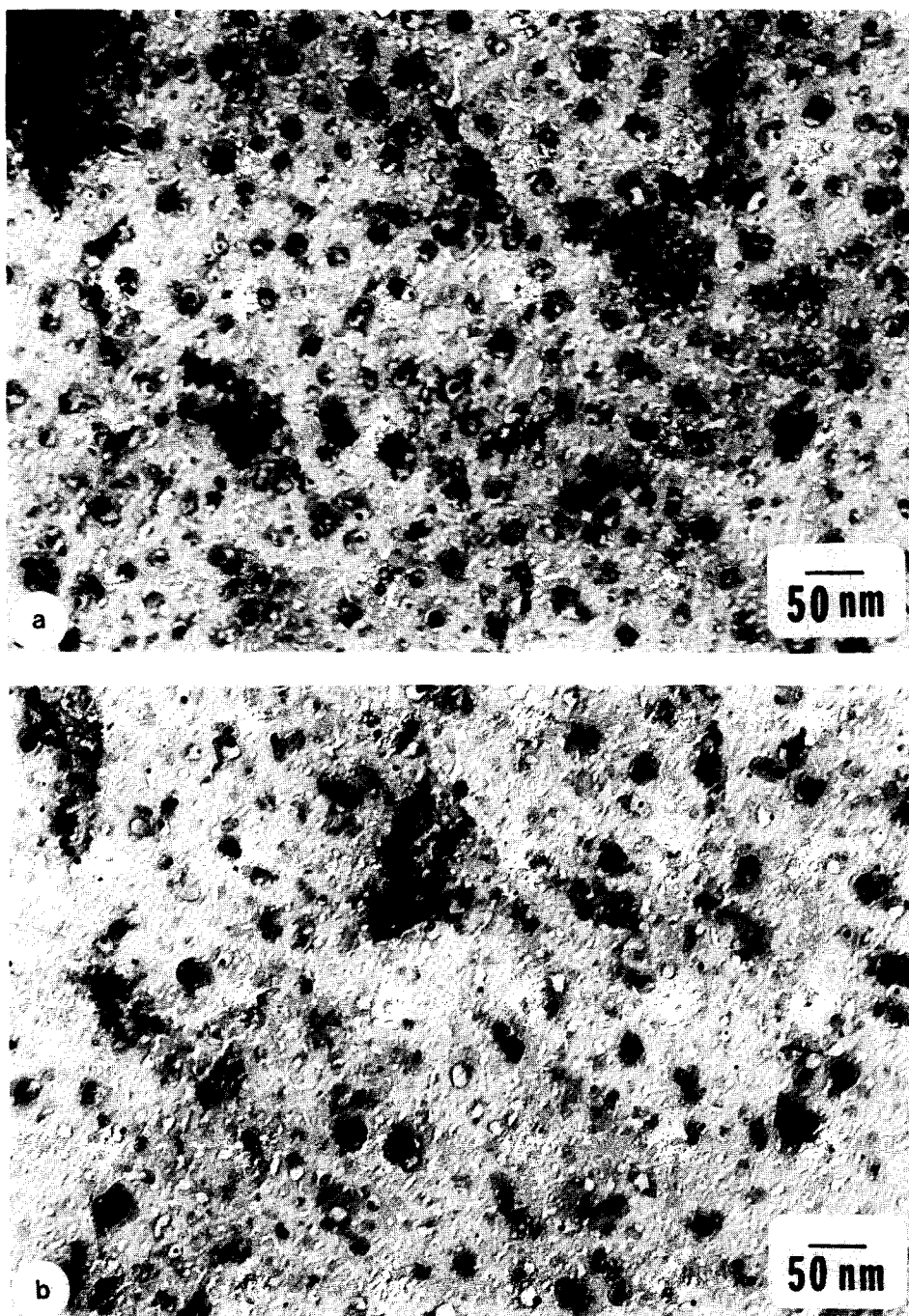


FIG. 6. Sequence of changes on heating a 7.5-Å loading Fe/Al<sub>2</sub>O<sub>3</sub> specimen in methane at 700°C. (a) 10 h (5 h at 500°C and 5 h at 700°C) H<sub>2</sub>; (b) 20 min CH<sub>4</sub>; (c) 2 h CH<sub>4</sub>; (d) 15 h CH<sub>4</sub>; (e) 1 h H<sub>2</sub>.

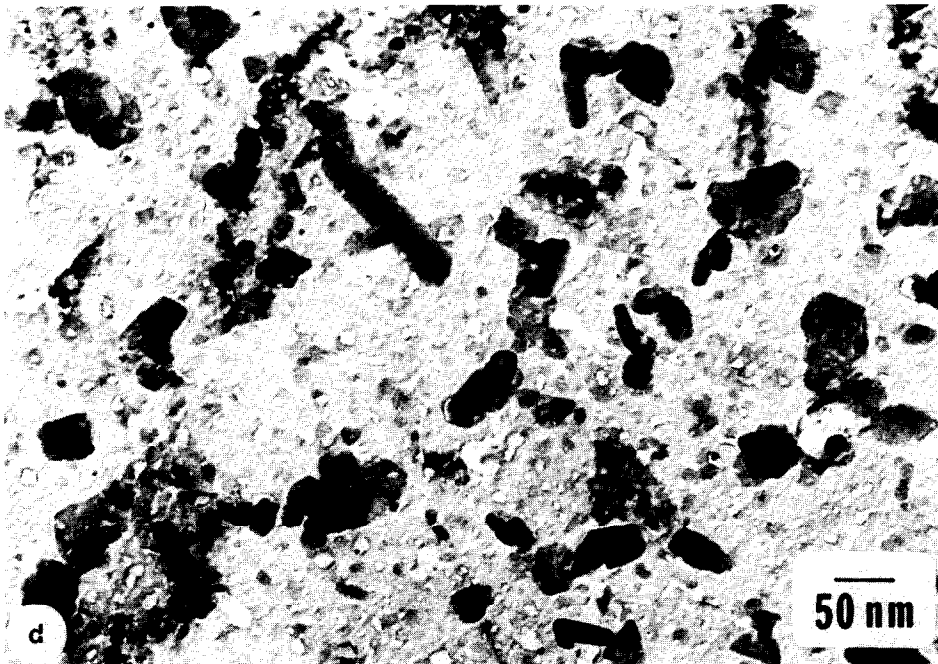
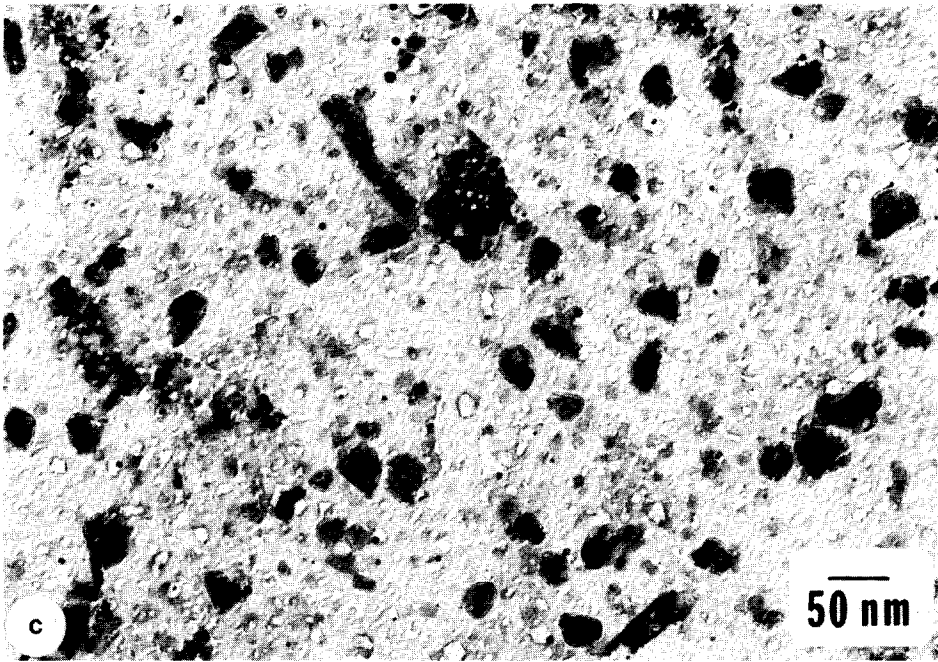


FIG. 6—Continued.

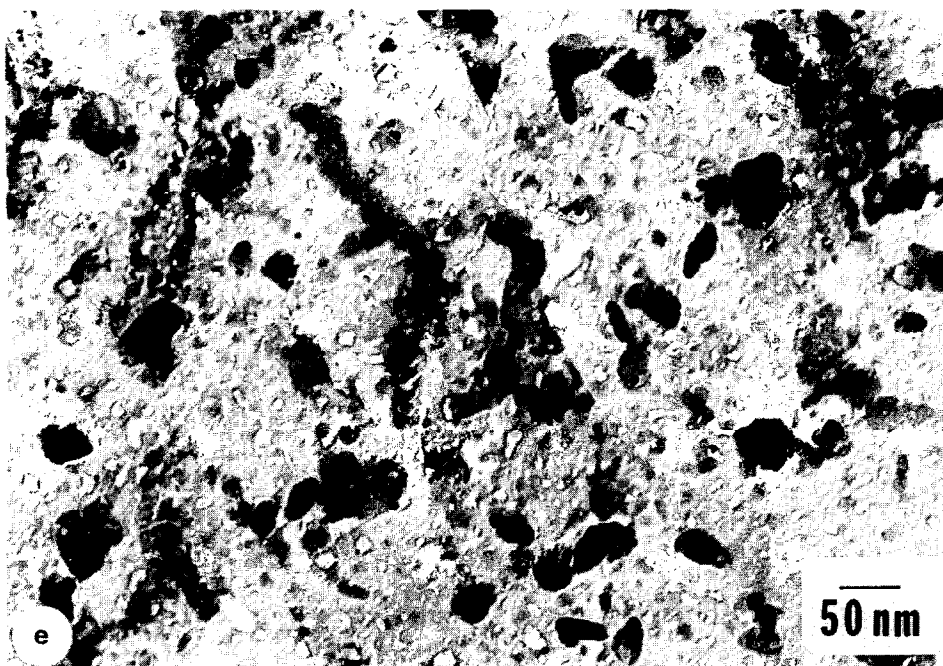


FIG. 6—Continued.

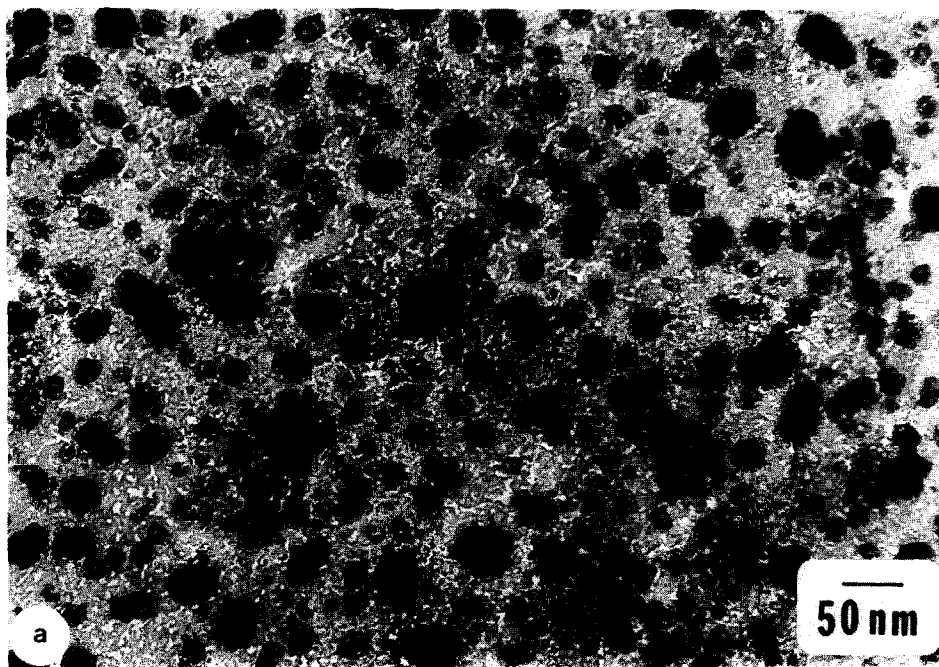


FIG. 7. Sequence of changes on heating a 15-Å loading Fe/Al<sub>2</sub>O<sub>3</sub> specimen in methane at 700°C. (a) 10 h (5 h at 500°C and 5 h at 700°C) H<sub>2</sub>; (b) 1.5 h CH<sub>4</sub>; (c) 14.5 h CH<sub>4</sub>.

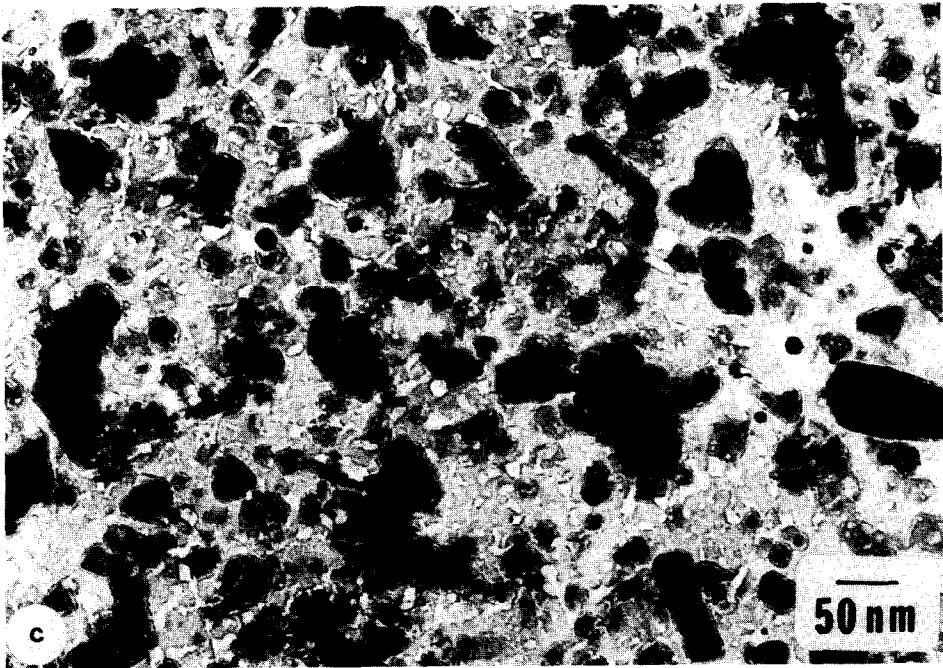
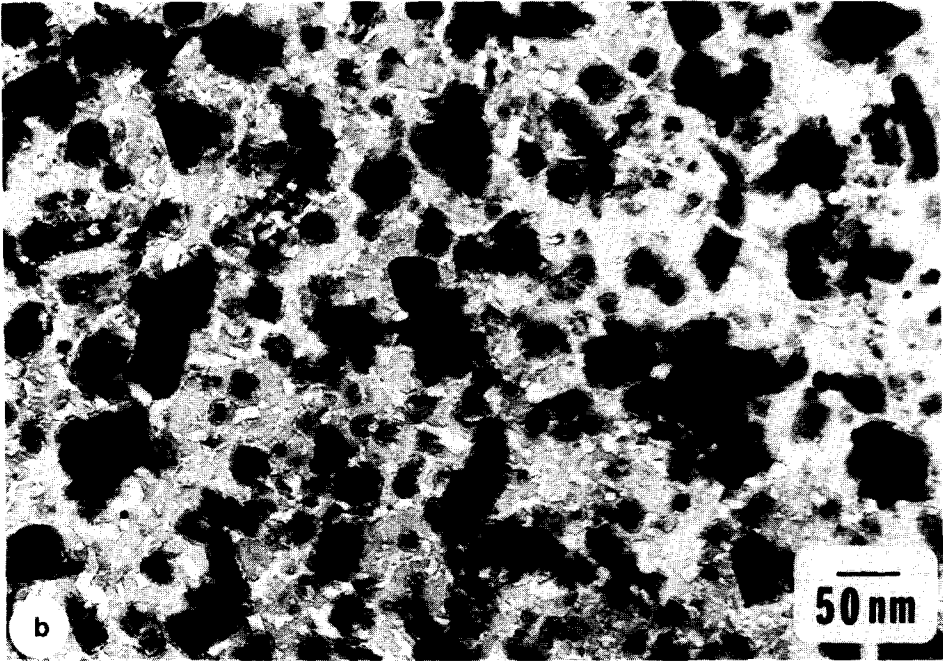


FIG. 7—Continued.



shape appeared (Fig. 7b). Coke was probably deposited around and on the particles, and/or carbon films interconnected neighboring particles, thus generating large patches. One may also note that some particles became elongated. In the electron diffraction pattern,  $\gamma$ - $\text{Fe}_2\text{O}_3$  (or  $\text{Fe}_3\text{O}_4$ ) was identified, indicating that most of the particles were oxidized probably because of the impurities, such as  $\text{O}_2$  and moisture, present in  $\text{CH}_4$ . The heating in  $\text{CH}_4$  for a total of 14.5 h (Fig. 7c) led to the growth of carbonaceous films around the particle and also to the formation of filaments, most likely composed of  $\gamma$ - $\text{Fe}_2\text{O}_3$  ( $\text{Fe}_3\text{O}_4$ ) and carbon deposits. It is worth noting that the filaments are straight and do not have a thick particle at their tip; in contrast, the filaments encountered in the case of  $\text{Ni}/\text{Al}_2\text{O}_3$  were not straight and did have a thick particle at their leading tip. In Fig. 7c, the particles are probably entirely covered by carbonaceous films and therefore their activity is expected to be extremely reduced. Indeed,

there was very little change on further heating for up to 19 h.

Another 15-Å loading specimen was heated continuously in  $\text{CH}_4$  for 20 h (Fig. 8). The obtained micrograph was very similar to that obtained after heating in several steps for the same length of time, indicating that repeated exposure to air had no significant effect on the morphology of the particles.

The specimen whose micrographs are given in Figs. 7 was further heated in various atmospheres. The micrographs given in Figs. 9a–9e represent a different area of the specimen. Figure 9a represents that area, after heating in  $\text{CH}_4$  for 19 h, and shows elongated and irregular particles which, very likely, contain carbon in addition to crystallite material. Electron diffraction indicated the presence of  $\gamma$ - $\text{Fe}_2\text{O}_3$  ( $\text{Fe}_3\text{O}_4$ ). On subsequent heating in  $\text{H}_2$  for 6 h, the carbon was gasified, and the filaments retracted to more globular shapes, leaving traces on the substrate (Fig. 9b). The contracted par-



FIG. 8.  $\text{Fe}/\text{Al}_2\text{O}_3$  specimen after heating in  $\text{CH}_4$  for 20 h continuously at  $700^\circ\text{C}$ , following heating in  $\text{H}_2$  for 10 h (5 h at  $500^\circ\text{C}$  and 5 h at  $700^\circ\text{C}$ ).

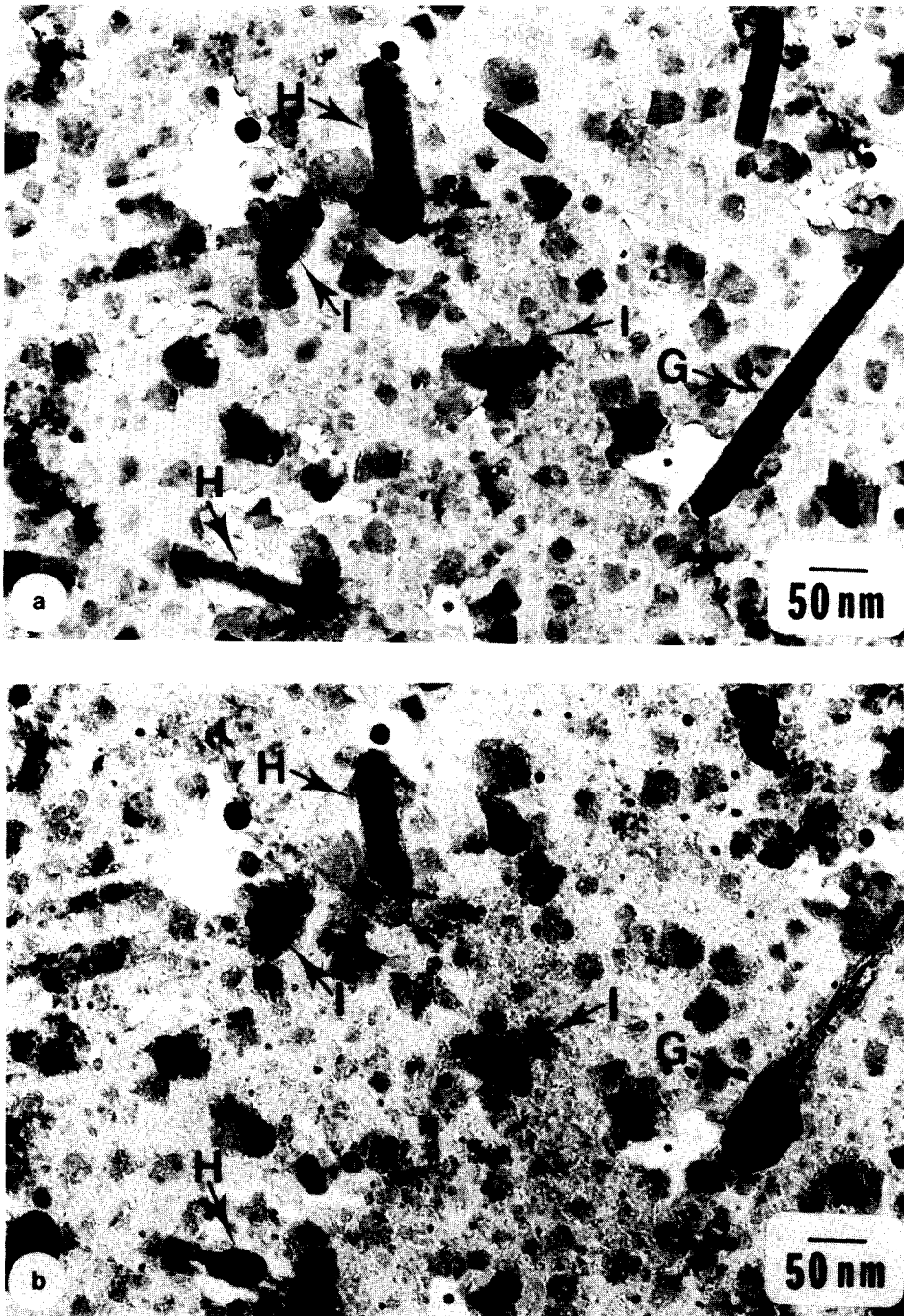


FIG. 9. Sequence of changes on heating the specimen of Fig. 7. The region shown here is different from that of Fig. 7. (a) 19 h  $\text{CH}_4$ ; (b) 6 h  $\text{H}_2$ ; (c) 2 h steam; (d) 4 h  $\text{H}_2$ ; (e) 1 h  $\text{CH}_4$ .

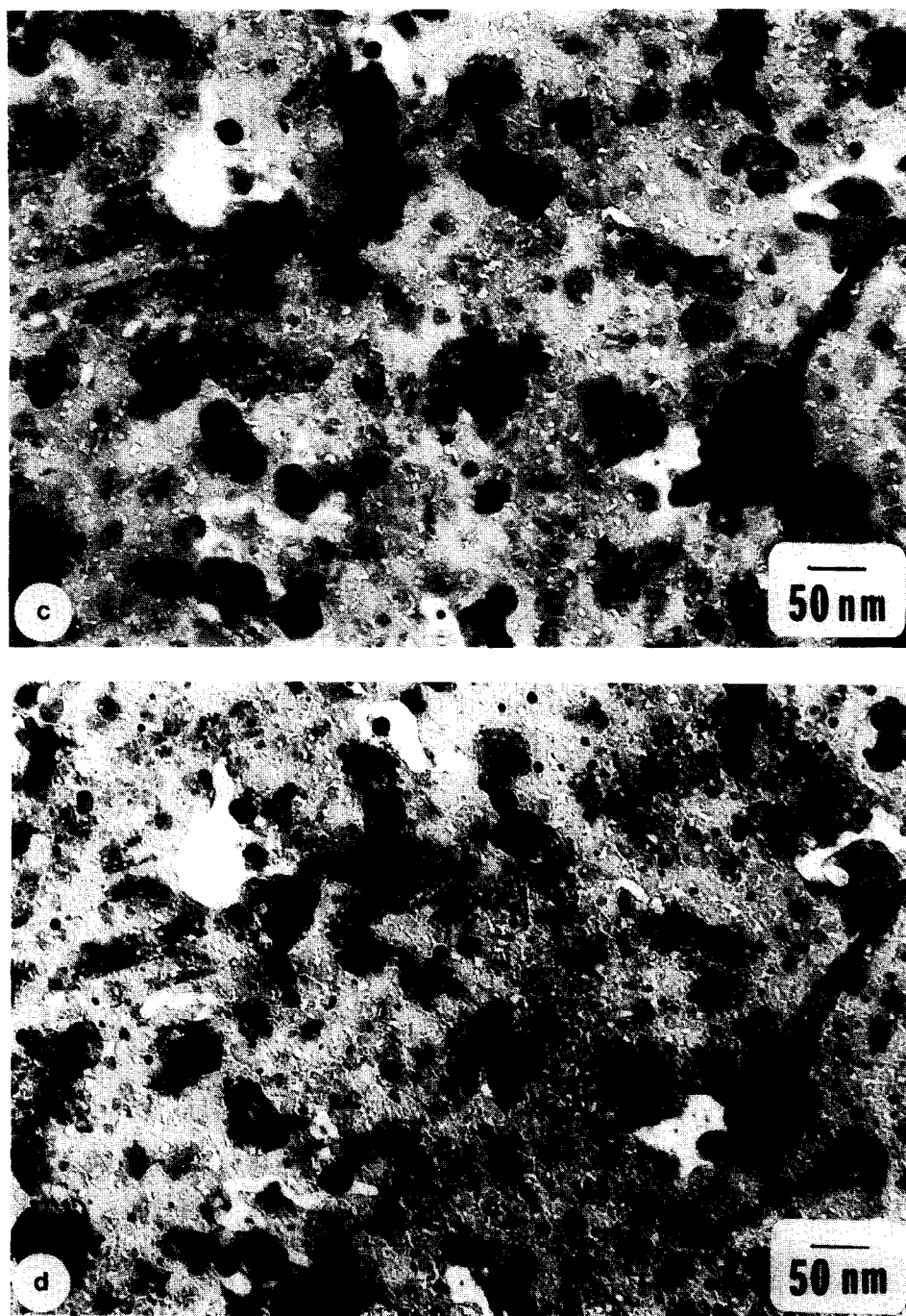


FIG. 9—Continued.

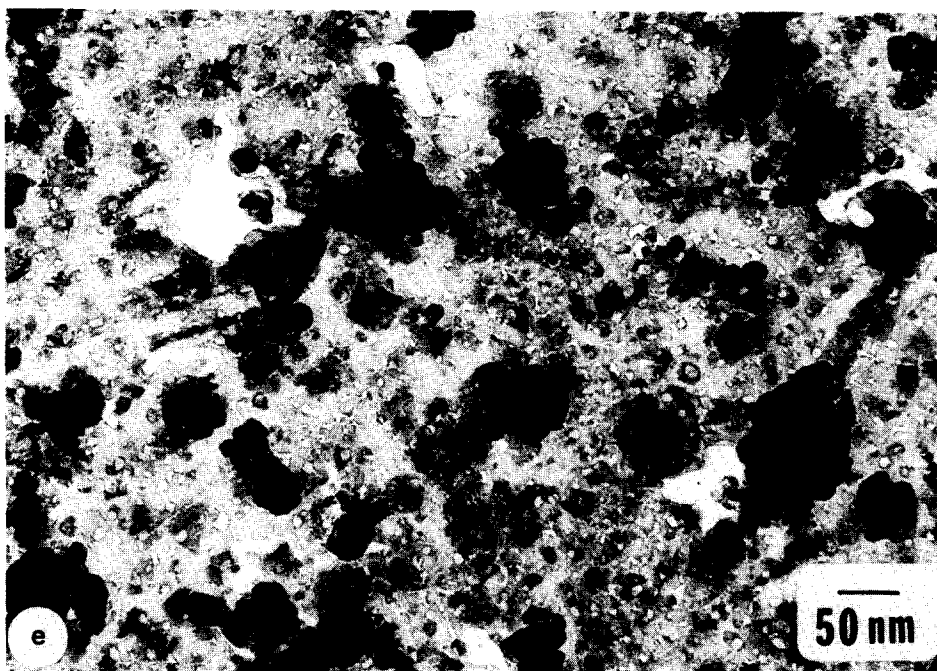


FIG. 9—Continued.

ticles were in some cases located at one of the ends of the previous filaments (G) and in other cases in their middle (H). Some of the irregular particles contracted to form thick small particles having films beneath them (I).  $\alpha$ -Fe was detected by electron diffraction. The bottom films were probably ungasified carbon and/or partially reduced or unreduced  $\gamma$ -Fe<sub>2</sub>O<sub>3</sub> (Fe<sub>3</sub>O<sub>4</sub>). In addition, many small new particles appeared on the substrate, most probably because the undetectable  $\gamma$ -Fe<sub>2</sub>O<sub>3</sub> (Fe<sub>3</sub>O<sub>4</sub>) films which spread out during heating in CH<sub>4</sub> ruptured and contracted to form particles after their reduction to  $\alpha$ -Fe. In order to verify whether the bottom films and the remnant traces remaining after the filament contraction were carbonaceous deposits, the specimen was heated in steam for 2 h (Fig. 9c). As shown in the micrograph, the films and the remnant traces did not disappear, indicating that they were composed mostly of iron or iron oxides. One may note that the thick particles extended on the substrate.

$\gamma$ -Fe<sub>2</sub>O<sub>3</sub> (Fe<sub>3</sub>O<sub>4</sub>) was detected in the electron diffraction pattern. On subsequent heating in H<sub>2</sub> for 4 h, the particles contracted (Fig. 9d). Further, the specimen was once again heated in CH<sub>4</sub>. On heating for 1 h (Fig. 9e) the particles extended; it was however little change on additional heating for up to 5 h. One may note that the filamentous structures, which were identified on the fresh specimen, have no longer appeared.

## 2. HEATING IN CH<sub>4</sub> + STEAM

### A. Ni/Al<sub>2</sub>O<sub>3</sub>

First, the specimen was heated in H<sub>2</sub> for 10 h, 5 h at 500°C and another 5 h at 700°C (Fig. 10a). The specimen was further heated in CH<sub>4</sub> + steam for 20 min at 700°C (Fig. 10b). The micrograph shows that most of the particles extended over the substrate as thin patches having small particles at one of the corners. Some particles acquired an elongated filamentous shape (J in Fig. 10b).

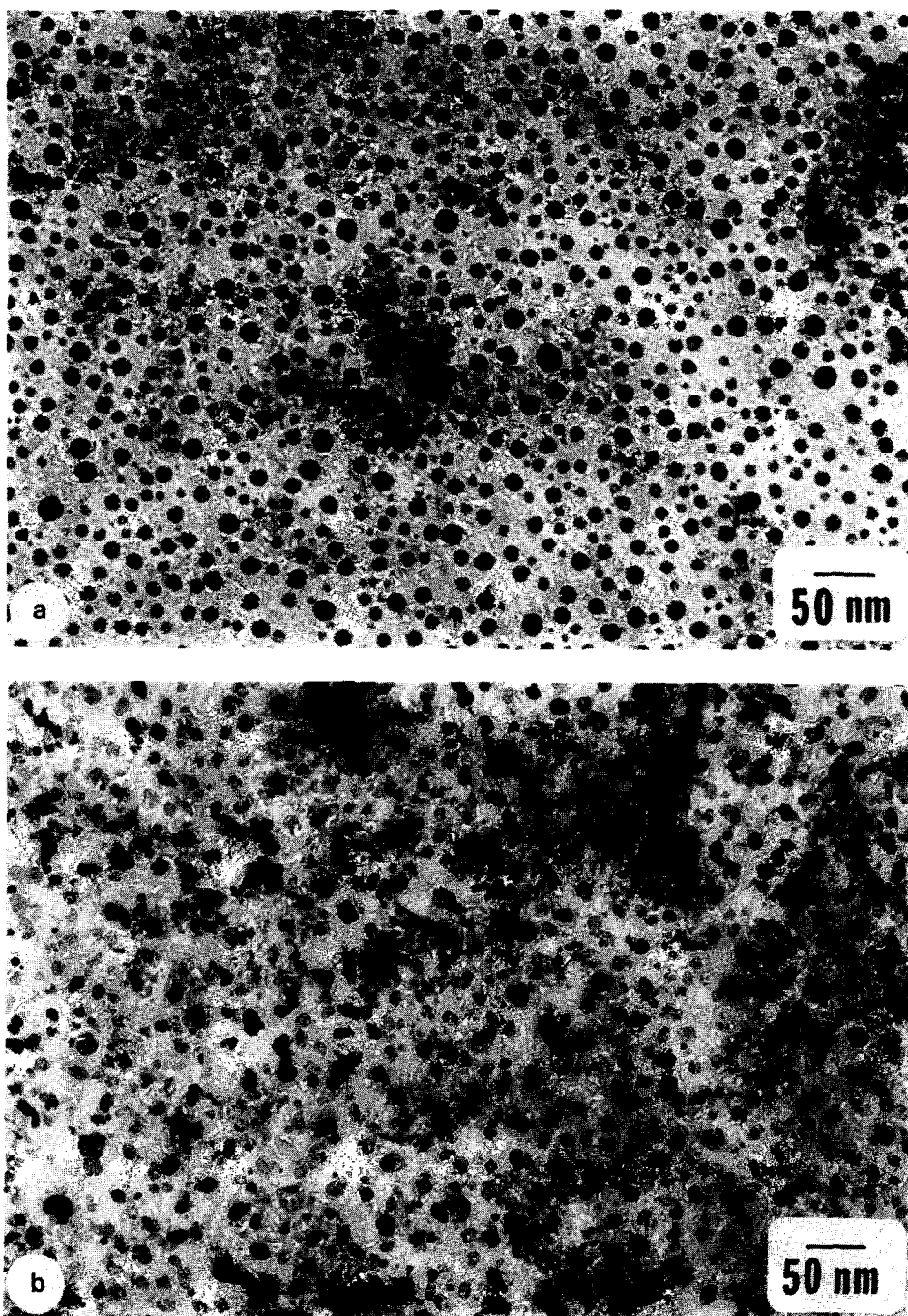


FIG. 10. Sequence of changes on heating a Ni/Al<sub>2</sub>O<sub>3</sub> specimen in methane plus steam at 700°C. (a) 10 h (5 h at 500°C and 5 h at 700°C) H<sub>2</sub>; (b) 20 min CH<sub>4</sub> + steam; (c) 1 h CH<sub>4</sub> + steam; (d) 2 h CH<sub>4</sub> + steam (the specimen was heated for additional 3 h in CH<sub>4</sub> + steam after the heat treatment (d)); (e) 2 h H<sub>2</sub>; (f) 1 h CH<sub>4</sub> + steam.

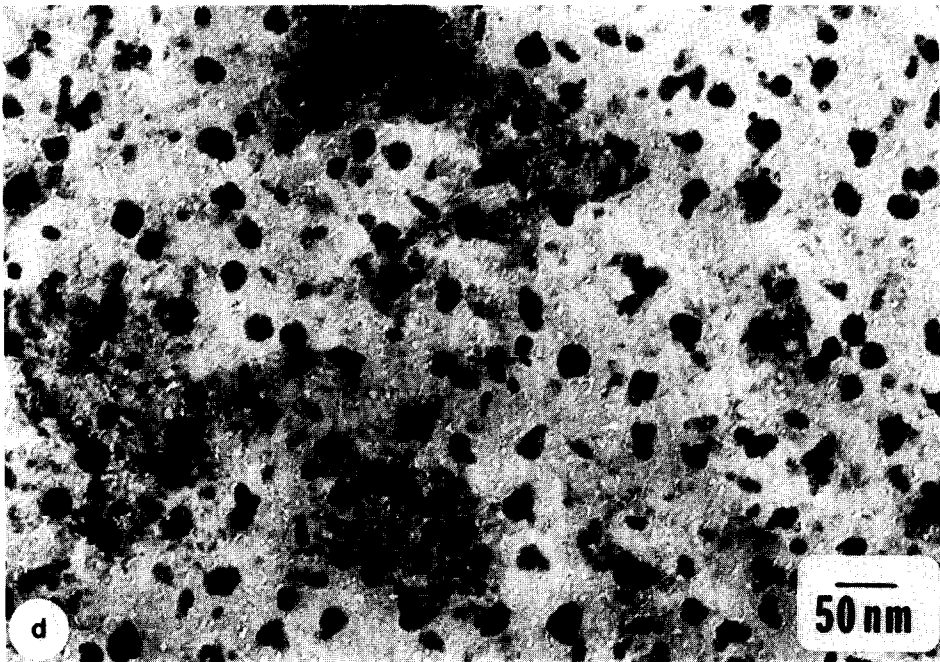
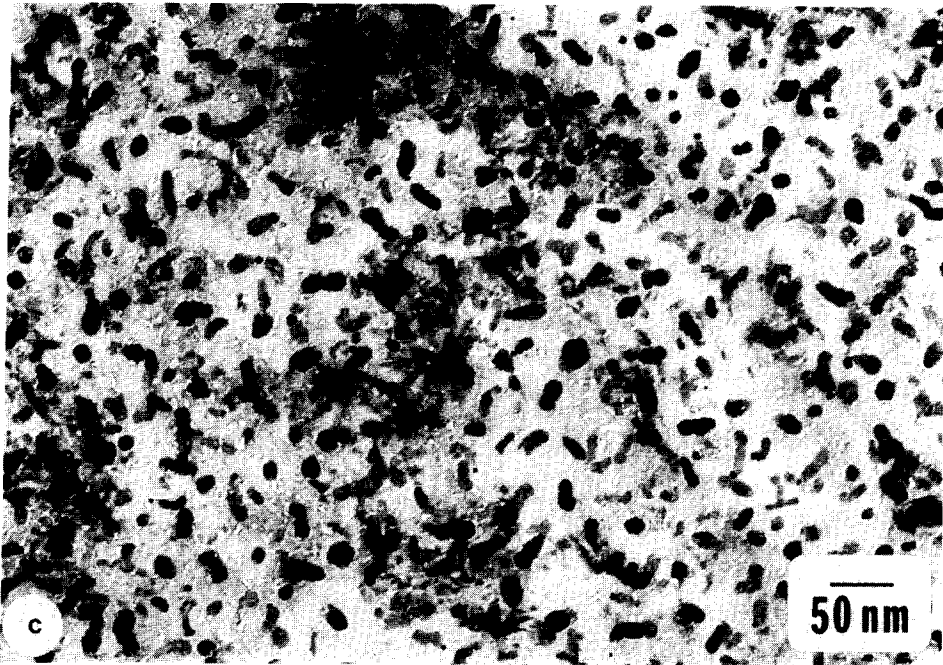


FIG. 10—Continued.

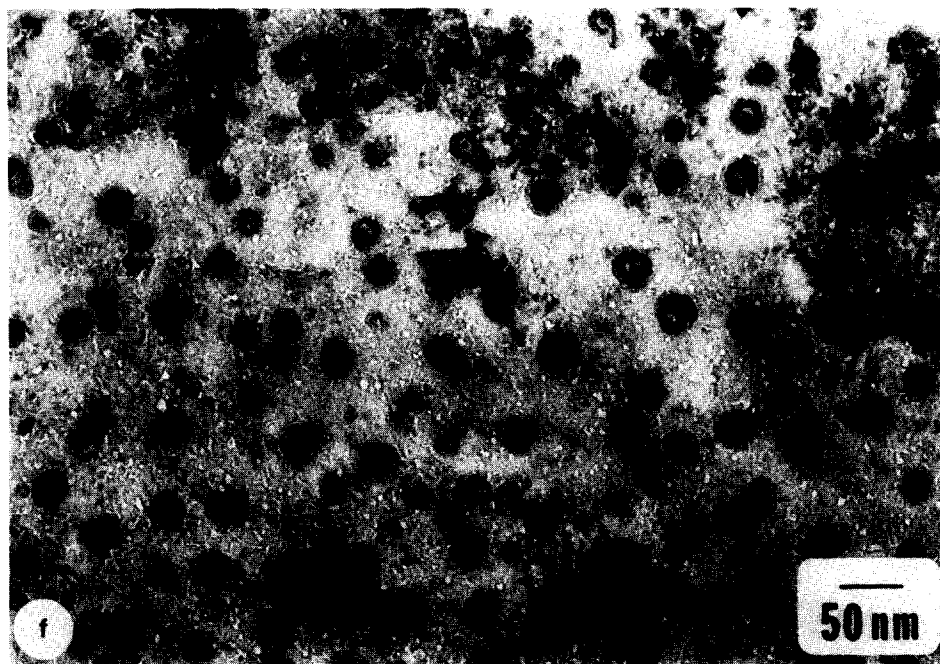
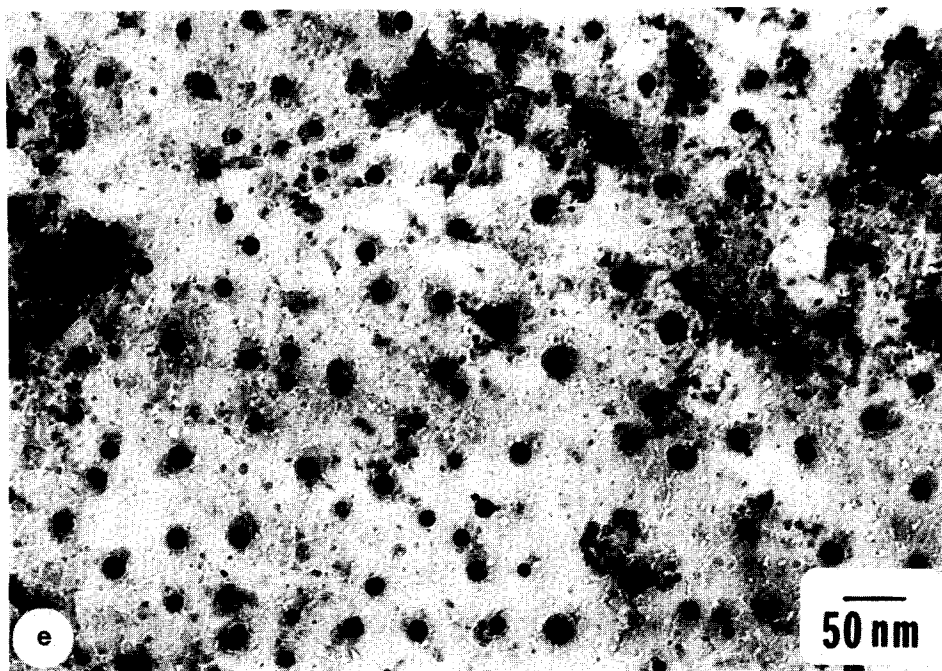


FIG. 10—Continued.

NiO was detected by electron diffraction. On further heating in  $\text{CH}_4 + \text{steam}$  for 40 more min, most of the particles acquired short filamentous shapes (Fig. 10c). Some of the filaments had a dense particle at their tip, while others did not. This suggests that, as in the  $\text{CH}_4$  atmosphere, the nickel particles transformed into filaments by depositing material behind them on the substrate during their migration. The electron diffraction pattern indicated NiO as the major component. Perhaps, the filaments contain also some carbon; this compound could not, however, be detected by electron diffraction. Compared to the filaments produced during heating in  $\text{CH}_4$ , the present ones are shorter. In addition, the number of filaments is smaller than the number of particles present before the last heat treatment (compare Figs. 10b and 10c). On further heating for 1 more hour, the filamentous particles changed their shape, becoming more irregular, and their number decreased (Fig. 10d). This indicates that the particles had relatively high mobilities on the substrate and coalesced. This probably happened because of the gasification by steam of the carbon deposits; the resulting gas lifted the particles, displacing them over the substrate. After the particles were heated for an additional 3 h, very little change occurred. After heating in  $\text{CH}_4 + \text{H}_2\text{O}$ , the specimen was heated in  $\text{H}_2$  for 2 h at  $700^\circ\text{C}$ . The result is shown in Fig. 10e. The particles contracted and, in addition, new very small particles appeared. This is a result of the reduction of NiO to Ni, which was detected by electron diffraction. The small particles were formed by the rupture of the undetectable films, which spread out over the substrate during heating in  $\text{CH}_4 + \text{steam}$ , and the subsequent contraction of the resulting patches. The specimen was heated again in  $\text{CH}_4 + \text{steam}$ , but the results were different from those of the previous heating in  $\text{CH}_4 + \text{steam}$ . After heating for 1 h, the shape of the particles changed to a torus which contained a core particle in the cavity (Fig. 10f). The outside

diameter of the torus was larger than that of the particle before heating. This indicates that the change in shape is associated with the extension of the particles on the substrate. Electron diffraction indicated the presence of NiO. This (torus and core) structure is very similar to that observed upon heating  $\text{Ni}/\text{Al}_2\text{O}_3$  in  $\text{O}_2$  at  $500^\circ\text{C}$  (20). On heating for 3 additional hours in  $\text{CH}_4 + \text{steam}$ , little change occurred and no filaments were formed. This indicates that, in these circumstances, carbon was not deposited, probably because the catalyst has lost its catalytic activity for methane decomposition.

### B. $\text{Co}/\text{Al}_2\text{O}_3$

Figure 11a represents the initial state after heating in  $\text{H}_2$ . Electron diffraction indicated the presence of  $\alpha\text{-Co}$ . After heating in  $\text{CH}_4 + \text{steam}$  for 30 min, some particles extended on the substrate (L in Fig. 11b) and other smaller particles (M) decreased in size, most likely because of the spreading out from them of thin films undetectable by electron microscopy. Electron diffraction indicated that the particles contained mostly CoO. This suggests that the extension of the particles is associated with their oxidation. One may note that some particles are composed of one or several small and dark particles located on the top or on the edge of an extended patch (N1 in Fig. 11b). Some of these dark particles moved away from the main body (N2 in Fig. 11b). On further heating for up to 2 h, most of the particles decreased in size (Fig. 11c), becoming thinner, either because of the emission of thin undetectable films, or because of the loss of material to the substrate or to the gas stream. In addition, large patches (O) appeared in a few regions as a result of either extension and subsequent interconnection of neighboring particles and/or more likely because of carbon deposition. After heating for 1.5 more hours, a large amount of material was lost from the large patches (O in Fig. 11d), while most of the particles remained unchanged.



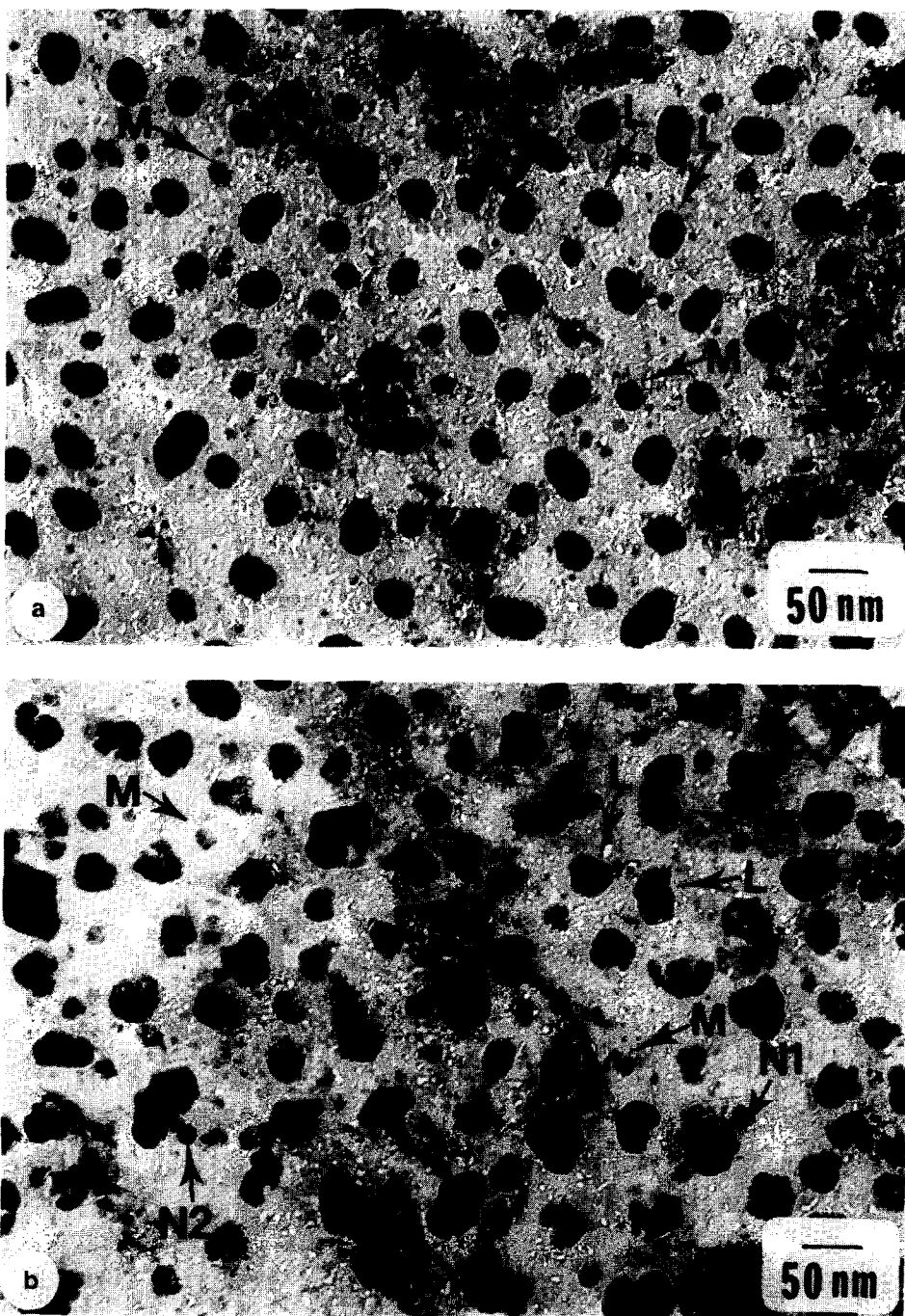


FIG. 11. Sequence of changes on heating a  $\text{Co}/\text{Al}_2\text{O}_3$  specimen in methane plus steam at  $700^\circ\text{C}$ . (a) 10 h (5 h at  $500^\circ\text{C}$  and 5 h at  $700^\circ\text{C}$ )  $\text{H}_2$ ; (b) 30 min  $\text{CH}_4$  + steam; (c) 2 h  $\text{CH}_4$  + steam; (d) 3.5 h  $\text{CH}_4$  + steam; (e) 1 h  $\text{H}_2$ .

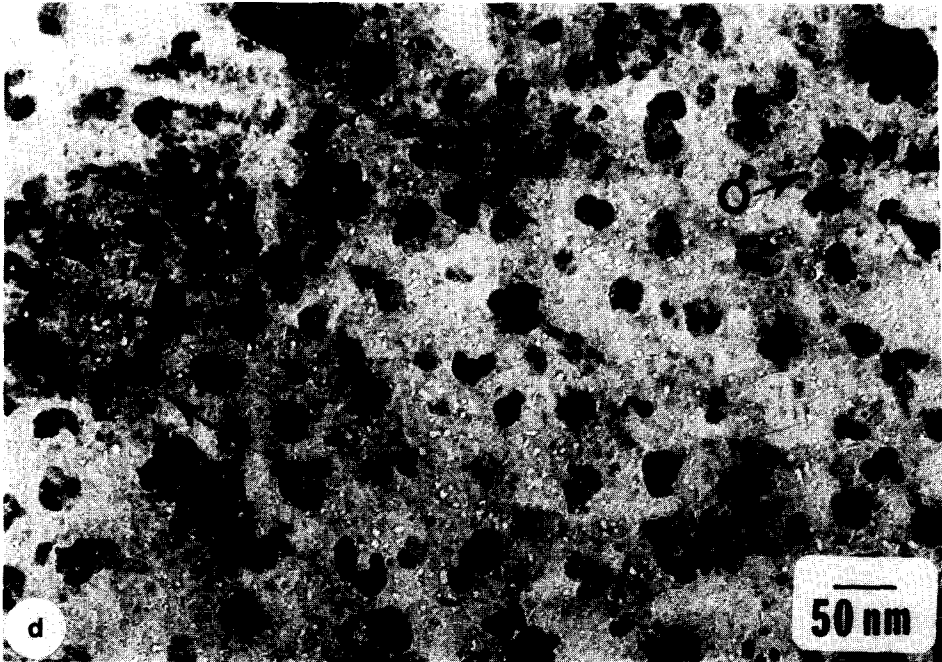
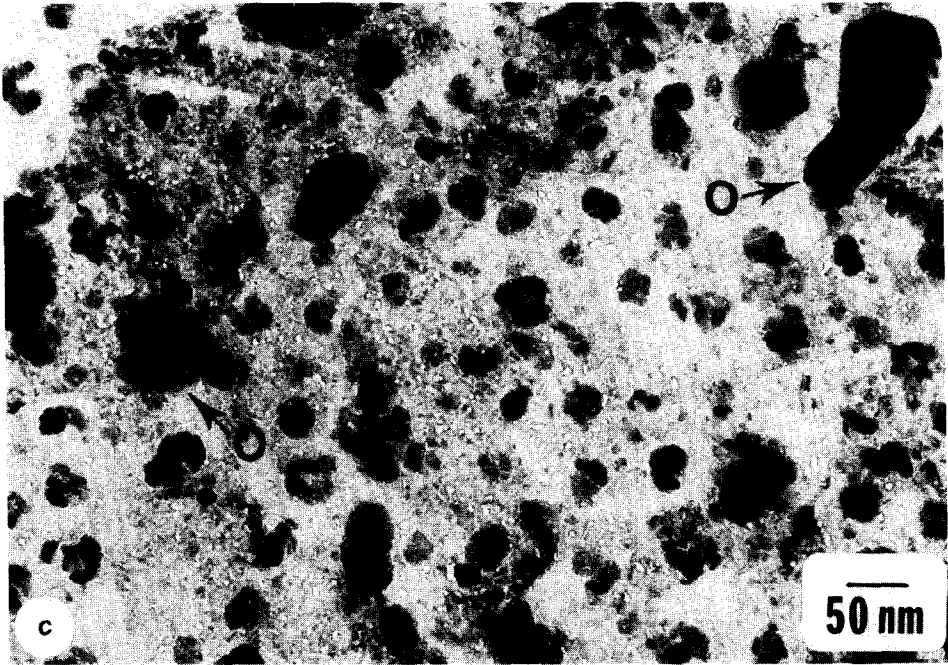


FIG. 11—Continued.

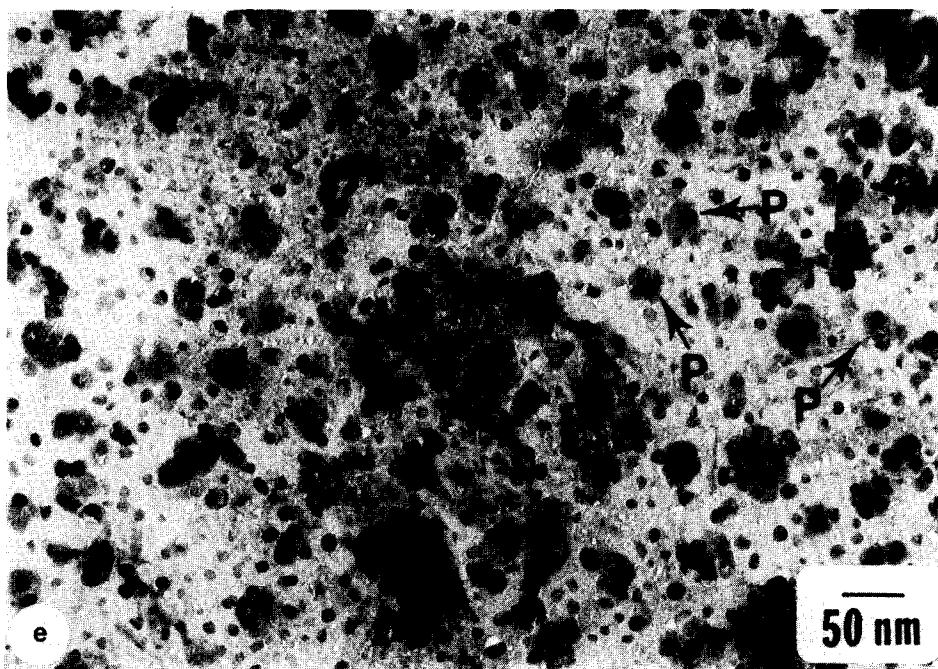


FIG. 11—Continued.

This suggests that the patches contained carbon deposits, which were subsequently gasified by steam. Further, the specimen was heated in  $H_2$  for 1 h (Fig. 11e). Some particles contracted and formed small thick particles on the top of thin extended patches (P in Fig. 11e). The electron diffraction patterns indicated the presence of  $\alpha$ -Co,  $Co_2O_3$ , and  $Co_3O_4$ . One may note again that many new particles appeared in regions where particles were not present before the heating in  $H_2$ . This is probably a result of the rupture of the undetectable films and the contraction of the resulting thin particles; it also indicates that most of the "lost material" from the particles remained on the substrate and was not permanently lost to the gas stream.

### C. $Fe/Al_2O_3$

After heating for 30 min in  $CH_4$  + steam, the shape of the particles of Fig. 12a changed to a torus with a small remnant particle in the cavity (Fig. 12b). The torus

and the core particle were interconnected by a film. Only  $\gamma$ - $Fe_2O_3$  (or  $Fe_3O_4$ ) was detected by electron diffraction. This indicates that the change in shape is associated with the oxidation of iron. Coke was also probably deposited around the particles, thus increasing their size, or the increase in size was a result of the extension of the particles. On further heating for up to 5 h, the cavities were filled, either because of the extension of the remnant particles and/or because of carbon deposition (Fig. 12c). After being heated in  $H_2$  for 2 h, the specimen was again heated in  $CH_4$  + steam. After heating for 1 h in  $CH_4$  + steam, in some of the particles a part, the small remnant particle in most of the cases, moved away from the main body, generating filamentous traces (Q in Fig. 12d). On heating for 3 additional hours, the growth of the filaments continued (Q in Fig. 12e). The leading particle, which was located at the tip of the filament, did not decrease in size, indicating, very likely, that the filament was

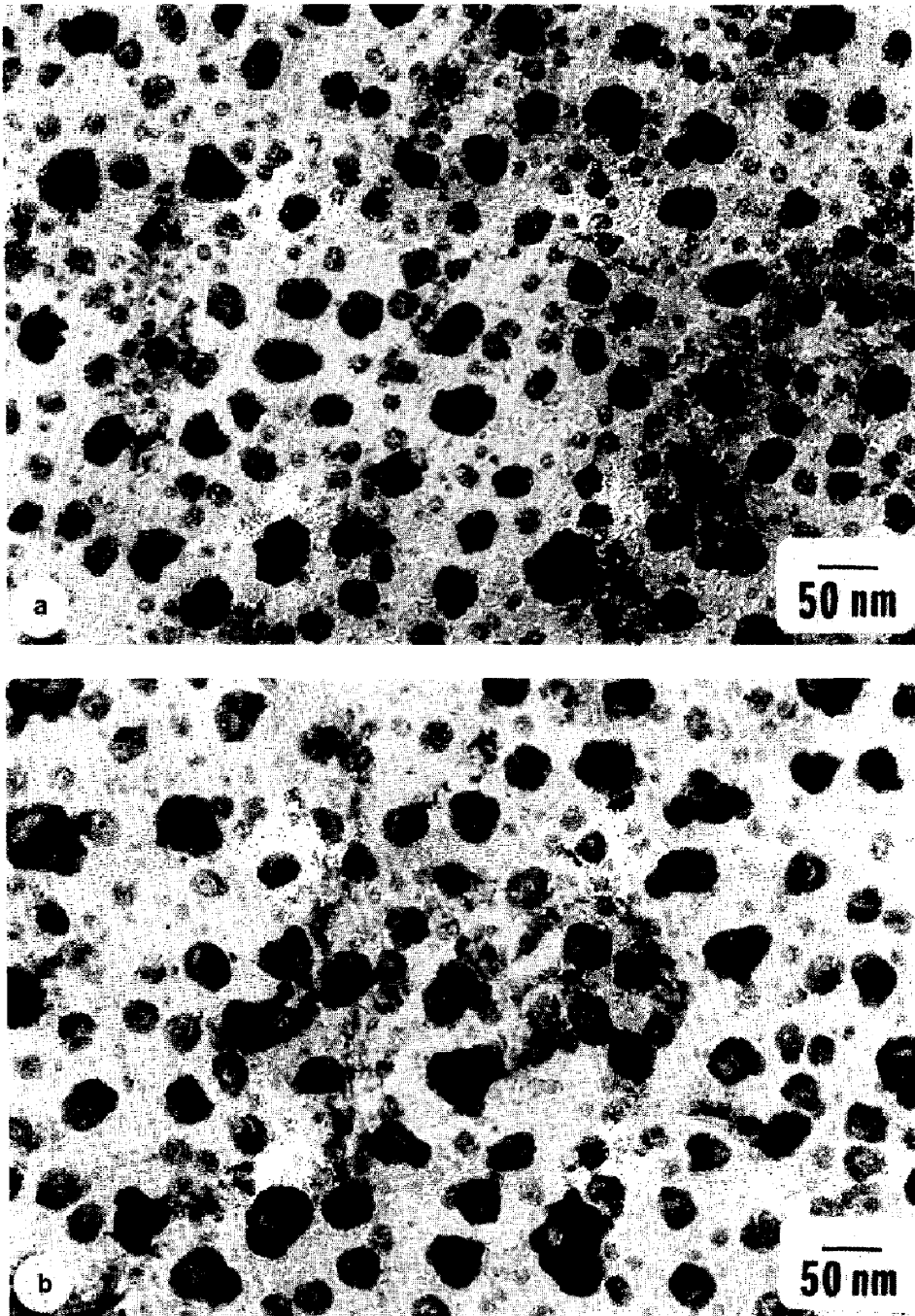


FIG. 12. Sequence of changes on heating a Fe/Al<sub>2</sub>O<sub>3</sub> specimen in methane plus steam at 700°C. (a) 10 h (5 h at 500°C and 5 h at 700°C) H<sub>2</sub>; (b) 30 min CH<sub>4</sub> + steam; (c) 5 h CH<sub>4</sub> + steam (the specimen was heated in H<sub>2</sub> for 2 h at 700°C between (c) and (d)); (d) 1 h CH<sub>4</sub> + steam; (e) 4 h CH<sub>4</sub> + steam.

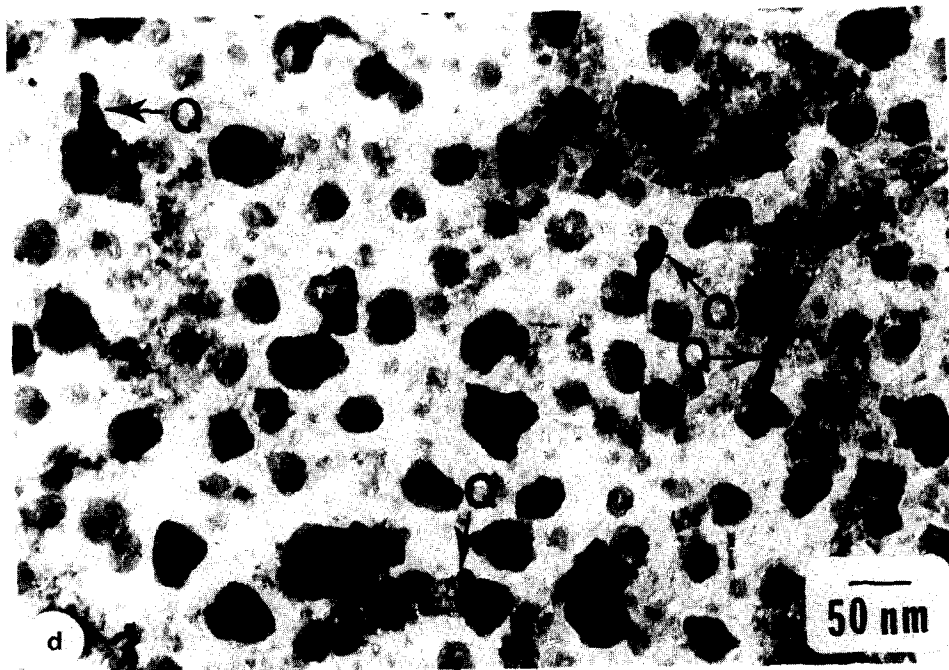
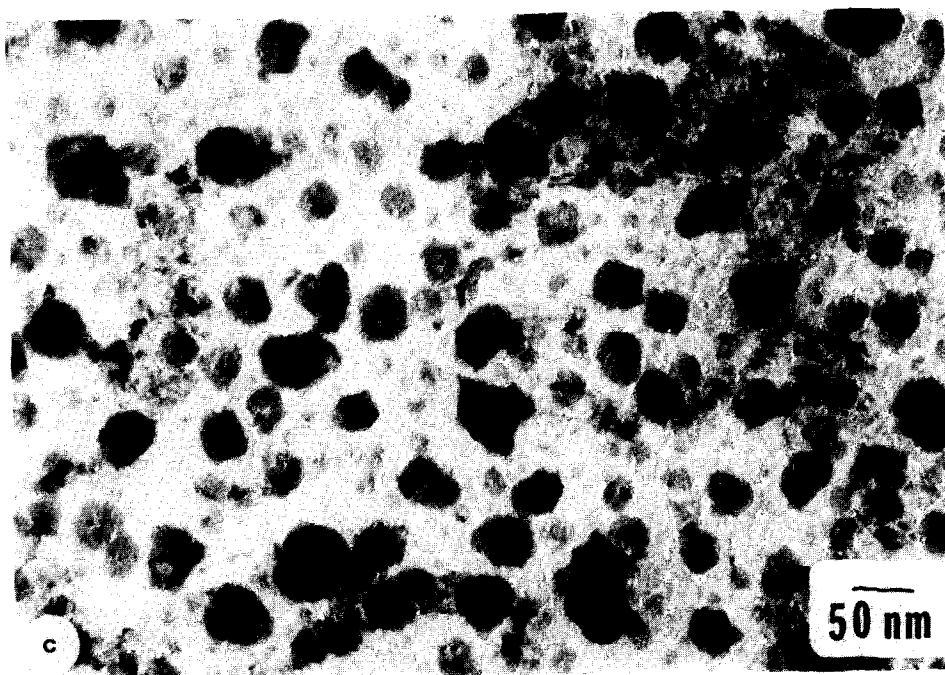


FIG. 12—Continued.

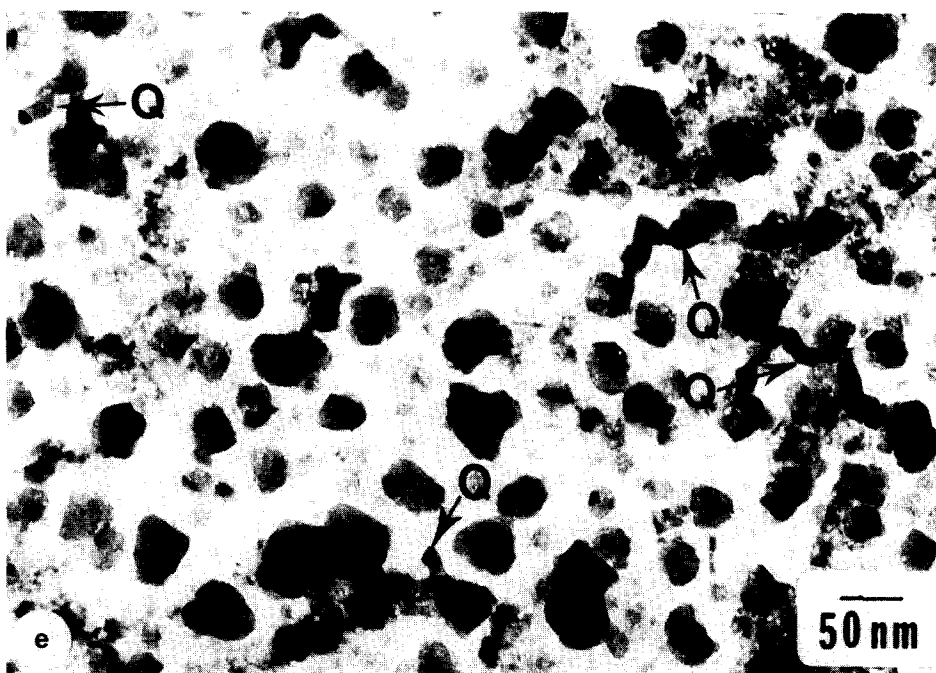


FIG. 12—Continued.

composed mostly of carbon. From this observation, one can infer that the heating of the coked specimen in  $H_2$  is more effective for the regeneration of  $Fe/Al_2O_3$  than of  $Ni/Al_2O_3$  for  $CH_4$  decomposition.

### 3. HEATING IN $CH_4 + STEAM + H_2$

#### A. $Ni/Al_2O_3$

As is well known, if the sample is heated in the individual components of the above gas mixture, the processes of sintering, coking, and redispersion are relatively slow. For instance, to increase the size of the particles by sintering from 60 to 120 Å, heating in hydrogen for more than 18 h (20) is needed; to redisperse particles of 400 to 200 Å in size, heating in steam for 10 h (17) must be employed. For this reason, in those cases it is easy to follow the history of individual particles. In contrast, by heating the specimen in the above mixture of gases the changes occur so rapidly that it is impossible to follow, in some cases, the

behavior of individual particles. The results obtained during heating of a specimen in  $CH_4 + steam + H_2$  are shown in Figs. 13a–13e. After heating for only 10 min, the particles formed tails with small thick particles at the tip of the tail (Fig. 13a). In the electron diffraction pattern, NiO was the only compound detected, indicating that the tails were composed of NiO, and perhaps, amorphous carbon, as discussed later in the Discussion section. Further heating for up to 1.5 h caused severe sintering (Fig. 13b). While the particles became larger, their shape remained similar to that present before heating, with only an increased ratio of width to length of the tails. After heating for 2 more hours, the particles changed their shape to a torus with a core particle in the cavity (Fig. 13c). Possibly, because of the carbon deposits, the particles lost their catalytic activity for  $CH_4$  decomposition and the gasification of the deposited carbon by  $H_2$  and steam that followed caused the changes in shape. On further heating for 1.5

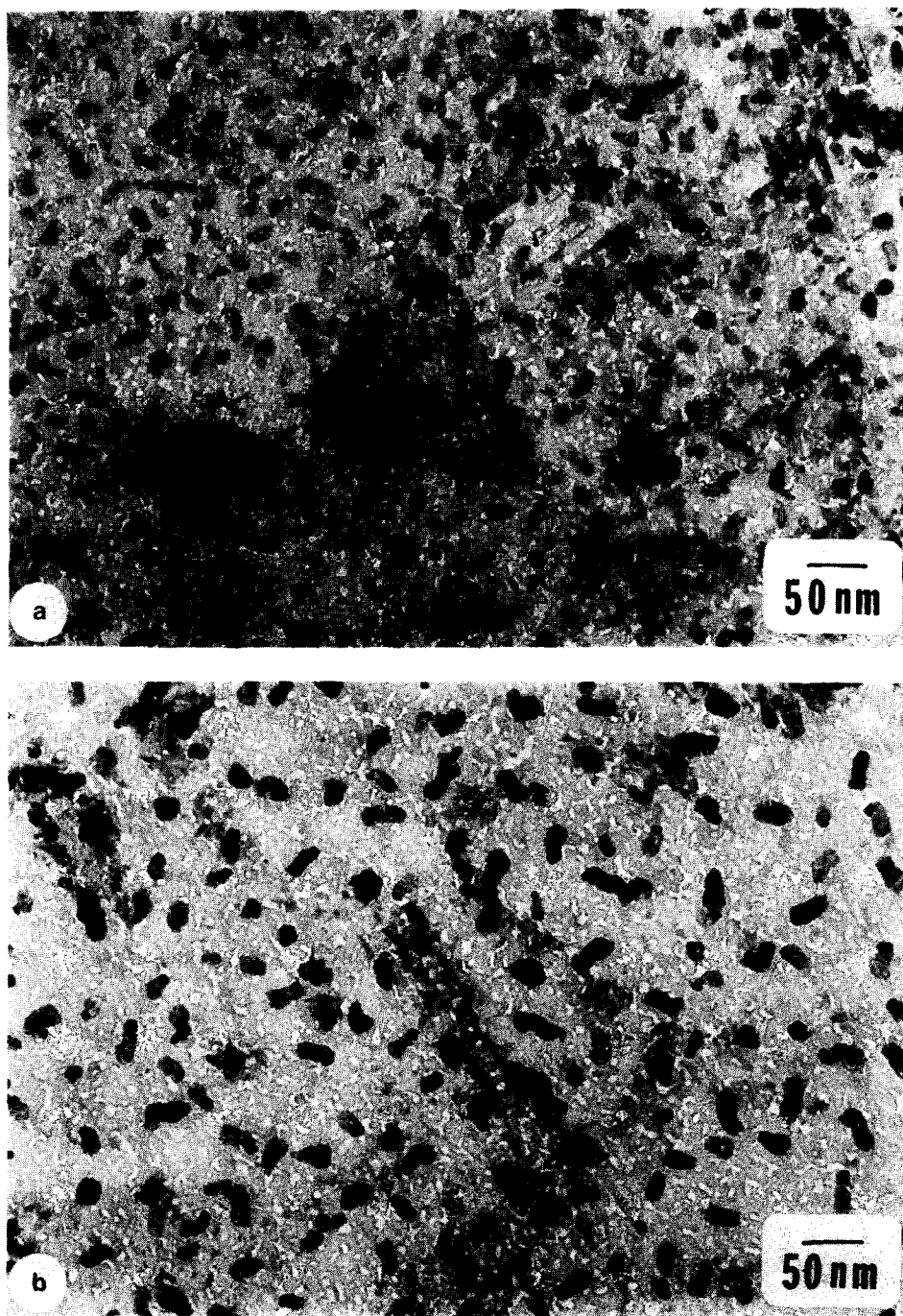


FIG. 13. Sequence of changes on heating a Ni/Al<sub>2</sub>O<sub>3</sub> specimen in CH<sub>4</sub> + steam + H<sub>2</sub> at 700°C after pretreatment in H<sub>2</sub> for 10 h (5 h at 500°C and 5 h at 700°C). (a) 10 min CH<sub>4</sub> + steam + H<sub>2</sub>; (b) 1.5 h CH<sub>4</sub> + steam + H<sub>2</sub>; (c) 3.5 h CH<sub>4</sub> + steam + H<sub>2</sub>; (d) 5 h CH<sub>4</sub> + steam + H<sub>2</sub> (the specimen was heated for 2 more hours in CH<sub>4</sub> + steam + H<sub>2</sub> after the heat treatment (d)); (e) 1 h H<sub>2</sub>.

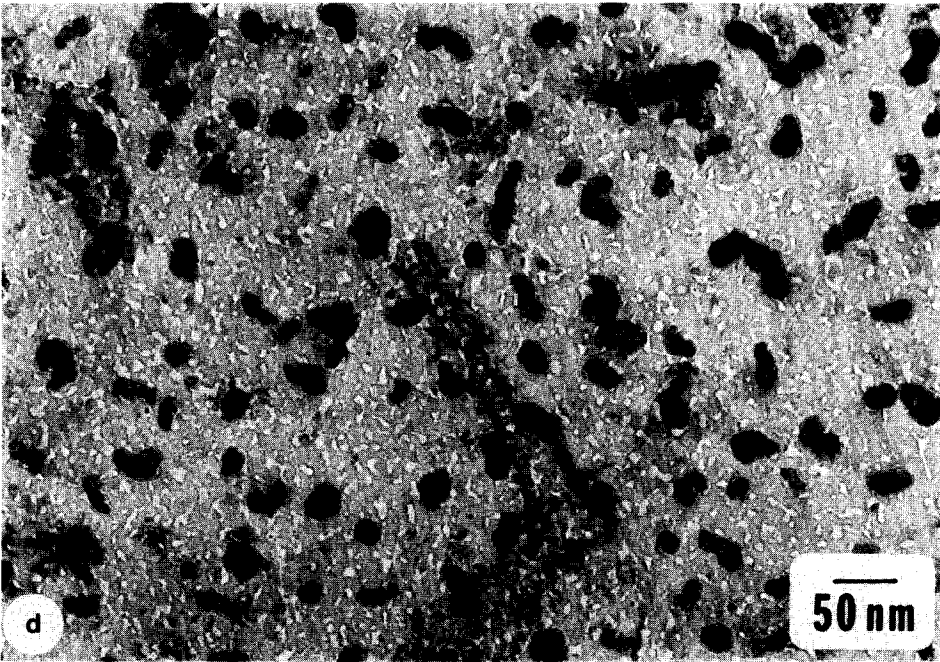
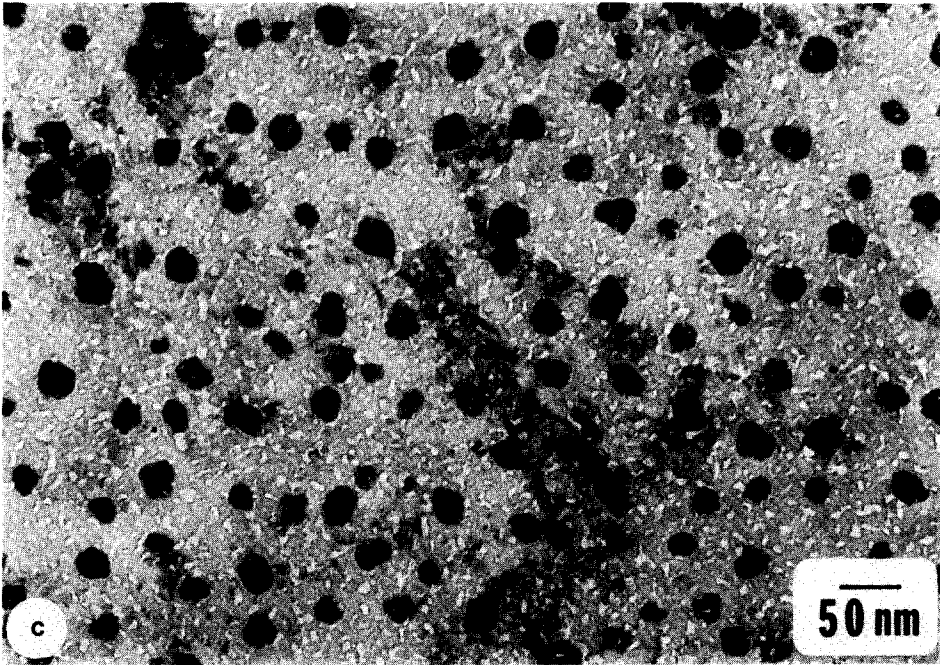
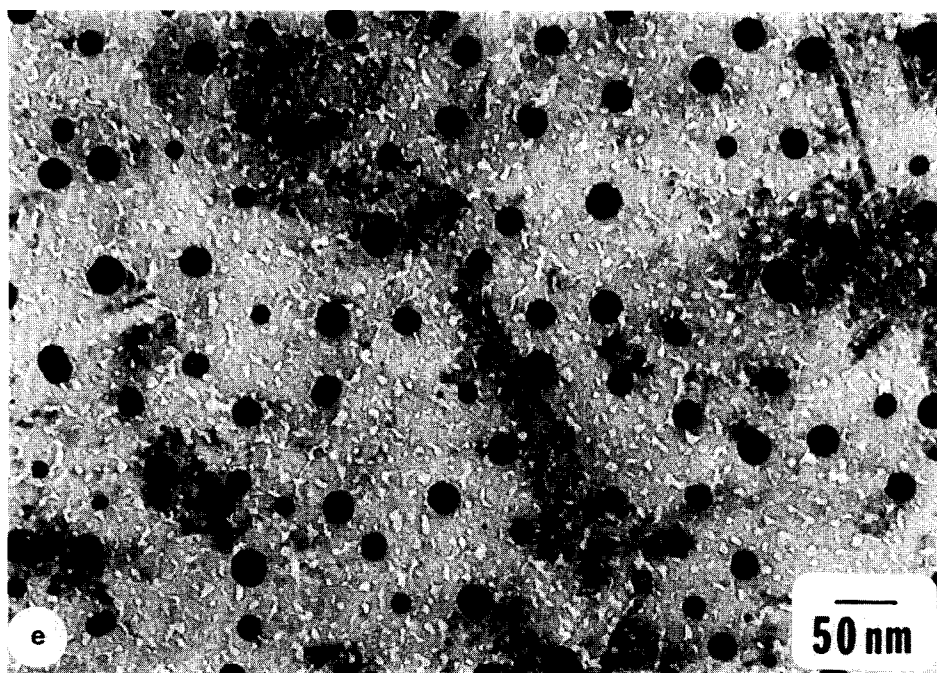


FIG. 13—Continued.



FIG. 13—*Continued.*

more hours, the shape of the particles became more irregular, and some of the particles became elongated (Fig. 13d). This suggests that after enough gasification of the deposited carbon, the particles regained their catalytic activity and could decompose  $\text{CH}_4$  again. After heating in  $\text{CH}_4 + \text{steam} + \text{H}_2$  for a total of 7 h, the specimen was heated in  $\text{H}_2$  for 1 h. As shown in Fig. 13e, the particles acquired a spherical shape.

The main events that occurred during heating in  $\text{CH}_4 + \text{steam} + \text{H}_2$  were somewhat similar to those observed during heating in  $\text{CH}_4 + \text{steam}$ . However, it is worth emphasizing the differences: (1) The particles formed tails more easily in  $\text{CH}_4 + \text{steam} + \text{H}_2$  than in  $\text{CH}_4 + \text{steam}$ . (2) The particles lost their catalytic activity for decomposition of  $\text{CH}_4$  more rapidly in the latter atmosphere. (3) The active catalyst had been better dispersed on the substrate, in the latter atmosphere. Indeed, for a specimen which was heat treated in  $\text{CH}_4 +$

steam, the subsequent heating in  $\text{H}_2$  produced numerous new small crystallites in regions where no particles were present before heating; this was not, however, the case with the specimen which was heated in  $\text{CH}_4 + \text{steam} + \text{H}_2$ .

Figures 14a–14c show the micrographs of a specimen similar to those of Figs. 13a–13e, but belonging to a different batch, whose initial average particle size was larger. After 10 min of heating in  $\text{CH}_4 + \text{steam} + \text{H}_2$ , the particles changed their shape from globular to a torus with a small particle in the cavity (Fig. 14a). NiO was detected by electron diffraction. In contrast, the particles of the similar specimen of Figs. 13a–13e elongated after 10 min of heating in the same mixture. The heating for 20 more minutes brought about, however, a dramatic change very different from that of the similar specimen of Figs. 13a–13e (Fig. 14b). Hollow, very likely, carbonaceous filaments grew over the surface of the substrate and cut across each

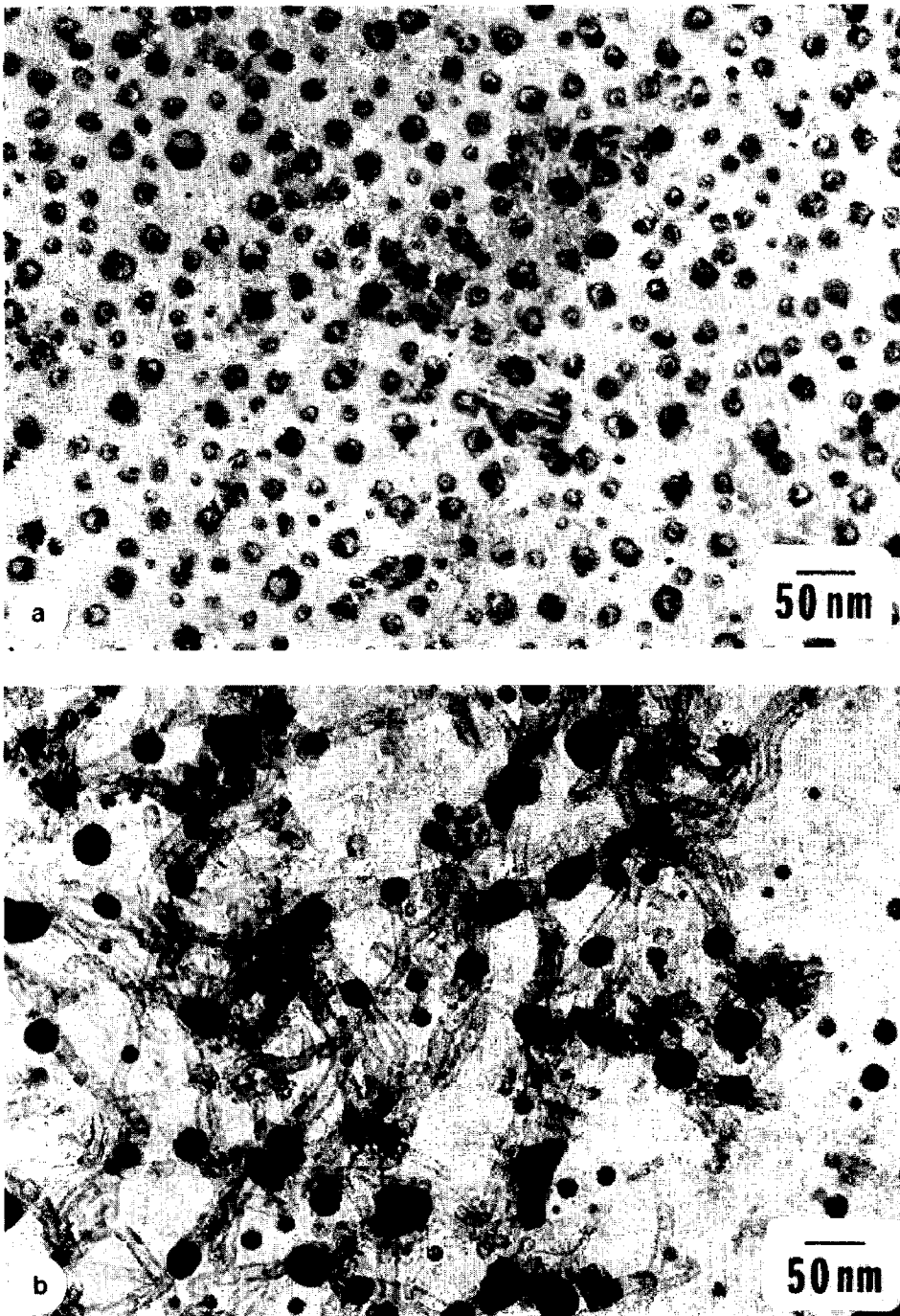


FIG. 14. Sequence of changes on heating a Ni/Al<sub>2</sub>O<sub>3</sub> specimen, which is different from the specimen of Fig. 13, in CH<sub>4</sub> + steam + H<sub>2</sub>, at 700°C after pretreatment in H<sub>2</sub> for 11.5 h (5.5 h at 500°C and 6 h at 700°C). (a) 10 min CH<sub>4</sub> + steam + H<sub>2</sub>; (b) 30 min CH<sub>4</sub> + steam + H<sub>2</sub>; (c) 1 h CH<sub>4</sub> + steam + H<sub>2</sub>.

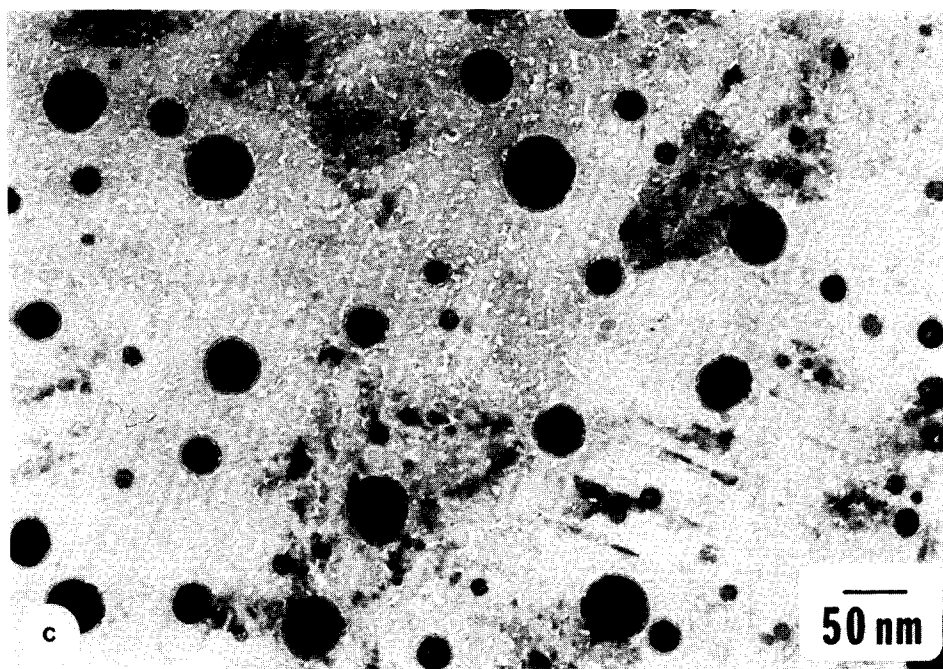


FIG. 14—Continued.

other, forming complex networks. Severe sintering of the particles also took place. Electron diffraction indicated that the particles were present mostly as Ni. Hence, the particles were reduced to metal nickel and sintered, (most probably) by migration followed by coalescence. It appears that the formation of the carbonaceous filaments is associated with the reduction of the particles. Indeed, in the specimen of Figs. 13a–13e, the particles were present as NiO throughout heating in  $\text{CH}_4 + \text{steam} + \text{H}_2$  and they did not produce carbonaceous filaments. In addition, it is worth noting that the heating in methane or in methane + steam did not produce carbonaceous filaments either and the particles were also present as NiO. However, after additional heating for 30 more minutes in  $\text{CH}_4 + \text{steam} + \text{H}_2$ , the filaments disappeared and sintering continued to occur (Fig. 14c). Electron diffraction identified the presence of Ni. On heating for 1 more hour in  $\text{CH}_4 + \text{steam} + \text{H}_2$  and subsequently in  $\text{H}_2$  for 1 h,

most of the particles remained without any significant change. Two similar specimens, from two different batches, behaved differently. The kinetics of oxidation and reduction of the crystallites, which is affected by the details of the preparation of the specimen, is probably responsible for the difference.

#### B. $\text{Co}/\text{Al}_2\text{O}_3$

On heating for 10 min in  $\text{CH}_4 + \text{steam} + \text{H}_2$ , the initial particles of Fig. 15a have extended over the substrate (Fig. 15b). The particles are now composed of an extended bottom that supports a darker small particle. One may also note the coalescence of neighboring particles (R1), as well as the dumbbell-shaped particles (R2). Heating for 20 more minutes caused the deformation of the particles, probably because of the penetration of deposited carbon (see Discussion) (Fig. 15c). It is worth noting that the dark particles moved over the extended bottom to its edge. Some of the dark parti-

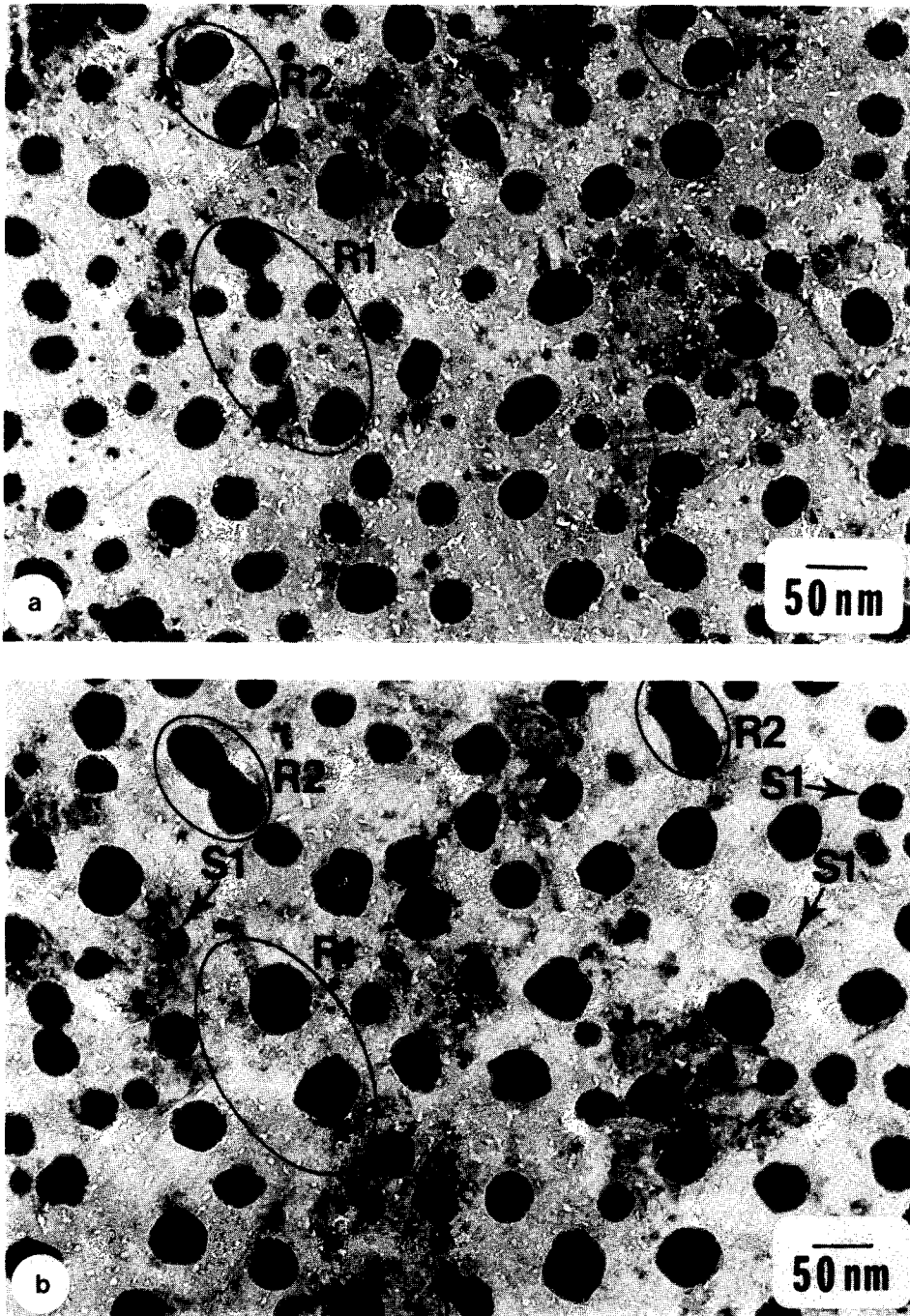


FIG. 15. Sequence of changes on heating a Co/Al<sub>2</sub>O<sub>3</sub> specimen in CH<sub>4</sub> + steam + H<sub>2</sub> at 700°C. (a) 10 h (5 h at 500°C and 5 h at 700°C) H<sub>2</sub>; (b) 10 min CH<sub>4</sub> + steam + H<sub>2</sub>; (c) 30 min CH<sub>4</sub> + steam + H<sub>2</sub>; (d) 1.5 h CH<sub>4</sub> + steam + H<sub>2</sub>; (e) 5.5 h CH<sub>4</sub> + steam + H<sub>2</sub> (the specimen was heated for additional 4.5 h in CH<sub>4</sub> + steam + H<sub>2</sub> after the heat treatment (e)); (f) 1 h H<sub>2</sub>.

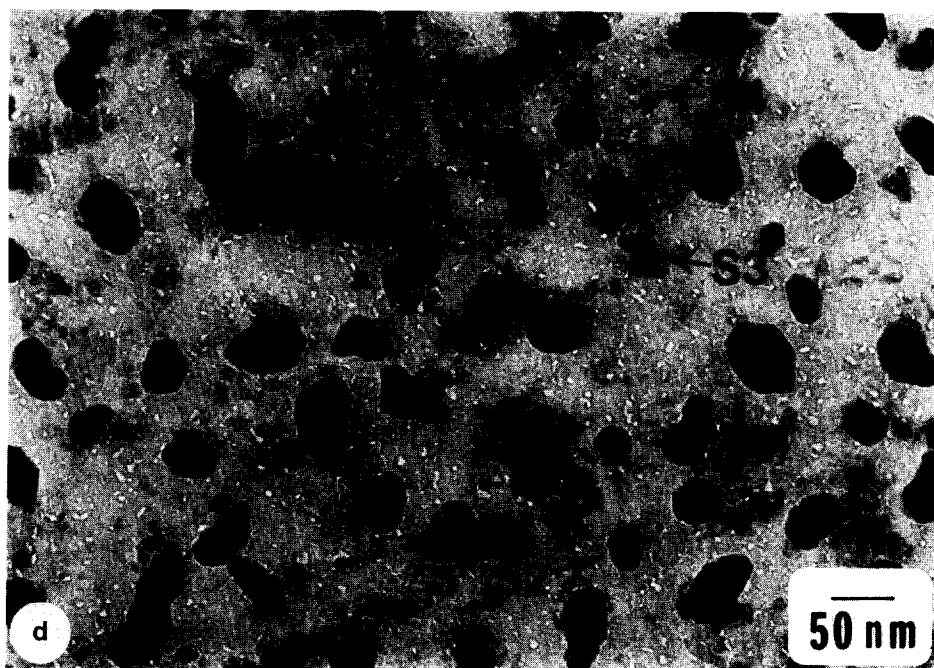
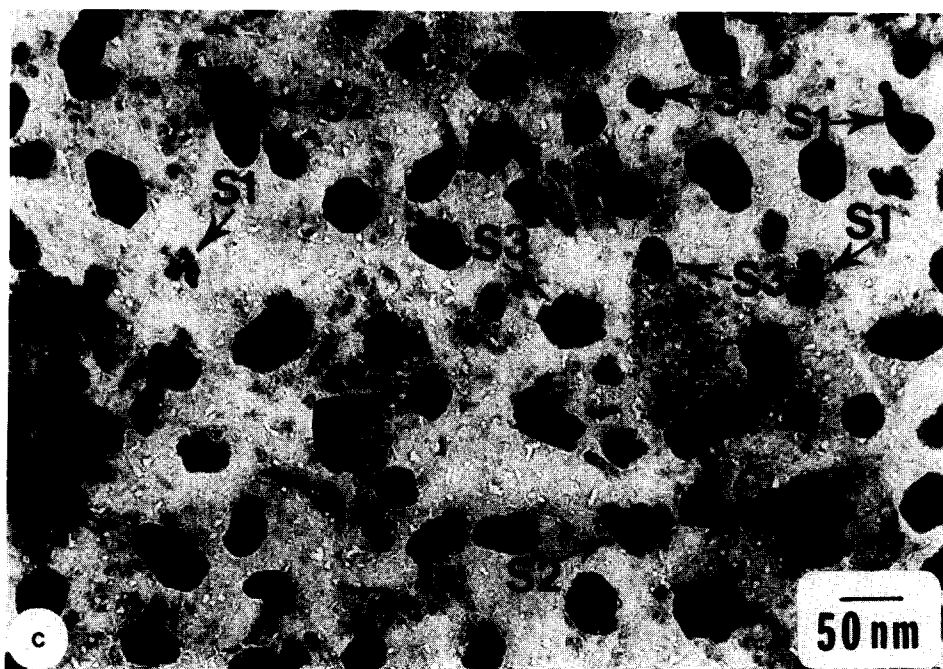


FIG. 15—Continued.

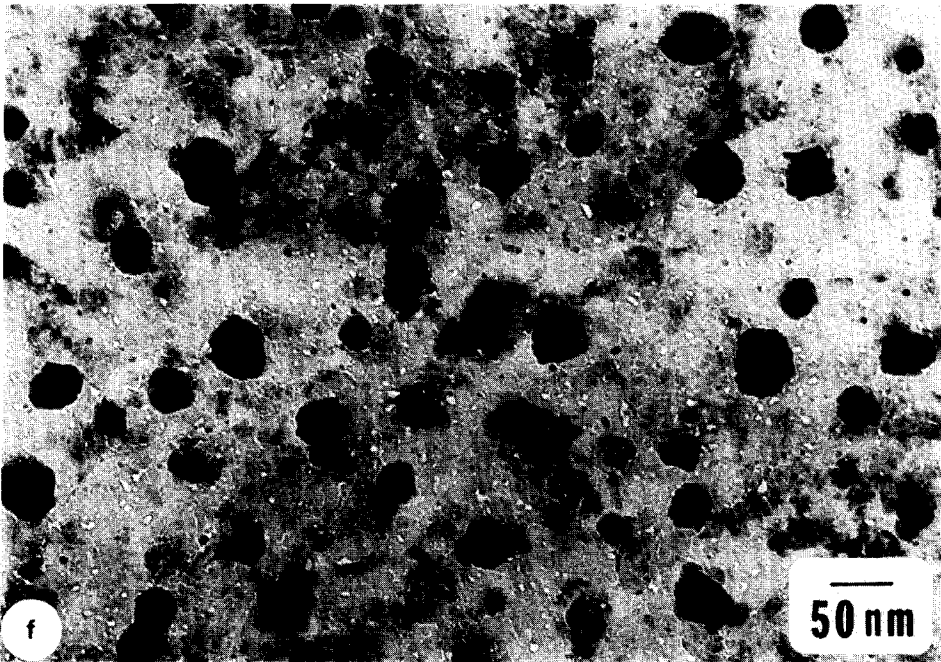
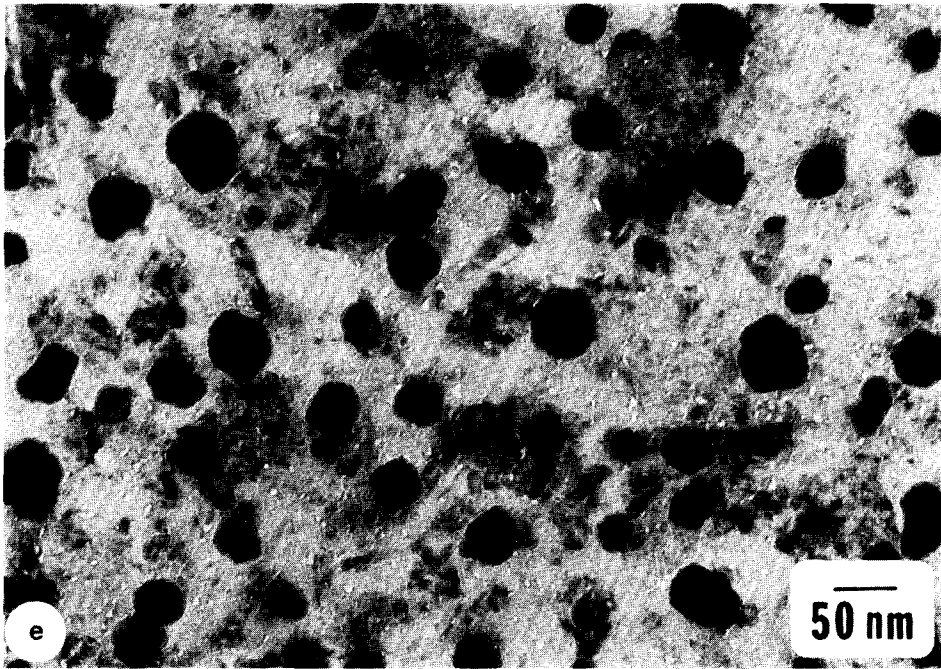


FIG. 15—Continued.

cles moved out from the extended bottom and tails were formed while they were migrating (S1 in Fig. 15c), perhaps because of the carbon formation. On further heating for up to 1.5 h, the dark particles changed their position within the extended bottom (S2 in Fig. 15d). In addition, a few dark particles moved further out from the extended bottom, forming tails which are probably composed of carbon and cobalt oxide (S3 in Fig. 15d). A few small particles disappeared, leaving some traces (S4 in Fig. 15d). After heating for a total of 5.5 h, the particles changed their shape, becoming more circular (Fig. 15e), and the dark particles moved from the edge of the extended bottom to their center. Now, the catalyst particles are no longer expected to be active for methane decomposition, because they are probably completely covered by carbon. However, heating for up to 10 h caused again tail formations, which were, however, shorter than before. This suggests that the coked particles were regenerated and able again to decompose methane, but with a lower activity than before. The specimen was subsequently heated in  $H_2$  for 1 h (Fig. 15f). The particles decreased in size, because of contraction. The appearance of new small particles in regions where no particles were observed before indicates that during heating in  $CH_4 + \text{steam} + H_2$  some particles and/or part of other particles spread over the substrate as undetectable films. The heating in  $H_2$  caused the rupture of that film, and the contraction of the thin patches thus formed generated the small particles. Comparing Figs. 15a and 15f, it is plausible to conclude that some material was permanently lost to the gas stream. As mentioned earlier, in the case of Ni the heating in  $H_2$  following heating in  $CH_4 + \text{steam} + H_2$  did not produce new particles in regions where no particles were present before. Compared to nickel, the cobalt particles emit to a greater extent undetectable thin films over the surface of the  $Al_2O_3$  substrate.

### C. $Fe/Al_2O_3$

After heating the specimen of Fig. 16a in  $CH_4 + \text{steam} + H_2$  for 10 min (Fig. 16b), one notes that most of the particles deformed and/or extended, and had one or several small darker particles supported on extended thin patches. In addition, a few particles elongated, acquiring a filamentous structure (T in Fig. 16b). Electron diffraction indicated the presence of  $\gamma\text{-Fe}_2O_3$  (or  $Fe_3O_4$ ). The filaments were most likely composed of carbon and some  $\gamma\text{-Fe}_2O_3$  (or  $Fe_3O_4$ ), and the extended thin patches contained probably deposited carbon. On heating for 20 more minutes (Fig. 16c), the particles became thinner and disintegrated in smaller, interconnected units, probably because of the formation of unstable carbides and their decomposition (see Discussion). It is likely that, because of disintegration, a part of the material was permanently lost to the gas stream. The only compound detected by electron diffraction was  $\gamma$ -alumina, probably because the particles were too thin. Further heating for up to 8.5 h did not cause any significant change. After particles were subsequently heated in  $H_2$ , no significant change was observed either. One may note that new particles did not appear in regions where no particles were observed before heating. This indicates that spreading as thin films, undetectable by electron microscopy, occurred in this case much less than for Co and that any "lost material" was permanently lost to the gas stream.

### 4. HEATING OF $Ni/Al_2O_3$ IN CO

On heating the specimen of Fig. 17a in CO for 0.5 h, one notes that severe sintering occurred (Fig. 17b). Some filamentous carbon (Y1), as well as some large patches of carbon which covered several particles (Y2 in Fig. 17b), was observed. On further heating for a total of 2 h, the carbonaceous filaments in region Y1 disappeared, while new carbonaceous filaments appeared in

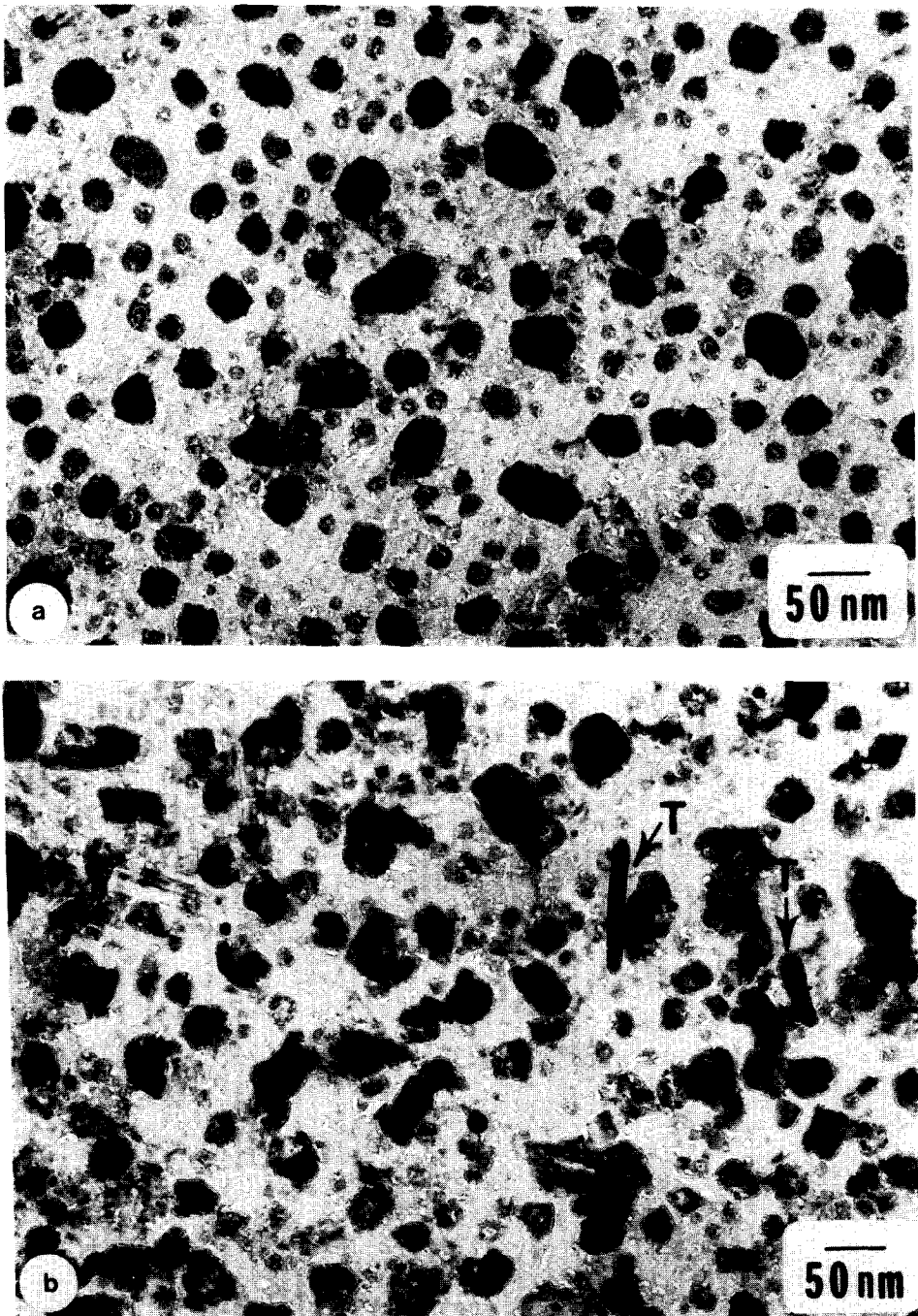


FIG. 16. Sequence of changes on heating a  $\text{Fe}/\text{Al}_2\text{O}_3$  specimen in  $\text{CH}_4 + \text{steam} + \text{H}_2$  at  $700^\circ\text{C}$ . (a) 10 h (5 h at  $500^\circ\text{C}$  and 5 h at  $700^\circ\text{C}$ )  $\text{H}_2$ ; (b) 10 min  $\text{CH}_4 + \text{steam} + \text{H}_2$ ; (c) 30 min  $\text{CH}_4 + \text{steam} + \text{H}_2$ .



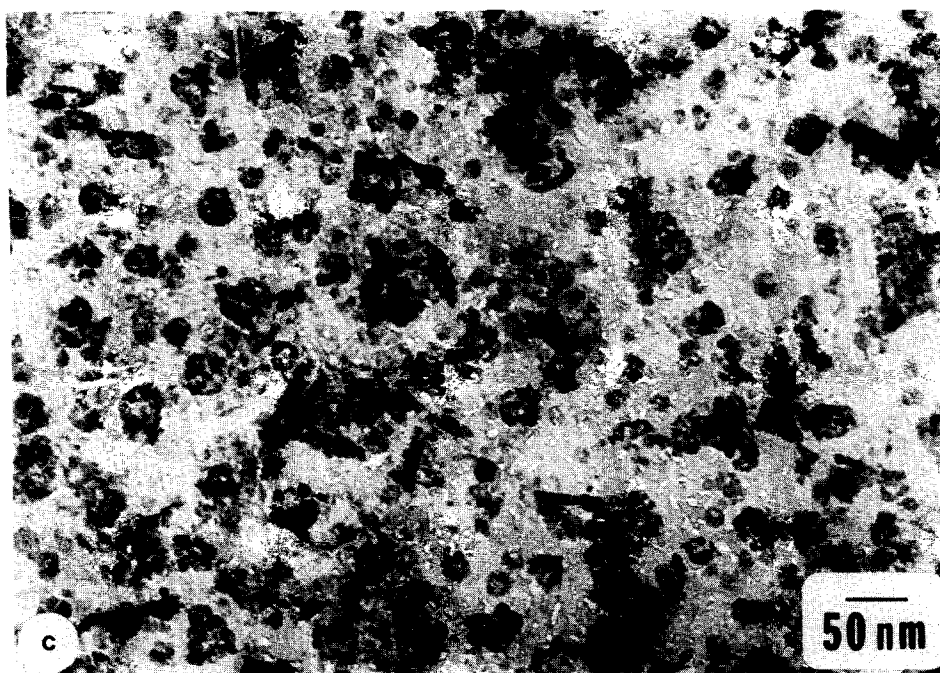
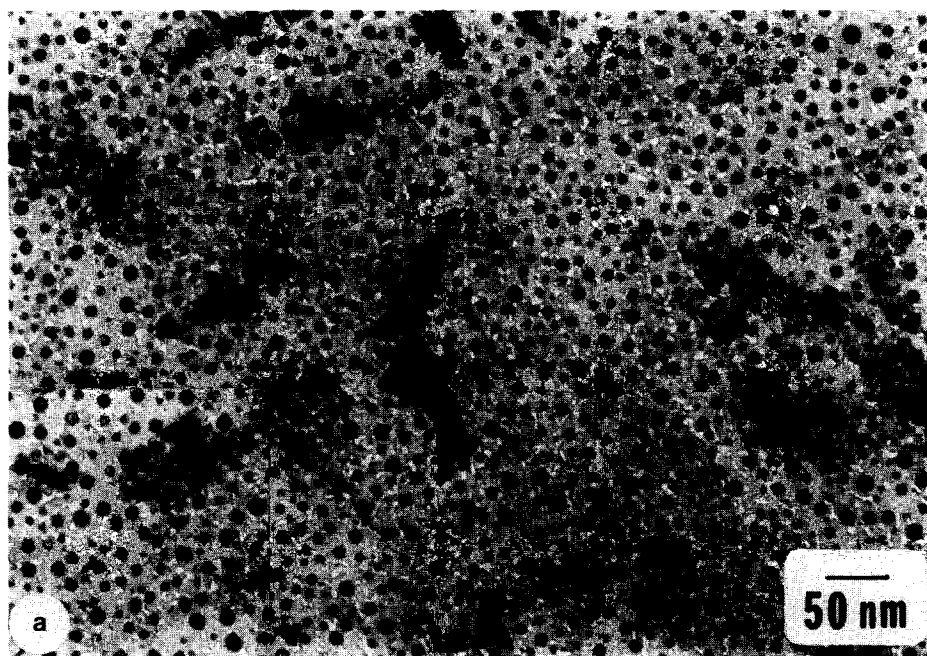
FIG. 16—*Continued.*

FIG. 17. Sequence of changes on heating a Ni/Al<sub>2</sub>O<sub>3</sub> specimen in carbon monoxide at 700°C. (a) 10 h (5 h at 500°C and 5 h at 700°C) H<sub>2</sub>; (b) 0.5 h CO; (c) 2 h CO; (d<sub>1</sub> and d<sub>2</sub>) 4 h CO (d<sub>1</sub> and d<sub>2</sub> show two different regions of the same specimen).

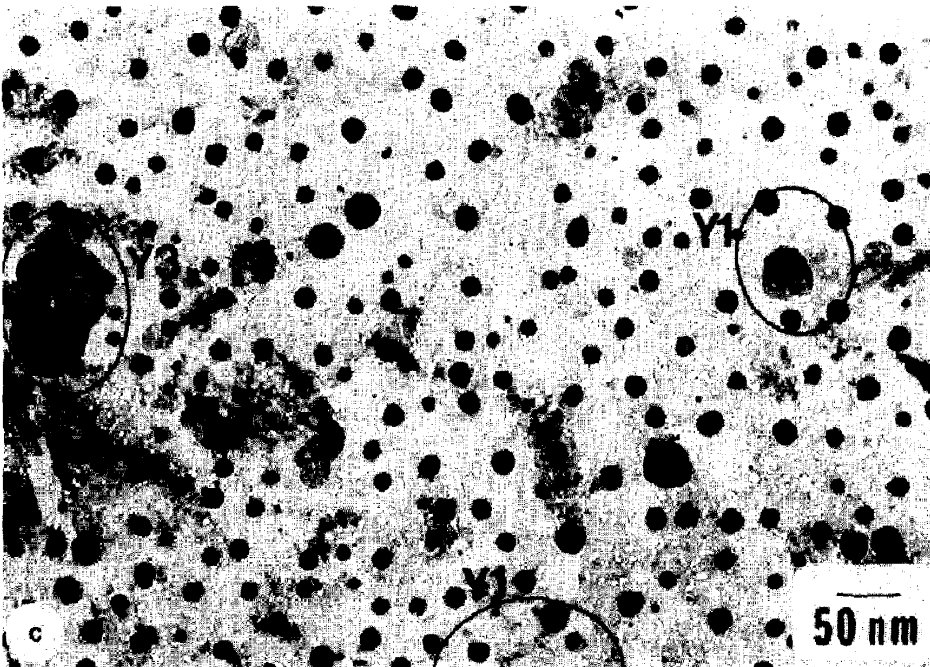
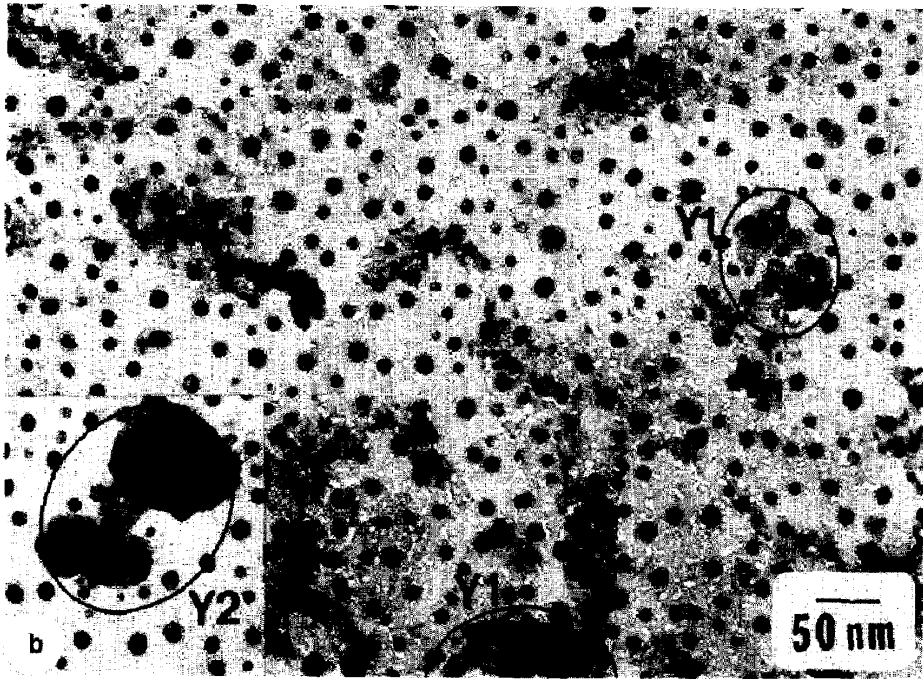


FIG. 17—Continued.

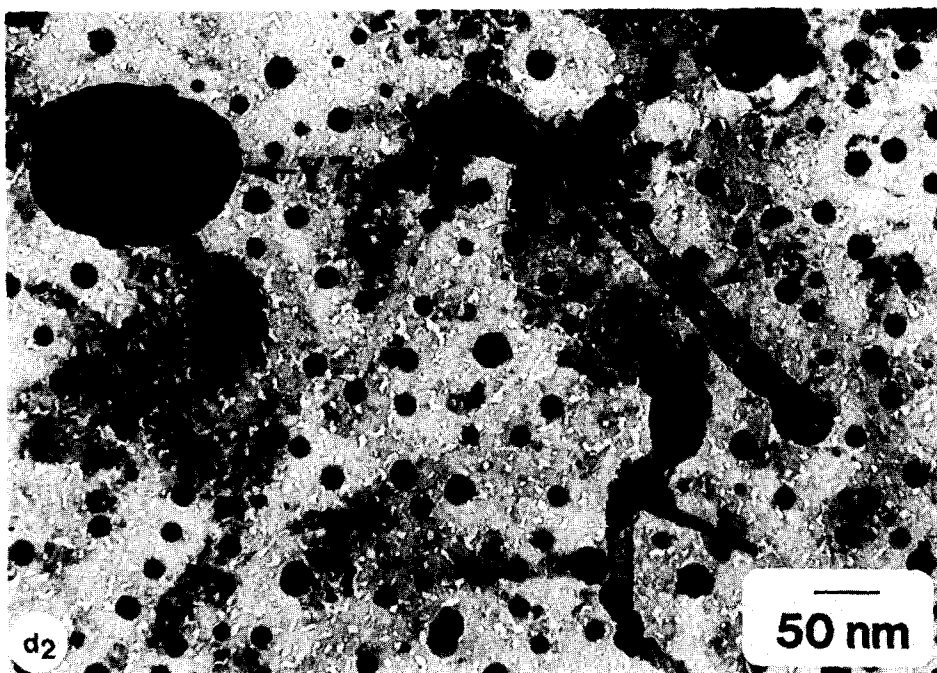
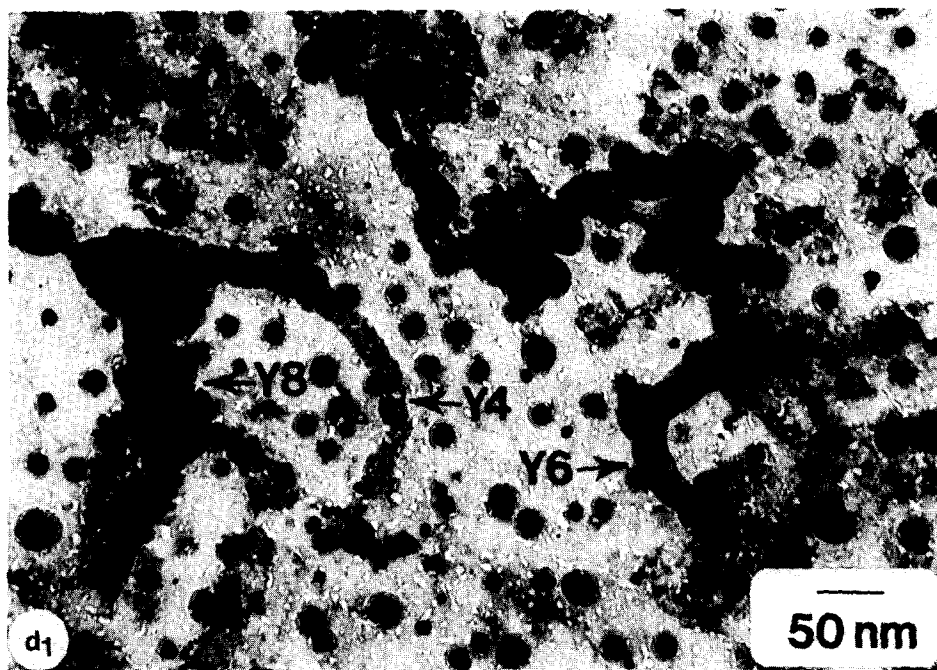


FIG. 17—Continued.

other regions (Y3 in Fig. 17c). In addition, severe sintering continued to occur. The specimen was further heated for up to 4 h. Figures 17d<sub>1</sub> and 17d<sub>2</sub>, which represent two different regions of the same specimen, show several types of carbon deposits:

- a. filamentous carbon (Y4 in Fig. 17d<sub>1</sub>),
- b. hollow filamentous carbon (Y5 in Fig. 17 d<sub>2</sub>),
- c. carbonaceous filament which wraps an elongated nickel particle (Y6 in Fig. 17 d<sub>1</sub>),
- d. thick large patches of carbon (Y7 in Fig. 17 d<sub>2</sub>), and
- e. films of carbon that cover a whole area of several neighboring particles (Y8 in Fig. 17 d<sub>1</sub>).

However, in the electron diffraction pattern, no rings corresponding to graphite were detected, indicating that the deposited carbon was amorphous. With the exception of the elongated particles which were wrapped in the carbonaceous filaments, the

catalyst particles maintained almost spherical shapes throughout the entire heating. Electron diffraction indicated that the crystallites were present as Ni. It is possible that a part of the metal was permanently lost to the gas stream as nickel carbonyl. It is, however, difficult to discriminate between the severe sintering that occurred and this loss of material.

Another specimen was heated continuously in CO for 4 h and its micrograph is shown in Fig. 18. All the types of carbon deposits, observed in the micrographs of the previous specimen which was heated in several steps for up to 4 h (Figs. 17a–17d<sub>2</sub>), can be identified in Fig. 18. However, the number of filaments was greater in the latter case and most of them were hollow. In addition, some filaments swung very slowly during observation in the transmission electron microscope and were not sharp, while others were well focused. This means that the former filaments were not completely supported on the substrate.

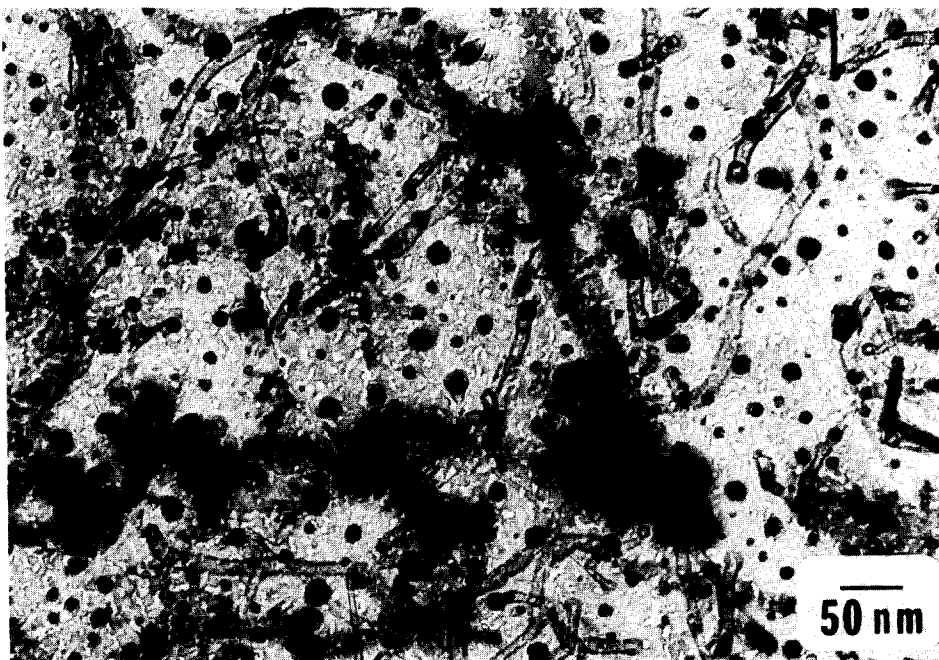


FIG. 18. Ni/Al<sub>2</sub>O<sub>3</sub> specimen after heating in CO for 4 h continuously at 700°C following heating in H<sub>2</sub> for 10 h (5 h at 500°C and 5 h at 700°C).

## 5. HEATING IN $\text{CH}_4 + \text{STEAM} + \text{H}_2 + \text{CO}$

As mentioned earlier, different deactivation processes are dominant for the three systems during heating in  $\text{CH}_4 + \text{steam} + \text{H}_2$ , namely sintering and coking for  $\text{Ni}/\text{Al}_2\text{O}_3$ , spreading and coking for  $\text{Co}/\text{Al}_2\text{O}_3$ , and loss of material and coking for  $\text{Fe}/\text{Al}_2\text{O}_3$ . When  $\text{CO}$  was added to the ternary mixture, the results remained similar to those in the ternary mixture, but the changes occurred more rapidly.

### A. $\text{Ni}/\text{Al}_2\text{O}_3$

After heating in the quaternary mixture for 5 min, most of the initial particles (Fig. 19a) became elongated (Fig. 19b) and the number of particles decreased, due to the mergence of the nearby particles (Z1 in Fig. 19b). In addition, some large patches, in which carbon interconnects and covers several particles, formed (Z2).  $\text{NiO}$  was detected by electron diffraction. On heating

for 15 additional minutes, the particles contracted and acquired spherical shapes (Fig. 19c). Some neighboring particles coalesced (Z3), while some elongated particles which contacted one another split into several particles of spherical shape (Z1). However, most of the particles remained at their original locations with a change in shape only. Electron diffraction indicated that most of the particles were reduced to  $\text{Ni}$ , but  $\text{NiO}$  was also present. Comparing with the heating in the gas mixture without  $\text{CO}$ , one may note that  $\text{NiO}$  particles are more rapidly reduced to  $\text{Ni}$  in the  $\text{CH}_4 + \text{steam} + \text{H}_2 + \text{CO}$  mixture. After particles were further heated for up to 2 h, severe sintering occurred (Fig. 19d). As suggested in the case of heating in  $\text{CO}$ , it is possible that a part of the metal was permanently lost to the gas stream, because of carbonyl formation. Electron diffraction indicated that the particles were almost completely reduced to  $\text{Ni}$  after 1 h of heating. Another sample

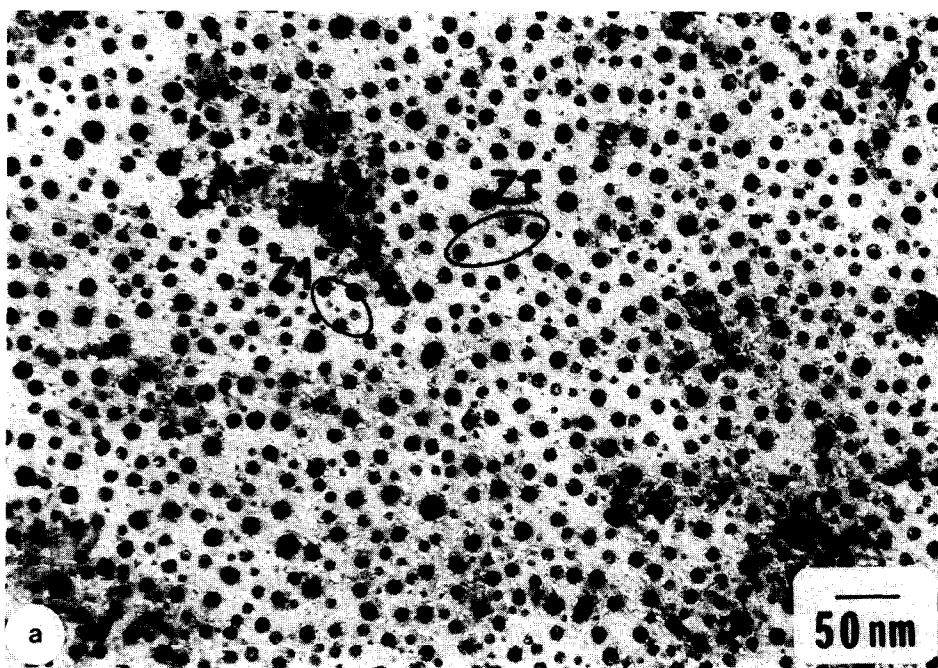


FIG. 19. Sequence of changes on heating a  $\text{Ni}/\text{Al}_2\text{O}_3$  specimen in  $\text{CH}_4 + \text{steam} + \text{H}_2 + \text{CO}$  at  $700^\circ\text{C}$ . (a) 10 h (5 h at  $500^\circ\text{C}$  and 5 h at  $700^\circ\text{C}$ )  $\text{H}_2$ ; (b) 5 min  $\text{CH}_4 + \text{steam} + \text{H}_2 + \text{CO}$ ; (c) 20 min  $\text{CH}_4 + \text{steam} + \text{H}_2 + \text{CO}$ ; (d) 2 h  $\text{CH}_4 + \text{steam} + \text{H}_2 + \text{CO}$ .

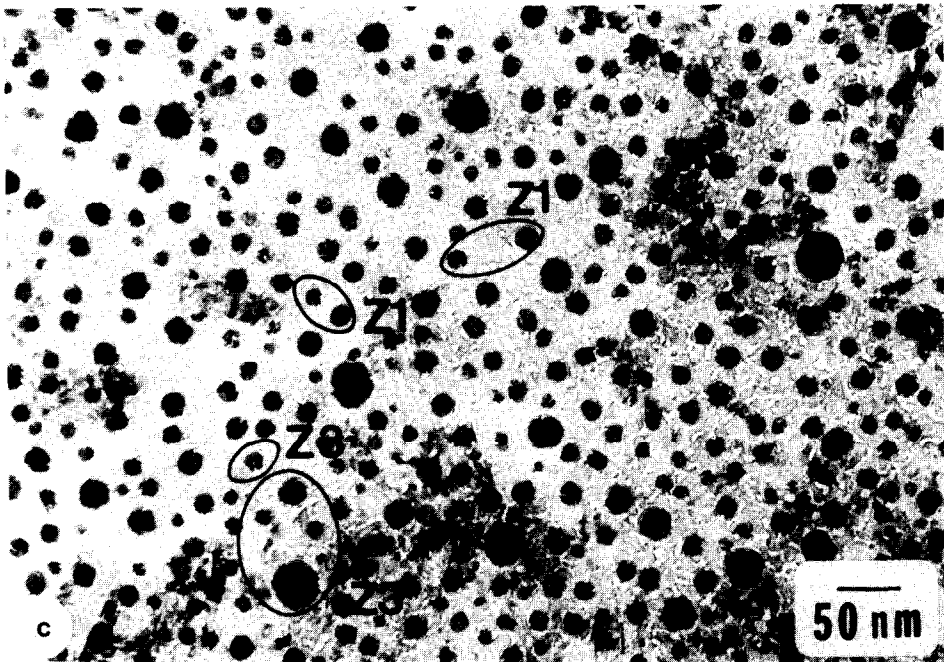
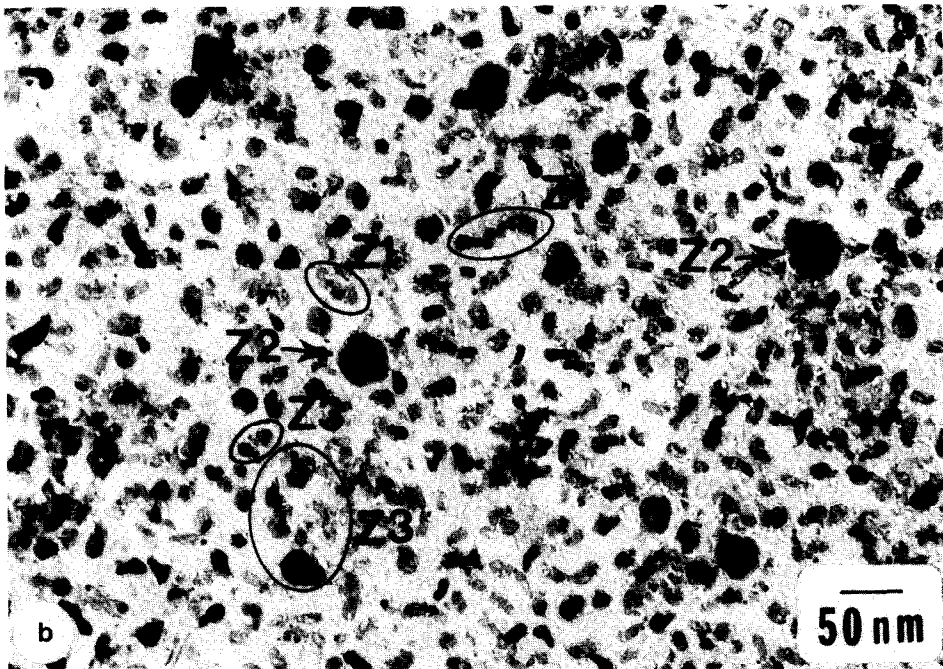


FIG. 19—Continued.

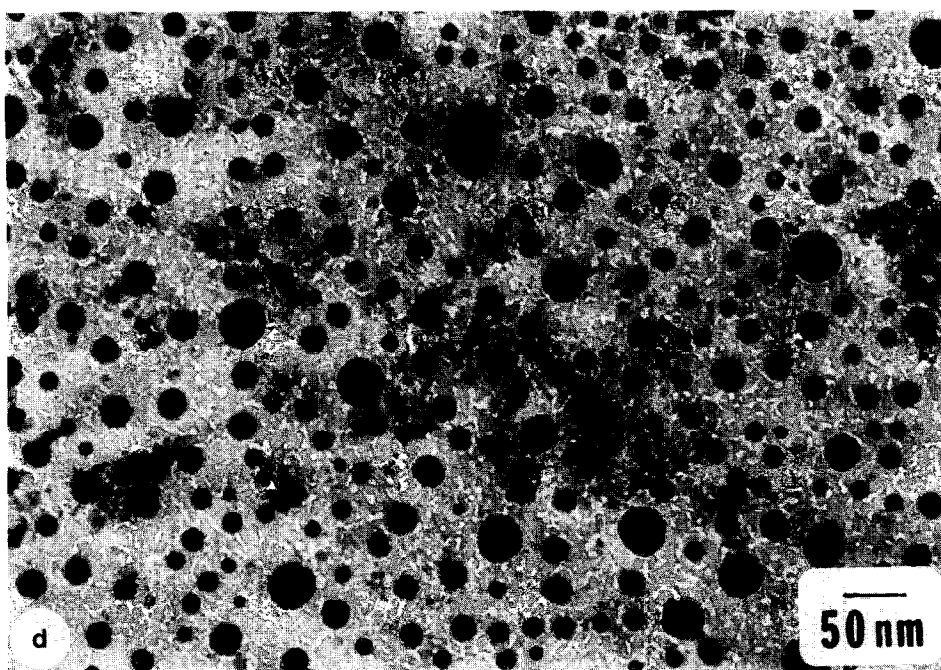


FIG. 19—Continued.

was heated continuously in the quaternary mixture for 2 h. The results were similar to those obtained with a specimen heated in several steps, for the same length of time.

#### B. $\text{Co}/\text{Al}_2\text{O}_3$

Many particles disappeared after heating the specimen of Fig. 20a in  $\text{CH}_4 + \text{steam} + \text{H}_2 + \text{CO}$  for only 5 min, and the remaining particles were deformed (Fig. 20b). The deformation is very likely associated with carbon deposition and its dissolution inside the particles (see Discussion). The electron diffraction pattern indicated that the particles were present mostly as  $\text{CoO}$  with traces of  $\text{Co}_2\text{O}_3$ . After heating for 15 more minutes, the particles acquired a more compact circular shape (Fig. 20c). One may also note that some particles split into two particles ((a) in Fig. 20c). On further heating for up to 1 h (Fig. 20d) a few new particles appeared (b), while some particles decreased in size (c) and some particles extended (d). The specimen was subsequently

heated in  $\text{H}_2$  for 1 h (Fig. 20e). Numerous new particles appeared, indicating that at least a fraction of the disappeared material was not lost to the gas stream, but remained on the substrate as undetectable films.

#### C. $\text{Fe}/\text{Al}_2\text{O}_3$

After heating the specimen of Fig. 21a for only 5 min, one notes that most of the particles became smaller and thinner, indicating that a considerable amount of material was lost to the substrate and/or to the gas stream (Fig. 21b). On heating for up to 1 h, most of the particles became increasingly thinner (Fig. 21c). In addition, some of the dark particles (e) migrated over the substrate leaving white tracks. These tracks can be a result of the catalytic gasification of the carbon deposited on the substrate during the migration of the crystallites, migration which is enhanced by the gasification process. The specimen was subsequently heated in  $\text{H}_2$  for 1 h (Fig. 21d). As shown in the micrograph, a few new parti-

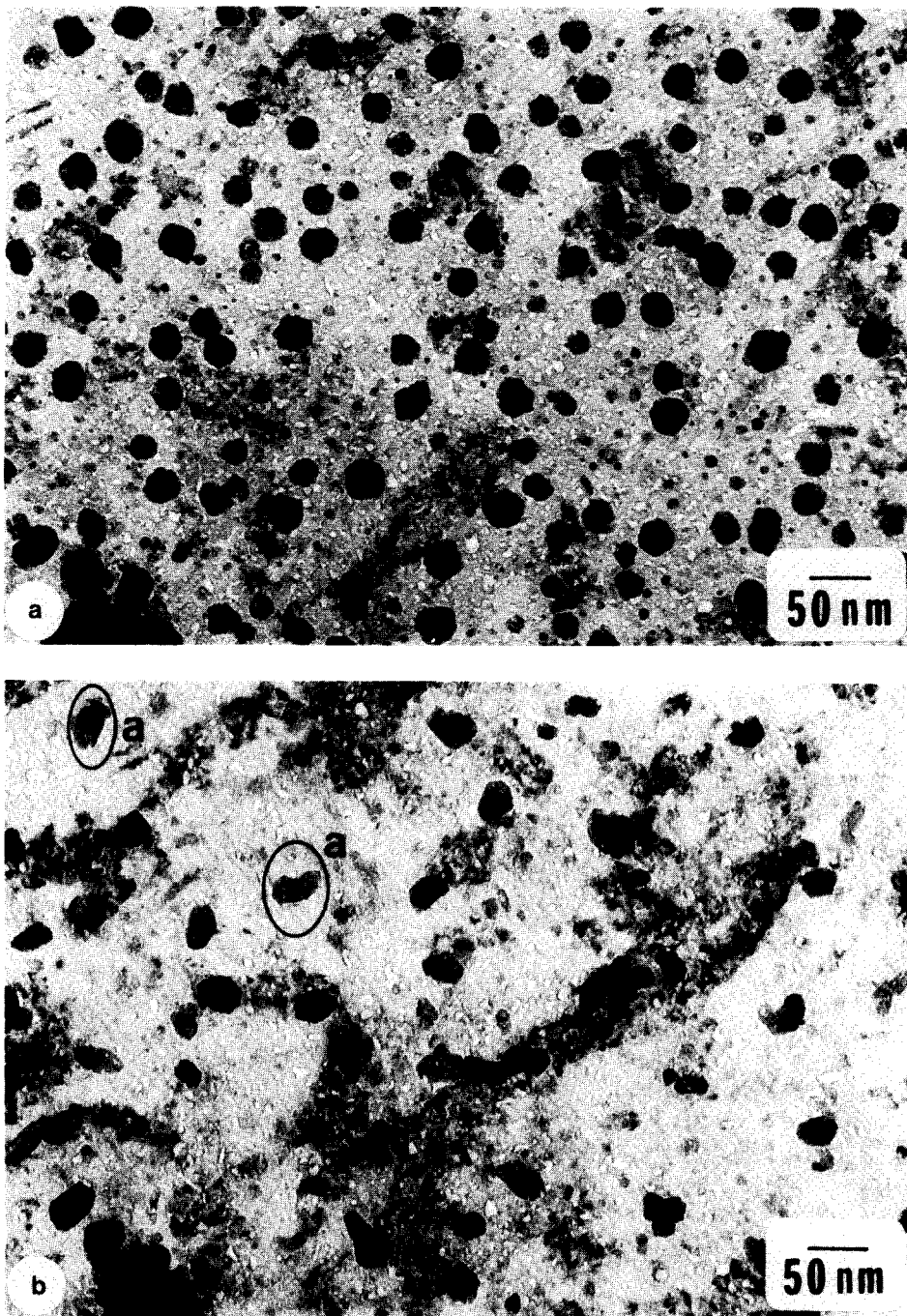


FIG. 20. Sequence of changes on heating a  $\text{Co}/\text{Al}_2\text{O}_3$  specimen in  $\text{CH}_4 + \text{steam} + \text{H}_2 + \text{CO}$  at  $700^\circ\text{C}$ . (a) 10 h (5 h at  $500^\circ\text{C}$  and 5 h at  $700^\circ\text{C}$ )  $\text{H}_2$ ; (b) 5 min  $\text{CH}_4 + \text{steam} + \text{H}_2 + \text{CO}$ ; (c) 20 min  $\text{CH}_4 + \text{steam} + \text{H}_2 + \text{CO}$ ; (d) 1 h  $\text{CH}_4 + \text{steam} + \text{H}_2 + \text{CO}$ ; (e) 1 h  $\text{H}_2$ .



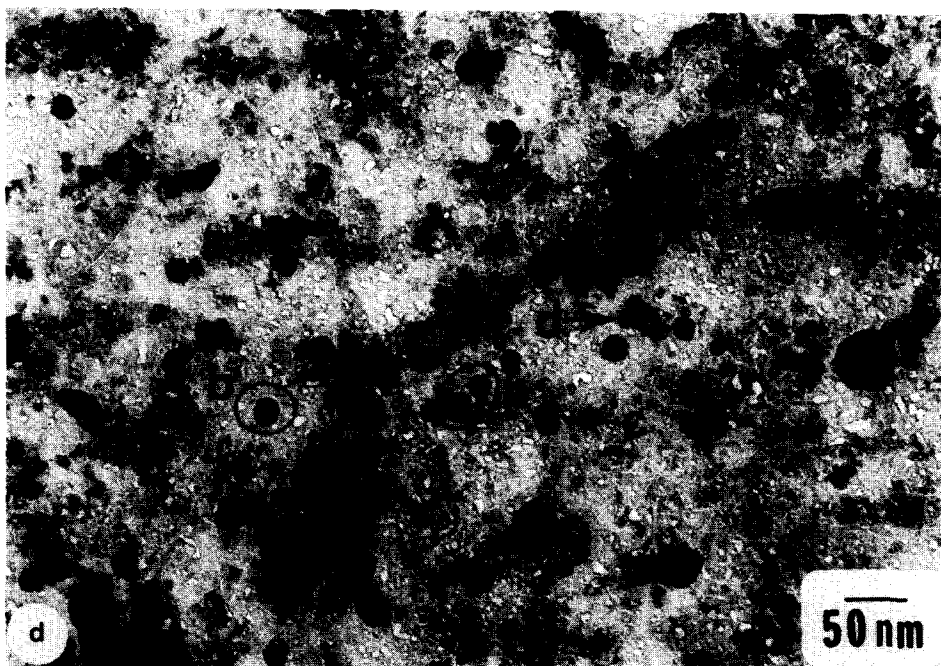
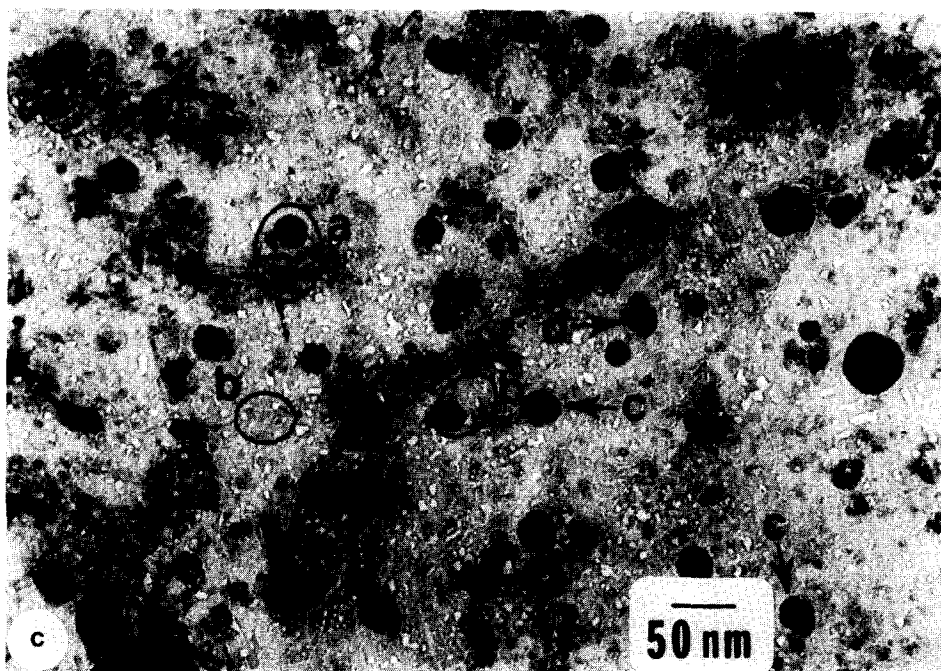


FIG. 20—Continued.

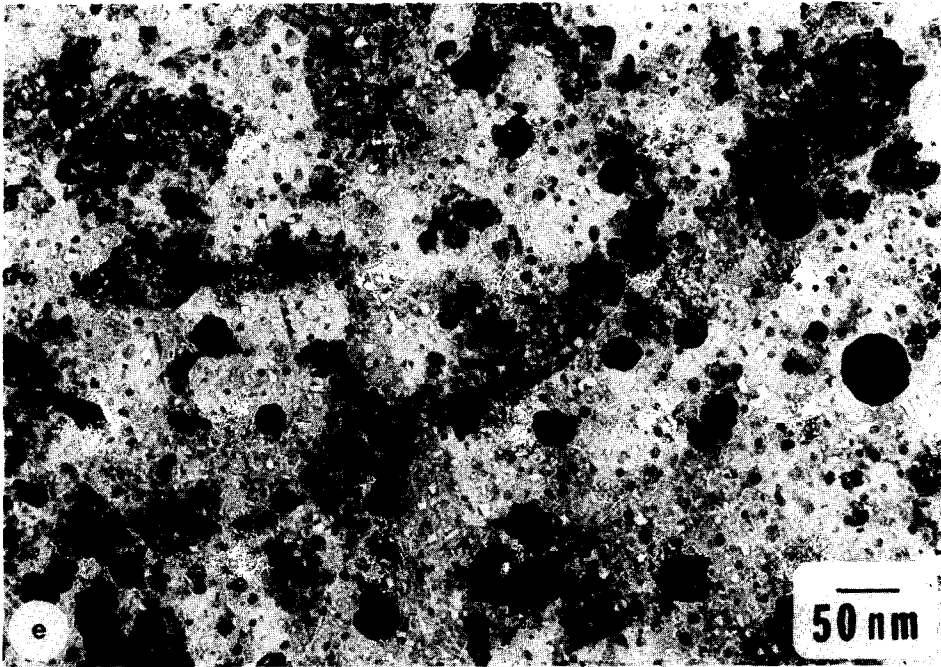


FIG. 20—Continued.

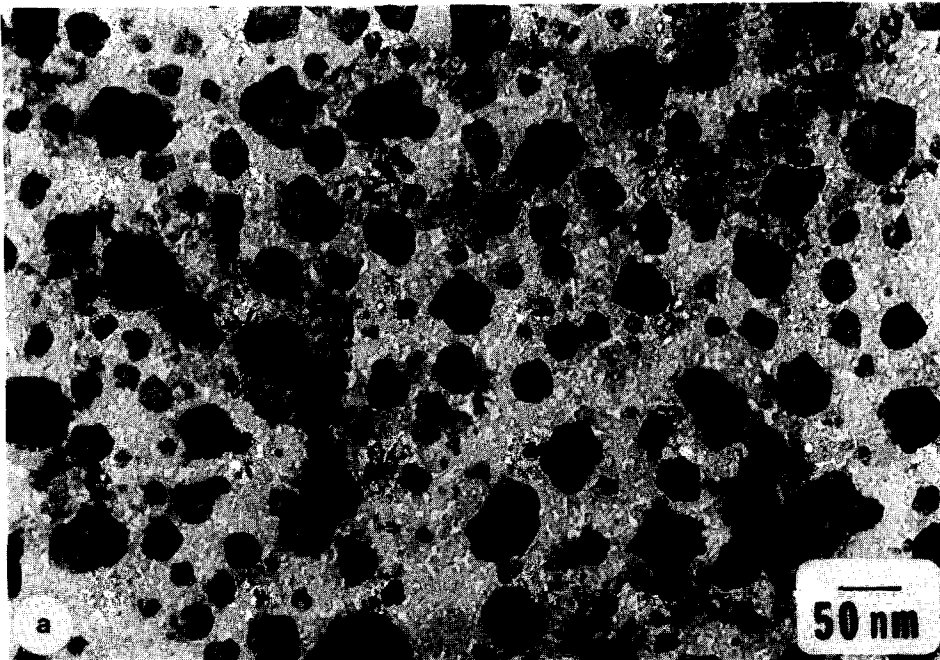


FIG. 21. Sequence of changes on heating a Fe/Al<sub>2</sub>O<sub>3</sub> specimen in CH<sub>4</sub> + steam + H<sub>2</sub> + CO at 700°C. (a) 10 h (5 h at 500°C and 5 h at 700°C) H<sub>2</sub>; (b) 5 min CH<sub>4</sub> + steam + H<sub>2</sub> + CO; (c) 1 h CH<sub>4</sub> + steam + H<sub>2</sub> + CO; (d) 1 h H<sub>2</sub>.

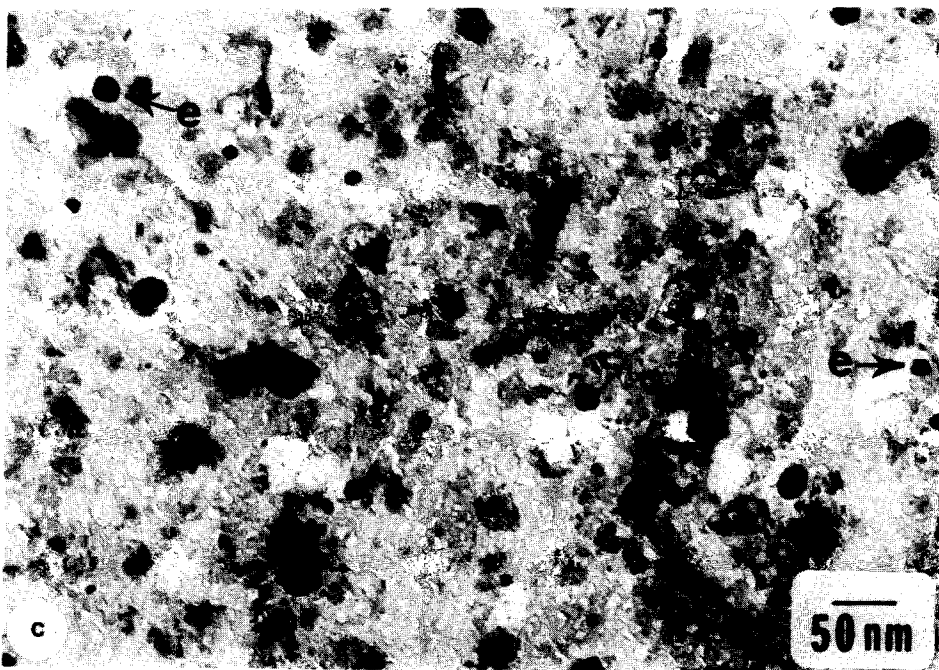
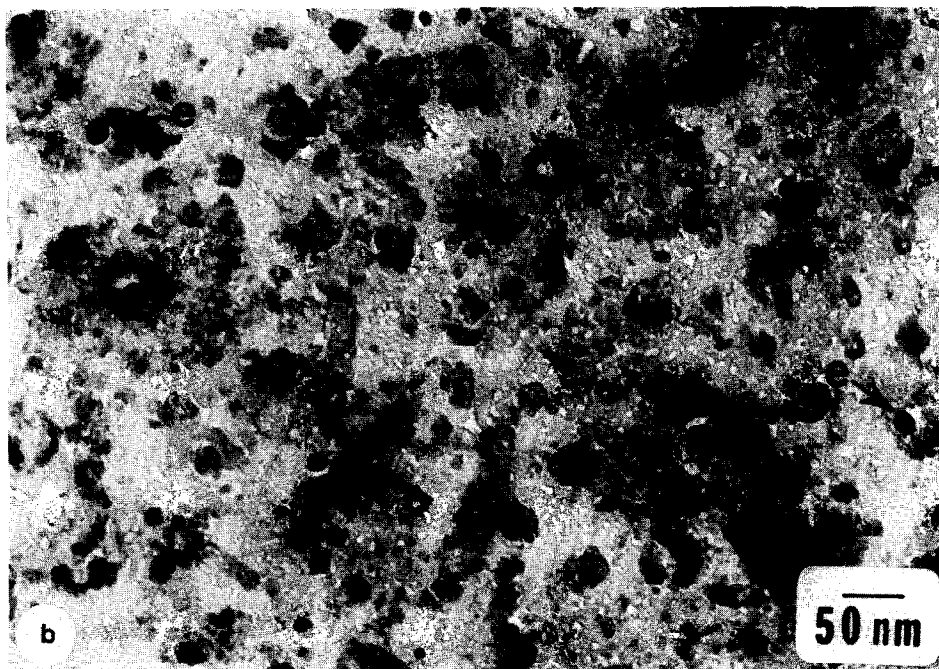


FIG. 21—Continued.

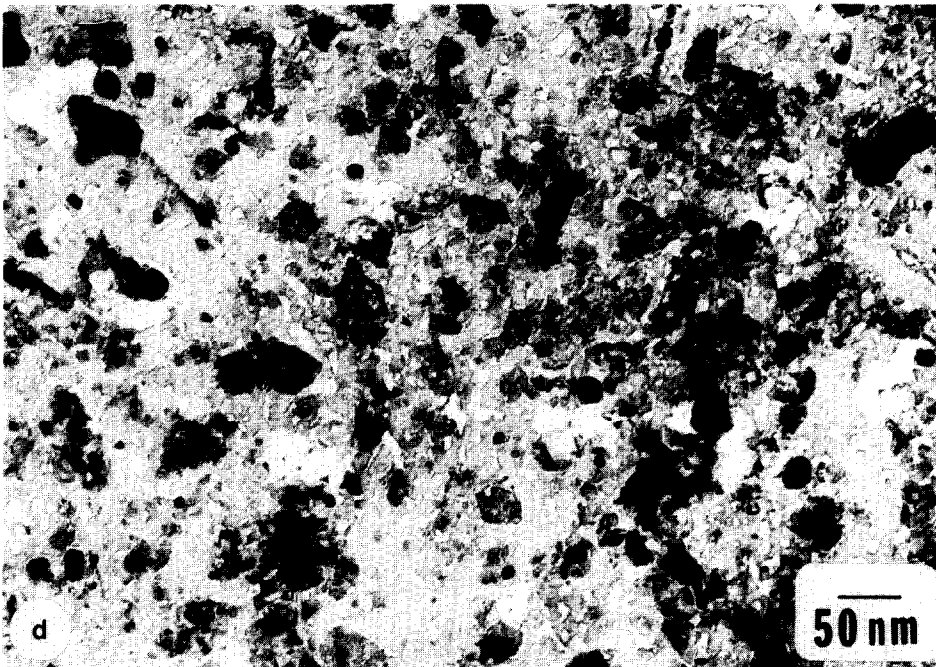


FIG. 21—Continued.

cles appeared, while most of the thin particles remained unchanged. Comparing with  $\text{Co}/\text{Al}_2\text{O}_3$ , one may note that the amount of material lost permanently to the gas stream during heating in  $\text{CH}_4 + \text{steam} + \text{H}_2 + \text{CO}$  is greater for  $\text{Fe}/\text{Al}_2\text{O}_3$ .

#### DISCUSSION

##### 1. Overall View of the Behavior of the Model Catalysts in Various Atmospheres

*1a. Individual components.* Before the phenomena that occur in the simulated reaction atmospheres are examined, a brief review of the effects of the individual components on the model catalysts is useful.

It is well known that the presence of  $\text{H}_2$  at elevated temperatures enhances sintering in the case of nickel on alumina catalysts. Although there is less information on the sintering of cobalt, the effect of  $\text{H}_2$  on cobalt should be similar to that on nickel. The sintering of  $\text{Fe}/\text{Al}_2\text{O}_3$  in  $\text{H}_2$  was exam-

ined in some detail by Sushumna and Ruckenstein (21). Since Fe is extremely reactive, only traces of  $\text{O}_2$  or  $\text{H}_2\text{O}$  are sufficient for the formation of iron oxide. The chemical interactions between this oxide and the alumina substrate appreciably diminish the rate of sintering.

The results reported by Ruckenstein and Hu (17) have shown that by heating in steam, the particles of  $\text{Ni}/\text{Al}_2\text{O}_3$ ,  $\text{Co}/\text{Al}_2\text{O}_3$ , and  $\text{Fe}/\text{Al}_2\text{O}_3$  extended and spread over the surface of the substrate, with a rate in the order  $\text{Co} > \text{Ni} > \text{Fe}$ .

All three metals are active and efficient catalysts for the decomposition of methane or disproportionation of carbon monoxide (10), and various types of carbon deposits have been reported (22–25).

The results presented in this paper show that heating in  $\text{CH}_4$  changes the shape of the particles; the change is, however, different for the three metals. In the case of Ni, the particles became elongated and transformed to filaments, by depositing

their material behind migrating leading particles, which decreased in size. The presence of small amounts of carbon was inferred from the subsequent heating of the specimen in  $O_2$ . The elongation of the particles is most likely a result of carbon deposition on the particles and its diffusion inside. In the case of Co, carbon was deposited around and on the particles, and, on further heating, the particles decreased in size, most probably because of spreading out from them of thin films, undetectable by electron microscopy. The presence of films could be inferred from the observation of new particles after the subsequent heating of the specimen in  $H_2$ . In the case of Fe, the particles transformed to extended patches and a few filaments formed, very likely as a result of carbon deposition. Carbonaceous filaments were not observed for any of the three metals. Baker *et al.* (26) also reported that carbonaceous filaments were not generated when heating in high-purity methane.

Upon heating  $Ni/Al_2O_3$  in  $CH_4$ , following its pretreatment in steam, one notes that carbon was deposited around and/or on the particles. In this case, the NiO formed during pretreatment interacted more strongly than Ni with alumina. As a result, the particles did not migrate over the substrate, and carbon could not penetrate at the interface between particles and substrate to form filaments, for reasons discussed later in the paper.

The present experiments indicate that the main difference between heating in single gas components and their mixtures is the rapid change of the morphologies of the metal particles in the latter case. This may explain the rapid decline, noted by many investigators (3, 14, 27, 28), in the activity of the catalysts after they were subjected to reaction conditions. The previous investigators attributed the early deactivation to either sintering or coking. In contrast, we conclude that this deactivation is due to the coupling of sintering and coking. In other words, the rapid deactivation reflects the

cooperative effect of the components of the gas mixture on the supported metal catalysts.

*1b.  $CH_4 + steam$ .* Let us examine how this cooperative effect acts for the three metals. In the case of  $Ni/Al_2O_3$ , on heating the specimen in methane plus steam, one notes that the nickel particles are first oxidized by steam to nickel oxide, which is believed to constitute both the active catalytic species for the decomposition of methane (29) and the species responsible for the extension and spreading of the particles (17). However, the carbon deposited as a result of methane decomposition is subsequently gasified by steam. The gases thus resulting lift the particles and displace them over the surface of the substrate. This appears to be the main cause for the severe sintering that occurs on heating for 2 h the nickel model catalyst in the binary mixture of methane and steam.

In the case of  $Fe/Al_2O_3$ , steam has a much smaller effect because even traces of  $O_2$  or water are enough for its oxidation, and therefore iron is already oxidized before the heating in methane plus steam and has already reacted with the substrate. Therefore, the particles did not migrate and remained at their initial locations, in spite of the gasification of carbon by steam.

In the case of  $Co/Al_2O_3$ , the cobalt particles acquired deformed shapes and undetectable films spread out from them over the substrate, indicating that cobalt spreads more easily than Ni or Fe over alumina. The undetectable films were inferred from the new particles which were formed after subsequent heating in  $H_2$ .

*1c.  $CH_4 + steam + H_2$ .* In a mixture of  $H_2 + CH_4 + steam$  two different behaviors were observed for similar specimens of  $Ni/Al_2O_3$ , belonging to two different batches. In one specimen, the particles became elongated, forming tails behind dark leading particles. Electron diffraction indicated the presence of NiO, but carbon was also probably present. The behavior was similar to that observed on heating in

$\text{CH}_4$  + steam, except that sintering occurred to a greater extent, because of the presence of  $\text{H}_2$ . This enhances gasification of carbon deposits and, in addition, ensures more contracted forms of the crystallites; both effects enhance sintering. In the other specimen, the particles acquired toroidal shapes with a small particle in the cavity, after 10 min of heating. NiO was identified by electron diffraction. Upon heating for 20 more minutes, the particles were reduced to Ni and sintered, and long hollow interlinked carbonaceous filaments appeared. However, on further heating, the carbonaceous filaments disappeared and sintering continued to occur. The disappearance of the carbonaceous filaments was due to the carbon gasification by  $\text{H}_2$  and  $\text{H}_2\text{O}$ . The severe sintering was caused by the formation of Ni, which has a higher mobility than NiO, and by the gases produced by gasification. Note that in the former specimen, the particles were present as NiO, while in the latter, they were present as NiO for the first 10 min of heating and were reduced to Ni on subsequent heating. The different behavior of the two similar specimens appears to be of kinetic origin, being probably related to the reducibility of the NiO. These results indicate that heating in  $\text{CH}_4$  + steam +  $\text{H}_2$  oxidizes the Ni particles during the initial period. On subsequent heating, the particles can be reduced or not, and then they will have one or the other kind of behavior.

In the case of  $\text{Co}/\text{Al}_2\text{O}_3$ , the particles deformed during heating in  $\text{CH}_4$  + steam +  $\text{H}_2$ , most likely (as discussed later) because of the penetration of the deposited carbon inside the particles. Compared to the heating in  $\text{CH}_4$  + steam, less spreading of the particles occurred, because the particles were less oxidized. However, since on subsequent heating in  $\text{H}_2$  only a few new particles appeared, it is clear that a large part of the material was permanently lost to the gas stream.

In the case of  $\text{Fe}/\text{Al}_2\text{O}_3$ , the particles were deformed throughout their heating in

$\text{CH}_4$  + steam +  $\text{H}_2$  and part of the material disappeared, being permanently lost to the gas stream. This was inferred from the subsequent heating in  $\text{H}_2$ , and happened, as discussed later in the paper, because of the disintegration of the particles.

*Id.* *CO.* The effect of heating in CO will be given only for  $\text{Ni}/\text{Al}_2\text{O}_3$ . Various types of carbon deposits, such as filamentous carbon, carbonaceous films around the particles, and large patches of carbon, were obtained. Compared with the heating in  $\text{CH}_4$ , the amount of carbon deposited was greater, indicating that on Ni particles the disproportionation of CO occurs more easily than the decomposition of  $\text{CH}_4$ . Electron diffraction indicated the presence of Ni during the entire heating in CO, as is in fact expected for such a strong reducing agent. As discussed later, the formation of filamentous carbon is associated with the reduced state of the particles.

*Ie.*  *$\text{CH}_4$  + steam +  $\text{H}_2$  + CO.* For  $\text{Ni}/\text{Al}_2\text{O}_3$ , on heating for 5 min, the particles became elongated, as throughout their heating in  $\text{CH}_4$ ,  $\text{CH}_4$  + steam, or  $\text{CH}_4$  + steam +  $\text{H}_2$ , and carbon deposits formed. Electron diffraction indicated the presence of NiO. This indicates that the oxidizing effect of steam is stronger during the initial heating. On further heating, the particles acquired spherical shapes and gradually were reduced to Ni, indicating that the reducing effect of  $\text{H}_2$  and CO gradually increased to become, finally, the stronger one. The absence of carbon deposits throughout the latter heat treatment was probably a result of a faster rate of gasification by  $\text{H}_2$  and steam than rate of carbon formation.

For  $\text{Co}/\text{Al}_2\text{O}_3$ , on heating for 5 min in the quaternary mixture numerous particles disappeared and the remaining particles became deformed, probably because of the penetration of the deposited carbon inside the particles. The particles disappeared, either because material was transferred to the substrate as undetectable films or because it was permanently lost to the gas

stream. On subsequent heating in  $H_2$ , new small particles appeared, indicating that at least a fraction of the disappeared material remained on the substrate as undetectable films.

For  $Fe/Al_2O_3$ , numerous particles disappeared on heating in the quaternary atmosphere. In contrast to  $Co/Al_2O_3$ , the material was permanently lost, as indicated by the fact that it was not restored as new particles on subsequent heating in  $H_2$ .

## 2. *The Growth of Carbonaceous Filaments and the Metal Support*

*Interactions.* For  $Ni/Al_2O_3$ , carbonaceous filaments appeared in CO, and, in some specimens, in  $CH_4 + steam + H_2$ , but as a transient phenomenon. In  $CH_4$  and  $CH_4 + steam$ , carbonaceous filaments were not observed, although elongated particles with filamentous structure did form. The pretreatment of a specimen in steam suppressed the formation of filamentous structures in  $CH_4$ .

The mechanism which was proposed for the carbon filament growth (10, 30, 31) involved the diffusion of carbon through the catalyst particles, driven either by a concentration difference (10) or by a temperature difference (31), and its precipitation between the particles and the support. The termination of the growth was attributed to the formation of a carbonaceous "skin" at the exposed (free) particle surface.

An additional important element should be, however, included. The initiation of carbon filaments, which have leading metal particles, implies that carbon can penetrate between crystallites and substrate. This, however, can happen only when the interfacial free energy between carbon and substrate plus the interfacial free energy between carbon and crystallite becomes smaller than the interfacial free energy between crystallite and substrate. This condition is satisfied in some cases. For instance, on heating metal foils in carbon containing atmospheres, one notes that filaments form with all three metals: Ni, Co, and Fe. This

probably happens because a thin surface layer, with a composition different from that of the bulk, exists, and the interfacial tension between the metal foil and the thin surface layer is higher than the sum of the interfacial tensions between carbon and the metal foil and between carbon and the thin layer. As a result, carbon penetrates between metal and thin layer.

In the case of supported metal catalysts, however, strong interactions between crystallites and support will lower their interfacial free energy (21), and the above condition may no longer be satisfied. Therefore, the strength of the above-mentioned interactions is critical for filament formation on supported metal catalysts. If the above condition is not satisfied, only changes in the particle shape and accumulation of carbon around and on the particles can occur.

When  $Ni/Al_2O_3$  specimen is heated in  $CH_4 + steam$ , Ni is easily oxidized by steam. The NiO which is thus formed interacts strongly with  $Al_2O_3$  (20) and the interfacial free energy between crystallites and support decreases. The absence of carbonaceous filaments during heating in  $CH_4 + steam$  indicates that the low interfacial free energy between NiO particles and substrate, which arises because of the strong interactions between them, does not satisfy the above thermodynamic inequality for filament formation. In contrast, the formation of carbonaceous filaments during heating in CO shows that the interfacial free energy between Ni particles and substrate is high enough for the above thermodynamic condition to be satisfied. When  $Ni/Al_2O_3$  specimens were heated in  $CH_4 + steam + H_2$ , different behaviors occurred, depending on the chemical state of the crystallites. When the crystallites were present as NiO throughout the entire heat treatment, no carbonaceous filaments were generated. But, in a very similar sample of a different batch, carbonaceous filaments were formed as a transient process after an induction period. The crystallites were present as NiO throughout the induction

period, but they were reduced to Ni when filaments were formed. The filaments disappeared after subsequent heating, because of their gasification.

Since Fe is easily oxidized even by traces of  $O_2$  and/or  $H_2O$ , and the oxide thus formed interacts strongly with  $Al_2O_3$  (for details see Ref. (21)), these interactions are indeed much stronger for  $Fe/Al_2O_3$  than for  $Ni/Al_2O_3$ . As a result, filaments should be absent in the former system. Indeed, carbonaceous filaments have not been observed on heating  $Fe/Al_2O_3$  catalyst in an atmosphere containing  $CH_4$  and/or  $CO$ . Co had a behavior similar to that of Fe, since it is also easily oxidized.

Once the particles are detached from the substrate, filaments will grow, by the further displacement of the particles. This can happen, however, only if the bulk diffusion of carbon through the particles and/or the surface diffusion of carbon over the surface of the particle are sufficiently rapid for a part of the metal to remain exposed to the chemical atmosphere, thus allowing the chemical decomposition of  $CH_4$  or  $CO$  to continue on the surface of the particle. The carbon which diffuses through the particles forms transient carbide phases (32), with a higher content of carbon at the particle surface and a lower one at the interface between particle and substrate. This gradient in carbon content probably constitutes the driving force for diffusion through the particle. The increase in the percentage of carbon inside the crystallites lowers their melting point, as indicated by the phase diagram, and the likelihood of defect formation is thus increased. This in turn increases the rate of diffusion of carbon through the crystallites and accelerates the process of precipitation of carbon between particle and substrate.

### 3. Deformation of the Particles

For Ni, the particles became elongated during heating in  $CH_4$ , or in mixtures containing  $CH_4$  and/or  $CO$ . For Co, the particles deformed on heating in mixtures con-

taining  $CH_4$  and/or  $CO$ . For Fe, the deformation of the particles was observed in  $CH_4 + \text{steam} + H_2$ . The elongation and deformation of the particles are probably associated with carbide formation. This is because carbon dissolves into the metal and forms carbides. The heating temperature being higher than the decomposition temperature of the stable carbides of Ni, Co, and Fe, only transient unstable phases form, from which some carbon can precipitate inside the particles. This generates internal stresses, leading to the deformation of the particles. Indeed, the carbides of Ni, Co, and Fe are not stable at the temperature of  $700^\circ C$  at which the specimens were heated.  $NiC$  decomposes in the temperature range of  $300\text{--}400^\circ C$  (33);  $Fe_2C$  and  $Fe_3C$  are not stable over  $450^\circ C$ , and decompose into iron and carbon (34);  $Co_3C$  decomposes in the temperature range of  $300\text{--}350^\circ C$  (35).

In addition, as the carbon content inside the particles increases, the melting point of the particles decreases, as indicated by the phase diagram, and thus the particles become softer. This may contribute to the deformation of the particles. In the case of  $Ni/Al_2O_3$ , the softened particles acquire high mobility and migrate over the substrate by liquid-like motion, depositing material behind the leading particle.

### 4. The Loss of Active Metal

During heating of  $Fe/Al_2O_3$  in the mixture of  $CH_4 + \text{steam} + H_2$ , a fraction of the particle material disappeared. This can be explained via unstable carbide formation, as follows: When small amounts of carbon penetrate and precipitate inside the particles, the latter will deform to release the internal stresses. This can disintegrate the particles, and at least a fraction of the resulting metal powder can be lost permanently to the gas stream. In the case of  $Co/Al_2O_3$ , a smaller amount of material was lost than in the case of  $Fe/Al_2O_3$ . This suggests that in the latter case, the particles disintegrate more easily.



On heating Fe/Al<sub>2</sub>O<sub>3</sub> in CH<sub>4</sub> + steam + H<sub>2</sub> + CO, one notes that the loss of material was even greater than on heating in the gas mixture without CO. This is most likely due to the formation of volatile carbonyl. Blackmond and Ko (36) reported a nearly 30% weight loss of Ni supported on SiO<sub>2</sub> after CO chemisorption at 273 K, due to the formation of Ni(CO)<sub>4</sub>. For Co/Al<sub>2</sub>O<sub>3</sub>, the loss of material during heating in CO containing mixture was smaller than that for Fe/Al<sub>2</sub>O<sub>3</sub>. For Ni/Al<sub>2</sub>O<sub>3</sub>, it is not clear whether the material was permanently lost during the heat treatment in the gas mixtures containing CH<sub>4</sub> and/or CO, because of the sintering of the particles.

#### CONCLUSION

In order to investigate the effect of the gas atmosphere on the physical and chemical changes of the particles in the steam reforming reaction, Ni/Al<sub>2</sub>O<sub>3</sub>, Co/Al<sub>2</sub>O<sub>3</sub>, and Fe/Al<sub>2</sub>O<sub>3</sub> model catalysts were heated at 700°C in various atmospheres, such as CH<sub>4</sub>, CO, and various gas mixtures containing CH<sub>4</sub> and/or CO.

During heating in CH<sub>4</sub>, the above metals behaved differently. For Ni/Al<sub>2</sub>O<sub>3</sub>, the particles became elongated, acquiring filamentous shapes, with leading migrating particles leaving their material along their trajectory until they disappeared. The elongated particles were composed mostly of NiO and probably some carbon. For Co/Al<sub>2</sub>O<sub>3</sub>, carbon deposits were formed around and on the particles, while for Fe/Al<sub>2</sub>O<sub>3</sub>, the particles initially extended on the substrate, and on further heating, carbon deposits were formed around the particles, as well as straight filaments, most likely composed of  $\gamma$ -Fe<sub>2</sub>O<sub>3</sub> (or Fe<sub>3</sub>O<sub>4</sub>) and some carbon deposits.

On heating Ni/Al<sub>2</sub>O<sub>3</sub> in CH<sub>4</sub> + steam, one notes that the particles extended initially on the substrate, because of their oxidation by steam. On further heating, the particles became elongated, but much less than in

CH<sub>4</sub>, and sintering occurred, because the gasification of deposited carbon enhanced the mobility of the particles on the substrate. For Co/Al<sub>2</sub>O<sub>3</sub>, the particles deformed, carbon deposits were formed around and on the particles, and undetectable films spread out from the particles over the substrate. For Fe/Al<sub>2</sub>O<sub>3</sub>, the particles extended on the substrate but less than for Co/Al<sub>2</sub>O<sub>3</sub>, because they were already partially oxidized before heating in CH<sub>4</sub> + steam and had therefore already reacted with the substrate.

On heating Ni/Al<sub>2</sub>O<sub>3</sub> specimens in the gas mixture of CH<sub>4</sub>, steam, and H<sub>2</sub>, one notes that severe sintering occurred. In addition, hollow carbonaceous filaments were formed when the crystallites were present as Ni, and did not form when the crystallites were present as NiO. Carbonaceous filaments have also appeared when Ni/Al<sub>2</sub>O<sub>3</sub> specimens were heated in CO. In this case, the crystallites were present as Ni. Hence, in the case of Ni/Al<sub>2</sub>O<sub>3</sub>, carbonaceous filaments can form if the particles are present as Ni and not as NiO.

A more general conclusion is that carbon filaments appear in those particular catalysts for which the interactions between crystallites and substrate are sufficiently weak. A thermodynamic criterion, based on wetting, is proposed for filament formation. The interfacial free energy between metal and substrate must be larger than the sum of the interfacial free energies between carbon and substrate, and carbon and metal. If this condition is satisfied, the crystallite can be detached from the substrate by a layer of carbon. The rate of growth of the filament is affected by the diffusion of carbon through the particles, diffusion which is probably facilitated by the formation of transient carbides.

In addition to filamentous carbon, other types of carbon deposits have also been identified. When steam-pretreated Ni/Al<sub>2</sub>O<sub>3</sub> was heated in CH<sub>4</sub>, carbon was deposited around and on the particles. Carbonaceous filaments were not generated because NiO

interacts strongly with the substrate. Therefore, the interfacial free energy between substrate and crystallite is small, and the thermodynamic condition for filament formation is not satisfied.

Deposits of carbonaceous films around and/or on the particles were also observed in other cases, such as Co/Al<sub>2</sub>O<sub>3</sub> and Fe/Al<sub>2</sub>O<sub>3</sub> in CH<sub>4</sub> and in gas mixtures containing CH<sub>4</sub>, and Ni/Al<sub>2</sub>O<sub>3</sub> in CO. Carbonaceous filaments wrapping elongated particles, as well as thick large patches of carbon deposits, were observed throughout heating of Ni/Al<sub>2</sub>O<sub>3</sub> in CO.

Upon heating Co/Al<sub>2</sub>O<sub>3</sub> and Fe/Al<sub>2</sub>O<sub>3</sub> in CH<sub>4</sub> + steam + H<sub>2</sub>, one notes that the particles deformed, and some material was permanently lost to the gas stream, because of the disintegration caused by the precipitation of carbon inside the particles.

When Ni/Al<sub>2</sub>O<sub>3</sub> was heated in CH<sub>4</sub> + steam + H<sub>2</sub> + CO, severe sintering occurred because the particles were reduced after a short time to Ni which sinters more easily, and the gasification of the deposited carbon increased the mobility of the particles. For Co/Al<sub>2</sub>O<sub>3</sub>, spreading of the particles and permanent loss of material were observed. For Fe/Al<sub>2</sub>O<sub>3</sub>, a considerable amount of material was permanently lost.

Unstable carbides are suggested to be responsible for the observed deformation of the particles. Carbide formation inside the particle, followed by carbon separation, generates internal stresses, which, in turn, lead to the deformation of the particles.

The investigation also indicates another aspect of catalyst deactivation, namely, the loss of active metal crystallites to the gas stream. This process occurs in different atmospheres for different reasons. On heating in the mixtures containing methane, the precipitation of carbon inside the metal disintegrates the crystallites, a part of which is then carried away by the gas stream. On heating in the mixtures containing carbon monoxide, the metal carbonyl that possibly forms may be in part responsible for the loss of particles.

#### ACKNOWLEDGMENT

Preliminary experiments regarding the present paper have been carried out by X. D. Hu (37).

#### REFERENCES

1. Satterfield, C. N., in "Heterogeneous Catalysis in Practice," Chemical Engineering Series, p. 286. McGraw-Hill, New York.
2. Schaper, H., Ames, D. J., Doesburg, E. B. M., and Van Reijen, L. L., *Appl. Catal.* **9**, 129 (1984).
3. Takemura, Y., Yamamoto, K., and Morita, Y., *Int. Chem. Eng.* **7**(4), 737 (1967).
4. Rostrup-Nielsen, J. R., "Symposium on the Science of Catalysis and its Application in Industry, FPDIL, Sindri, February 22-24, 1979." Paper No. 39.
5. Rostrup-Nielsen, J. R., *J. Catal.* **33**, 184 (1974).
6. Gardner, D. C., and Bartholomew, C. H., *Ind. Eng. Chem. Prod. Res. Dev.* **20**, 80 (1981).
7. Bartholomew, C. H., *Catal. Rev. Sci. Eng.* **24**, 67 (1982).
8. Trimm, D. L., *Catal. Rev. Sci. Eng.* **16**, 155 (1977).
9. Baker, R. T. K., and Harris, P. S., in "Chemistry and Physics of Carbon" (P. L. Walker, Jr., Ed.), Vol. 14, p. 83. Dekker, New York, 1979.
10. Rostrup-Nielsen, J. R., and Trimm, D. L., *J. Catal.* **48**, 155 (1977).
11. Jackson, S. D., Thomson, S. J., and Webb, G., *J. Catal.* **70**, 249 (1981).
12. Satterfield, C. N., in "Heterogeneous Catalysis in Practice," p. 288. McGraw-Hill, New York, 1980.
13. James, P., and Van Hook, O., *Catal. Rev. Sci. Eng.* **21**, 1 (1980).
14. Williams, A., Butler, G. A., and Hammons, J., *J. Catal.* **24**, 352 (1972).
15. Borowiecki, T., Denis, A., Nazimek, B., Grzegorzczak, W., and Barcicki, J., *Chemia Stosowana* **27**(3), 229 (1983).
16. Phillips, T. R., Yarwood, T. A., Mulhall, J., and Turner, G. E., *J. Catal.* **17**, 28 (1970).
17. Ruckenstein, E., and Hu, X. D., *J. Catal.* **100**, 1 (1986).
18. Ruckenstein, E., and Malhotra, L., *J. Catal.* **41**, 303 (1976).
19. Ruckenstein, E., and Sushumna, I., *J. Catal.* **97**, 1 (1986).
20. Ruckenstein, E., and Lee, S. H., *J. Catal.* **86**, 457 (1984).
21. Sushumna, I., and Ruckenstein, E., *J. Catal.* **94**, 239 (1985).
22. Baird, T., Fryer, J. R., and Grant, B., *Nature (London)* **233**, 329 (1971).
23. Evans, E. L., Thomas, J. M., Thrower, P. A., and Walker, P. L., *Carbon* **11**, 441 (1973).

24. Boehm, H. P., *Carbon* **11**, 583 (1973).
25. Hofer, L. J. E., Sterling, E., and McCartney, J. T., *J. Phys. Chem.* **59**, 1153 (1955).
26. Baker, R. T. K., Harris, P. S., Henderson, J., and Thomas, R. B., *Carbon* **13**, 17 (1975).
27. Hayer, R. E., Thomas, W. J., and Hayer, K. E., *J. Catal.* **92**, 312 (1985).
28. Jackson, S. D., Thomson, S. J., and Webb, G., *J. Catal.* **70**, 249 (1981).
29. Renshaw, G. D., Roscoe, C., and Walker, P. L., Jr., *J. Catal.* **18**, 164 (1970).
30. Lobo, L. S., Trimm, D. L., and Figueredo, J. L., "Proc. 5th Int. Congr. Catal. 1972," p. 1125. 1973.
31. Baker, R. T. K., Barber, M. A., Harris, P. S., Feates, F. S., and Waite, R. J., *J. Catal.* **26**, 52 (1972).
32. Renshaw, G. D., Roscoe, C., and Walker, P. L., Jr., *J. Catal.* **22**, 394 (1971).
33. Hofer, L. J. E., Cohn, E. M., and Peebles, W. C., *J. Phys. Colloid. Chem.* **54**, 1161 (1950).
34. Jack, K. H., *Proc. R. Soc. London. Ser. A* **195**, 56 (1948).
35. Kosolapova, T. Ya., in "Carbides," p. 177. Plenum, New York, 1971.
36. Blackmond, D. G., and Ko, E. I., *J. Catal.* **94**, 343 (1985).
37. Hu, X. D., MS. thesis, State University of New York at Buffalo, 1985.